A poised negative feedback circuit balances continual self-renewal with rapid restriction of developmental potential across asymmetric stem cell division.

By

Derek H. Janssens

A dissertation submitted in partial fulfillment
of the requirements for the degree of
Doctor of Philosophy
(Cellular and Molecular Biology)
The University of Michigan
2016

Doctoral Committee:

- **Associate Professor Cheng-Yu Lee, Chair**
- **Associate Professor Scott E. Barolo**
- **Professor Kenneth M. Cadigan**
- **Professor Tom K. W. Kerppola**
- **Associate Professor Yukiko Yamashita**

Table of Contents

List of Figures

List of Tables

Abstract

The identities of stem cells and their differentiated progeny are controlled by transcription factor networks that interact with chromatin modifying enzymes to package the genome into active and repressed domains. These transcription factor networks maintain stem cell identity across numerous rounds of self-renewing division through extensive auto- and feedforward-regulation, and by activating genes that are important for stem cell function. In addition, stem cell transcription factor networks directly regulate pro-differentiation genes, which are maintained in a poised chromatin state by the Polycomb group (PcG) and Trithorax group (TrxG) of chromatin modifying enzymes. How transcription factor networks maintain the poised chromatin state in stem cells, and coordinate the transition to an active chromatin state in their differentiating progeny remains unclear, and how this translates into the restriction of developmental potential is completely unknown.

To elucidate mechanisms that regulate stem cell self-renewal and differentiation my thesis work focuses on a subset of neural stem cells in the fly larval brain, called type II neuroblasts, and their production of intermediate neural progenitors (INPs). Type II neuroblast identity is maintained by a core group of self-renewal transcriptional repressor proteins including Klumpfuss, Deadpan and E(spl)my, as well as lineage-specific transcriptional activators including Pointed-P1 and Buttonhead that endow type II neuroblasts with the competence to produce INPs. My work demonstrates that

earmuff (*erm*) is specifically expressed in immature INPs, and functions as the master regulator of INP commitment, restricting their competence to respond to members of the self-renewal network by acting as a transcriptional repressor. In addition, we find the self-renewal transcriptional repressor network, lineage-specific transcriptional activators, and PcG and TrxG proteins converge to maintain the *erm* locus in a poised chromatin state in type II neuroblasts. Following asymmetric division, selective down-regulation of self-renewal transcriptional repressors in the immature INP allows rapid activation of *erm* expression. Erm then ensures stable commitment to a restricted INP identity by directly repressing components of the neuroblast transcription factor network. We propose the use of similar poised negative feedback circuits as a universal mechanism to balance continual self-renewal and rapid restriction of developmental potential across asymmetric stem cell division.

Chapter 1: Introduction

Stem cells are broadly defined by two cardinal features: (1) the ability to undergo long term self-renewal to maintain their own identity across numerous rounds of division, and (2) multipotency, meaning they have the capacity to give rise to a variety of more restricted or differentiated cell types. Thus, the term “stem cell” has become a catch-all in biology to refer to a variety of cells that differ greatly in their developmental potential. Embryonic Stem (ES) cells populate the inner cell mass (ICM) of the blastocyst and possess an extremely wide developmental potential, ultimately giving rise to cells within all three germ layers of the developing embryo. In comparison, tissue specific stem cells possess a more restricted developmental potential, and are responsible for generating and replenishing the specialized differentiated cell types within the tissues they reside (including the blood, gut, brain, and germline) throughout lifespan. Due to their potential use in regenerative medicine, stem cells have garnered immense interest in the medical and scientific communities. In addition, accumulating evidence suggests that numerous types of cancer arise from stem cell lineages that have acquired mutations which limit their differentiation programs. Realizing the immense therapeutic potential of stem cell biology requires an in-depth understanding of the mechanisms that control their self-renewal and differentiation. Here we discuss advances toward elucidating the molecular mechanisms controlling these cellular processes in both ES cells and tissue specific stem cells, as well as some of the current limitations in our understanding. In addition,

we discuss the regulation of neural stem cells in the fruit fly *Drosophila* to emphasize how studies of this relatively simple model organism may address some of the remaining enigmas in the field of stem cell biology.

The intimate relationship between gene regulation and stem cell biology.

All of the information essential for producing the diverse cell types that comprise metazoan organisms, including both stem cells and their progeny, is precisely encoded within the sequence of the genome. Although almost all cells within an organism contain a full complement of the genome, individual cell types only utilize, or express, a subset of the information their genome encodes. Thus, establishment and maintenance of specific cellular identities requires precise organization of the genome into active and repressed domains. This is achieved in part by wrapping the DNA around core octamers of proteins called histones to form nucleosomes. These nucleosome subunits are then chemically modified by large protein complexes known as chromatin modifiers to partition the genome into distinct domains, and establish the secondary chromatin structure (Sexton and Cavalli, 2015). However, few chromatin modifiers have the capacity to bind specific regions of the DNA on their own. Rather, recruitment of chromatin modifying enzymes to specific sites in the genome is often achieved through physical interaction with sequence specific transcription factor proteins that typically recognize short (6-10bp) motifs within the DNA. These motifs can occur by chance in the genome, potentially resulting in noisy or inappropriate transcription factor binding, so functional transcription factor binding elements often contain clusters of several binding sites in close proximity to one another. In addition, the open or closed state of the chromatin at particular regions of the genome can also determine which motifs a

transcription factor will actually bind in a given cell type (Lupien et al., 2008; McKay and Lieb, 2013; Teytelman et al., 2009). Ultimately, decoding the information contained in the sequence of the genome into specific cellular expression patterns is achieved through a complex interaction of the chromatin state, transcription factor binding and recruitment of chromatin modifying enzymes. Thus, understanding stem cell biology requires an in depth knowledge of the transcription factor networks they express, and how these networks interact with chromatin modifying enzymes to both maintain the chromatin state during self-renewal, and re-organize the chromatin during the generation of more restricted cell types.

Self-propagating transcription factor network maintain stem cell identity across self-renewing division.

Extensive investigation of mammalian ES cells and tissue-specific stem cells has revealed their self-renewal is dependent on intricate transcription factor networks. Although the networks that maintain the identity of distinct stem cell populations are comprised of unique, sometimes partially over-lapping, collections of transcription factors, the overall network architecture and regulatory logic appears to be very similar between stem cell types. Genome-wide association studies indicate stem cell transcription factors often bind their own distal- and proximal- cis-regulatory elements, called enhancers and promoters respectively, as well as cis-regulatory elements of other stem cell transcription factors (Boyer et al., 2005; Kim et al., 2008; Loh et al., 2006; Mateo et al., 2015; Schütte et al., 2016; Wilson et al., 2010). Furthermore, these transcription factors also share numerous additional common targets, including genes important for stem cell identity (i.e. chromatin modifiers and cell-signaling genes). Thus,

two of the defining features of stem cell transcription factor networks are: (1) they are self-propagating, engaging in extensive auto- and feedforward-regulation to maintain their own expression across numerous rounds of self-renewing division, and (2) they function cooperatively to maintain the activation of numerous genes required for stem cell function (Figure 1).

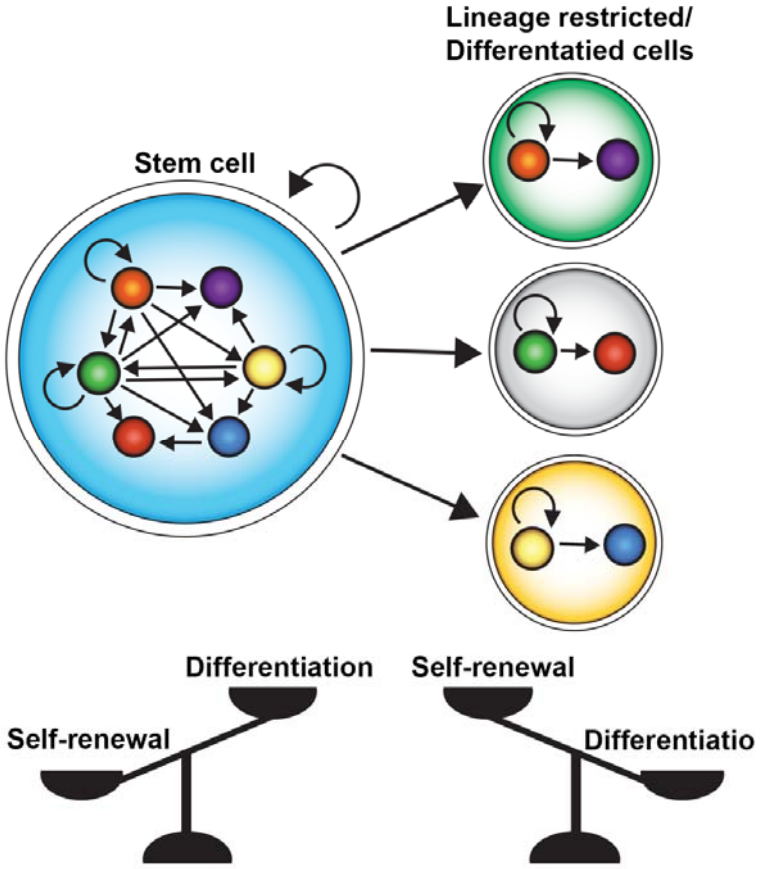

Figure 1: Stem cell transcription factor networks balance self-renewal and differentiation. Illustration of a hypothetical stem cell transcription factor network. Altering the activity of this network shifts the balance from self-renewal to differentiation. Small colored balls: transcription factors.

Stem cell transcription factor networks prime the genome for lineage commitment and differentiation.

In addition to binding the regulatory regions of genes involved in self-renewal, stem cell transcription factors networks also bind the enhancers and promoters of genes that control the subsequent lineage commitment and differentiation of stem cell progeny (Boyer et al., 2005; Kim et al., 2008; Loh et al., 2006). This was initially suggested to imply a context dependent role of stem cell transcription factor networks to activate self-renewal genes and repress differentiation genes; however, several lines of evidence

indicate an alternative scenario. While overexpression of certain components of the stem cell transcription factor network enhances self-renewal capacity (Chambers et al., 2003; Kim et al., 2008; Martello et al., 2013; Nichols and Smith, 2009), others induce stem cells to prematurely differentiate into distinct, more restricted cell types (Kopp et al., 2008; Niwa et al., 2000; Zhao et al., 2004). Although it's possible the pro-differentiation effect of this second class of stem cell transcription factors is a non-physiological artifact of overexpression, this is unlikely. During development, distinct components of stem cell transcription factor networks remain active in the lineage restricted or differentiated cell types they produce, and contribute to their respective cell-fate choices (Figure 1) (Heinz et al., 2010; Imayoshi and Kageyama, 2014; Novershtern et al., 2011; Weidgang et al., 2016). Thus, the unique collection of transcription factors that maintain the identity of a given stem cell type likely establishes their fixed developmental potential by priming their genome for the generation of specific differentiated cell types. This suggests maintenance of stem cell identity likely depends on an intricate balance between components of the transcription factor network to prevent premature activation of their pro-differentiation targets. Shifting this balance likely contributes to the precise timing and directionality of differentiation (Figure 1). Ultimately, elucidating how stem cell transcription factor networks control self-renewal and differentiation requires continued investigation of (1) the functional consequence of specific transcription factor binding events on their pro-differentiation targets (i.e. activation vs. repression), and (2) the mechanisms that selectively alter the activity of components of these networks in stem cell progeny.

Regulation of the chromatin state by Polycomb and Trithorax group proteins.

By modulating the accessibility of the genome to transcription factor binding, the chromatin state of a given cell type influences the functional output of their transcription factor network. The Polycomb group (PcG) and Trithorax group (TrxG) of proteins are chromatin modifying enzymes that play a central role in organizing the genome into active and repressed domains, as well as the heritable propagation of these transcriptional states across cell division.

PcG and TrxG genes were originally identified by genetic studies in *Drosophila* based on their common homeotic mutant phenotypes in which anterior-posterior patterning is disrupted (Ingham, 1998; Kennison, 1995). Extensive genetic analysis eventually revealed the homeotic mutant phenotype of PcG and TrxG genes is the result of mis-regulation of Hox genes in the Bithorax Complex (BX-C) (Ingham, 1983). Mutation of PcG genes results in de-repression of components of the BX-C, leading to ectopic expression within segments along the anterior-posterior axis. Conversely, TrxG genes are required for both the normal and ectopic activation of the BX-C (Ingham, 1983). This analysis led to the prevailing “red-light/green-light” model of gene regulation by PcG and TrxG proteins, in which these complexes work antagonistically to one another, mediating repression versus activation of their common target genes respectively (Geisler and Paro, 2015; Piunti and Shilatifard, 2016).

Genetic identification and cloning of PcG and TrxG proteins enabled biochemical analysis of these complexes which demonstrated their function as chromatin modifying

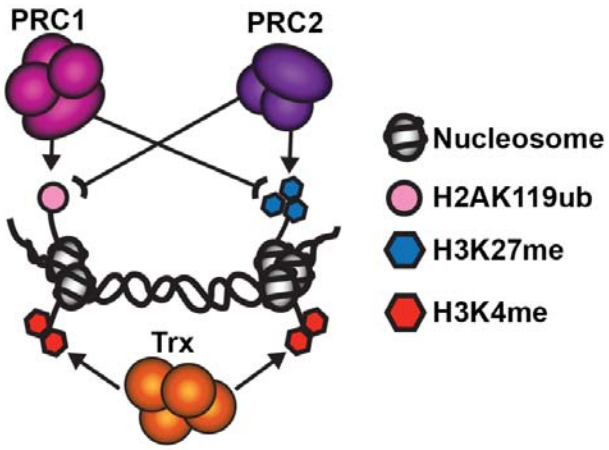

Figure 2: PcG and TrxG proteins functions as chromatin modifying enzymes to establish and maintain active and repressed genomic domains.

enzymes. The purification of PcG genes showed they comprise two distinct complexes: (1) Polycomb Repressive Complex 1 (PRC1), which contains the core subunits Polycomb (Pc), Posterior sex combs, dRing1, and Polyhomeotic, and (2) Polycomb Repressive Complex 2 (PRC2), which contains the core subunits Extra sex combs, Enhancer of zeste (E(z)), and Suppressor of zeste 12 (Su(z)12) (Figure 2) (Müller et al., 2002; Saurin et al., 2001; Shao et al., 1999). PRC1 catalyzes mono-ubiquitination of lysine 119 on histone 2A (H2AK119ub) though its Ring1 E3 ubiquitin ligase subunit (Figure 2) (Wang et al., 2004). PRC2 also functions as a chromatin modifying complex, and catalyzes methylation of lysine 27 on histone 3 (H3K27me) (Figure 2) (Müller et al., 2002). PRC2 is the sole H3K27 methyltransferase in *Drosophila* and vertebrates, catalyzing mono-, di-, and tri-methylation of H3K27 (Ferrari et al., 2014). Regions of the genome associated with prolonged PRC2 occupancy, and PRC2 mediated repression, are primarily marked by H3K27me3 (Ferrari et al., 2014). Interestingly, the PRC1 component Pc can bind to PRC2-deposited H3K27me3 through its chromodomain, and this interaction is important for recruiting PRC1 to specific sites in the genome (Figure 2) (Min et al., 2003). In addition, PRC2 has an increased affinity for nucleosomes bearing H2AK119ub, and this interaction stimulates the H3K27 methyltransferase activity of PRC2 *in vitro* (Figure 2) (Blackledge et al., 2014). The

reciprocal interaction of PRC1 and PRC2 with their modified histone substrates provides a biochemical explanation for their co-occupancy of numerous target loci in the genome, and their cooperation during gene regulation (Blackledge et al., 2015). In addition, this suggests PcG genes may be able to propagate their own interaction with specific regions of the genome, and may partially explain the heritable nature of PcG regulated domains (Steffen and Ringrose, 2014).

The *Drosophila* genome encodes three known H3K4 methyltransferases including Trithorax (Trx), Set1, and Trithorax-related (Piunti and Shilatifard, 2016). Set1 is responsible for global di- and tri-methylation of H3K4 (Ardehali et al., 2011), whereas the role of Trx appears to be more nuanced (Mohan et al., 2011). Although Trx catalyzes methylation of lysine 4 on histone 3 (H3K4me) *in vitro* (Tie et al., 2014), reducing the activity of Trx does not have a dramatic effect on global H3K4 methylation (Mohan et al., 2011). Thus, it is likely that Trx mediates a subset of H3K4 methylation in the genome (Figure 2). Consistent with this model, Trx is recruited to specific regions of the *Drosophila* genome, such as the BX-C, through interactions with Trx response elements (TREs), and is required for transcriptional activation of these genes (Ringrose and Paro, 2007). The vast majority of the TREs that have been molecularly defined in *Drosophila* occur in close proximity to Polycomb response elements (PREs), suggesting the TrxG proteins may have a specific role during the activation of PcG regulated genes (Figure 2) (Ringrose and Paro, 2007).

The role of Polycomb and Trithorax group proteins during stem cell regulation

The PcG and TrxG proteins are highly conserved in mammals, and in addition to their conserved role in regulating anterior-posterior patterning they also contribute to the

regulation of stem cell biology (Aloia et al., 2013; Luis et al., 2012; Sauvageau and Sauvageau, 2010). Genome-wide association studies in human and mouse ES cells found PRC2 binds the Hox gene clusters as well as a large number of additional transcription factors that function as master regulators of lineage commitment and differentiation in the developing embryo (Boyer et al., 2006; Lee et al., 2006d). Consistent with direct regulation by PRC2, the local chromatin of these genes was enriched with H3K27me3, and mutation of *EED*, the vertebrate homologue of *Drosophila extra sexcombs*, results in de-repression of multiple PRC2 targets in mouse ES cells (Boyer et al., 2006). Thus, it was suggested PRC2 promotes ES cell self-renewal by maintaining repression of genes involved in lineage commitment.

Subsequent work focusing on the chromatin state of ES cells found a large number of these PRC2 bound genes have distal-regulatory elements, referred to as “poised enhancers”, that in addition to H3K27me3, also display high levels of mono- and di- H3K4 methylation (presumably catalyzed by the mammalian homologue of *trx*) (Calo and Wysocka, 2013; Heintzman et al., 2007; Rada-Iglesias et al., 2011). Consistent with the proposed role of PRC2 bound genes during lineage commitment and differentiation, these poised enhancers are sufficient to drive cell-type and stage-specific gene expression in the developing embryo (Rada-Iglesias et al., 2011). Following the identification of poised enhancers in ES cells, a similar chromatin signature was identified on numerous distal-regulatory elements in NSCs (Amador-Arjona et al., 2015; Bergsland et al., 2011; Mateo et al., 2015). Functional studies indicate that the vertebrate homologue of *trx*, *mixed-lineage leukemia 1* (*Mll1*), is required in adult NSCs in the subventricular zone of mice to maintain the proneural gene *Dlx2* in a poised state

for subsequent activation in their progeny (Lim et al., 2009). Thus, maintenance of a poised chromatin state by PcG and TrxG genes may be a universal mechanism to prime the genome of stem cells for subsequent differentiation. In agreement with the red-light/green-light model of PcG/TrxG gene regulation, PcG proteins are thought to maintain repression of poised enhancer in stem cells, while TrxG proteins maintain these regions of the genome for subsequent activation during lineage commitment (Heinz et al., 2010).

Regulation of the transition from a poised to active chromatin state.

The finding that lineage-commitment and differentiation genes are maintained in a poised chromatin state in stem cells strongly suggests that proper regulation of the poised enhancers is likely important to balance self-renewal and differentiation. Elucidating how the poised chromatin state is maintained during stem cell self-renewal, and how the transition from a poised to active state is regulated in stem cell progeny will likely have a broad impact on our understanding of stem cell biology.

In contrast to poised enhancers, enhancers associated with active genes frequently display high levels of acetylated lysine 27 on histone 3 (H3K27ac), whereas H3K27me3 is absent (Creyghton et al., 2010). Furthermore, when ES cells are induced to differentiated into neuroectoderm, enhancers of developmental regulators of neurogenesis, which display a poised chromatin signature (H3K4me1+, H3K27me3+, H3K27ac-) in ES cells, transition to an activate chromatin state (H3K4me1+, H3K27me3-, H3K27ac+) (Rada-Iglesias et al., 2011). In contrast, distal-regulatory elements associated with genes involved in mesoderm or endoderm lineage commitment maintain their poised chromatin signature during neuroectoderm

differentiation (Rada-Iglesias et al., 2011). This indicates the transition from methylation to acetylation of H3K27 is involved in the activation of poised enhancers, and likely drives expression of the pro-differentiation genes they regulate. In addition, this suggests stem cell multipotency is dependent on maintaining the enhancers of genes that control the lineage commitment or differentiation of their progeny in a poised chromatin state, and that production of a specific lineage or differentiated cell type involves precise activation of a subset of these poised enhancers.

How is the transition from a poised to active chromatin state regulated? Numerous components of the transcription factor networks that maintain ES cell and tissue specific stem cell identity bind to poised enhancers, and likely contribute to their regulation (Amador-Arjona et al., 2015; Bergsland et al., 2011; Creyghton et al., 2010; Heinz et al., 2015; Mateo et al., 2015; Rada-Iglesias et al., 2011). In the blood, components of the hematopoietic stem cell (HSC) transcription factor network maintain distinct subsets of H3K4me1+ enhancers in differentiated macrophages and B-cells through cooperative binding with lineage-specific transcription factors (Heinz et al., 2010). Maintenance of these H3K4me1+ enhancers facilitates subsequent binding and activation by signal dependent transcription factors (Heinz et al., 2010; Heinz et al., 2015). This provides a compelling model to explain how cell-type specific enhancers are regulated, however, these studies did not examine H3K27me3 or H3K27ac, and so the relevance of this model to poised enhancers specifically remains to be tested. In neural stem cells (NSCs) the H3K27 specific demethylase JMJD3 is required for robust activation of the poised gene *Dlx2* in the progeny of adult NSCs (Park et al., 2014). However, JMJD3 is expressed in both NSCs and their progeny, and how the activity of

JMJD3 is coordination on the *Dlx2* locus remains unclear. Thus, continued investigation is necessary to elucidate how transcription factor networks interact with chromatin modifying enzymes to maintain the poised state of enhancers in stem cells, and coordinate the transition of these enhancers to an active state in stem cell progeny.

The link between stem cell biology and the formation of cancer.

Tissue specific stem cells divide asymmetrically to regenerate while producing intermediate progenitors, also called transit-amplifying cells, which function to amplify the output of each stem cell division. As opposed to their parental stem cells, intermediate progenitors, have a restricted developmental and proliferative potential, limiting their number of divisions and the differentiated cell types they can produce. For example, HSCs can give rise to either common lymphoid progenitors, which generate differentiated granulocytes and macrophages, or common myeloid progenitors, which give rise to differentiated B-cells, T-cells and natural killer cells (Chotinantakul and Leeanansaksiri, 2012). To meet the rapid pace of development and the fluctuating demands of adult tissues, intermediate progenitors need to rapidly commit to their restricted identity before entering the cell cycle within hours of their birth (Homem et al., 2013; Ponti et al., 2013). Precise specification of intermediate progenitor identity likely involves restriction of stem cell self-renewal pathways, and upregulation of intermediate progenitor specific programs. Mechanistic insight into this critical transition will have broad clinical applications.

Genetically engineered mouse models have revealed mutations commonly found in human tumors lead to oncogenic transformation when induced in stem cells or specific intermediate progenitor populations, but not their differentiated progeny

(Lamprecht and Fich, 2015; Liu et al., 2011; Liu and Zong, 2012; Zong et al., 2015). Also, human cancer cells that phenotypically resemble intermediate progenitors occasionally acquire the capacity to aberrantly revert to a less restricted stem cell-like identity. This inter-conversion between stem cells and intermediate progenitors may be a primary mechanism driving tumor expansion (Magee et al., 2012). Because of their unique susceptibility to oncogenic lesions that impair differentiation, intermediate progenitors are suspected to act as the cell-of-origin for numerous tumor types (Lamprecht and Fich, 2015; Zong et al., 2015). Thus understanding how the restricted identity of intermediate progenitors is established and maintained to ensure their subsequent differentiation will likely inform clinical efforts to combat cancer.

Interestingly, both gain- and loss-of-function mutations in PcG and TrxG proteins have been identified in distinct tumor types, and the molecular mechanisms by which these lesions contribute to tumor growth are just beginning to be elucidated (Herz et al., 2014; Piunti and Shilatifard, 2016; Sauvageau and Sauvageau, 2010; Slany, 2016). One attractive possibility is that context dependent mis-regulation of poised differentiation genes may contribute to the tumor-suppressive versus oncogenic effects of PcG and TrxG mutations in different tissues. While this model is gaining traction (Herz et al., 2014), further investigation is necessary to conclusively demonstrate the link between the tumorigenic effects of PcG and TrxG mutations and mis-regulation of poised differentiation genes.

Drosophila neuroblasts as a model of stem cell biology

Due to their fast generation time, amenability to genetic manipulation and their similar physiology to more complex metazoans, the fruit fly *Drosophila* has served as a work

horse to identity molecular mechanisms controlling many aspects of biology. The *Drosophila* nervous system is produced by neural stem cells (neuroblasts) that delaminate from the neural epithelium in the early embryo, perform the bulk of neurogenesis during the larval stages, and then terminally differentiate or die shortly after pupation (Doe, 2008; Homem et al., 2014; Maurange et al., 2008). The neuroblasts that populate the larval central brain can be broadly categorized into two classes, referred to as type I and type II neuroblasts, based on molecular marker expression, and their unique lineage hierarchies (Bello et al., 2008; Boone and Doe, 2008; Weng and Lee, 2011). Each larval brain lobe contains close to 100 type I neuroblasts that undergo repeated rounds of asymmetric division to self-renew while generating ganglion mother cells (GMCs). Shortly after their birth, these GMCs undergo a single differentiating division to produce two neurons (Homem et al., 2013). In comparison, each larval brain lobe contains only 8 type II neuroblasts which also invariably divide asymmetrically, but amplify the number and diversity of progeny produced by each division through generating intermediate neural progenitors (INPs) (Bello et al., 2008; Boone and Doe, 2008). Similar to vertebrate intermediate progenitors, INPs possess a restricted developmental and proliferative potential, and undergo 5-6 rounds of asymmetric division to produce GMCs before terminally differentiating (Bayraktar et al., 2010; Bayraktar and Doe, 2013). The GMCs produced by type II neuroblast lineages also undergo a single differentiating division, but can give rise to either terminally differentiated neurons or glia (Viktorin et al., 2011). Their similar physiology to mammalian tissue-specific stem cells makes *Drosophila* neuroblasts an excellent model to identity conserved mechanisms controlling stem cell self-renewal, intermediate

progenitor commitment, and the terminal differentiation of their progeny (Doe, 2008; Homem and Knoblich, 2012; Janssens and Lee, 2014).

The transcription factor networks controlling neuroblast identity

Genetic investigation of neuroblast regulation has revealed their self-renewal is controlled by a highly conserved transcription factor network. The Notch signaling pathway regulates many aspects of stem cell biology in both *Drosophila* and vertebrates (Liu et al., 2010; Pierfelice et al., 2011), and is a critical input into the neuroblast self-renewal transcription factor network. *Notch* encodes a transmembrane protein that upon extra-cellular ligand binding undergoes proteolytic activation, releasing the Notch intra-cellular domain (NICD). The NICD then translocates to the nucleus where it complexes with the DNA binding protein Suppressor of Hairless (Su(H)) to activate target gene expression (Hori et al., 2013; Liu et al., 2010).

In neuroblasts the NICD/Su(H) complex directly regulates activation of the self-renewal transcription factors *Enhancer of split-mγ* (*E(spl)mγ*), *deadpan* (*dpn*), *klumpfuss* (*klu*), and the O-isoform of *grainyhead* (*grhO*) (San-Juán and Baonza, 2011; Xiao et al., 2012; Zacharioudaki et al., 2015; Zacharioudaki et al., 2012). The basic-helix-loop-helix-orange transcription factors E(spl)mγ and Dpn are *Drosophila* homologues of the HES family of transcription factors, which also regulate vertebrate neural stem cell identity (Imayoshi and Kageyama, 2014). E(spl)mγ and Dpn bind DNA as either homo- or hetero-dimers that are all thought to recognize a similar consensus motif (Zacharioudaki et al., 2012). Whereas mutation of either the *E(spl)* locus or *dpn* alone does not lead to neuroblast loss, simultaneous mutation of the *E(spl)* locus and *dpn* together results in

the rapid premature differentiation of neuroblasts (Zacharioudaki et al., 2012). This indicates E(spl)mγ and Dpn act redundantly to promote neuroblast self-renewal, suggesting they likely regulate common target genes. The EGR-like transcription factor Klu is homologous to mammalian Wilms Tumor-1 (Pei and Grishin, 2015), and in contrast to *E(spl)* or *dpn*, the single mutation of *klu* results in premature neuroblast differentiation (Berger et al., 2012; Xiao et al., 2012). Thus, Klu function is required for neuroblast self-renewal. Lastly, GrhO is a member of the Grh family of transcription factors, which has expanded in mammals and includes *Grh-like 1,2 & 3* (Wang and Samakovlis, 2012). The single *grh* locus in *Drosophila* encodes multiple isoforms which all share a common DNA binging domain coupled to different trans-regulatory domains. GrhO is the sole isoform expressed in central brain neuroblasts, and is thought to act primarily as a transcriptional activator (Almeida and Bray, 2005). Indeed, GrhO has been included in models of the neuroblast self-renewal transcription factor network (Berger et al., 2012). However, the role of GrhO during maintenance of neuroblast identity remains unclear. Mutation of *grhO* results in mild neuroblast cell cycle defects, but does not lead to overt premature differentiation (Cenci and Gould, 2005). One possible explanation is that, like E(spl)mγ and Dpn, GrhO may act in a partially redundant manner with other neuroblast transcriptional activators, masking the role of GrhO during the regulation of neuroblast self-renewal.

In addition to the core neuroblast transcription factor network, type II neuroblasts also uniquely express the P1-isoform of the ETS-1 transcription factor *pointed* (*pntP1*), members of the SP1/KLF family of transcription factors including *buttonhead* (*btd*) and *Sp1,* as well as the homeodomain transcription factor *Distal-less* (*Dll*) (Carney et al.,

2012; Yang et al., 2015). Thus, PntP1, Btd, Sp1, and Dll constitute a type II neuroblast specific transcription factor network. During delamination from the optic placode neuroepithelium in the *Drosophila* embryo, the EGFR signaling pathway is necessary for activation of *pntP1* and establishment of a type II neuroblast identity (Hwang and Rulifson, 2011). However, EGFR signaling is dispensable for maintenance of a type II neuroblast identity and PntP1 expression in the larval brain (unpublished data). An attractive model to explain the temporal specific requirement of EGFR signaling is that the type II neuroblast-specific transcription factor network is self-propagating, and may include auto-regulatory and feedforward loops to maintains its own activity. Consistent with this possibility, mutation of *btd* results in reduction or loss of PntP1 expression in type II neuroblasts (Xie et al., 2014), and Btd and Sp1 have been show to directly activate *Dll* during *Drosophila* leg development (Estella and Mann, 2010). In addition, Mis-expression of *pntP1* or *btd* alone confers a type II neuroblast-like identity to type I neuroblasts, causing them to directly produce INP-like progeny rather than GMCs (Komori et al., 2014a; Xie et al., 2014; Zhu et al., 2011). This suggests expression of either *pntP1* or *btd* is sufficient to jump start the type II neuroblast specific transcriptional program, potentially by initiating a feedforward mechanism. However, additional experiments are necessary to test whether direct cross-talk between PntP1, Btd, Sp1, and Dll exists in type II neuroblasts.

Initiation of intermediate neural progenitor commitment in type II neuroblast lineages

Following their birth, INPs undergo a maturation phase lasting approximately 6-8 hours, during which their developmental potential becomes stably restricted prior to entry into

the cell cycle (Bowman et al., 2008; Homem et al., 2013; Weng et al., 2010). Importantly, immature INPs can be unambiguously identified based on proximity to their parental type II neuroblast and expression of a well characterized set of molecular markers. Thus, INP maturation provides an exceptional model to identify fundamental mechanisms that restrict the identity of intermediate progenitors following asymmetric stem cell division (Janssens and Lee, 2014). Genetic investigation has revealed that INP commitment is initiated by the asymmetrically segregated fate-determinants Brain-tumor (Brat) and Numb (Betschinger et al., 2006; Bowman et al., 2008; Lee et al., 2006a; Lee et al., 2006c). Brat and Numb are both expressed in type II neuroblasts and localize to the cell membrane where they are thought to be held in an inactive confirmation. During type II neuroblast mitosis, Brat and Numb become segregated to the basal membrane resulting in their exclusive inheritance by the newly born immature INP following asymmetric division (Figure 3). Brat and Numb initiate INP commitment by transiently down-regulating expression of the self-renewal transcription factors Notch, E(spl)mγ, Dpn, and Klu during INP maturation (Figure 3) (Haenfler et al., 2012; Janssens et al., 2014; Janssens and Lee, 2014; Xiao et al., 2012). The Brat protein functions as a translational repressor of specific mRNA targets, and has been shown to directly bind *dpn* and *klu* mRNA in the *Drosophila* embryo (Loedige et al., 2015). Numb

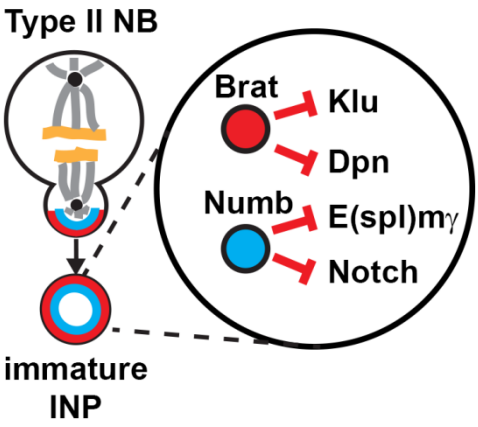

Figure 3: The asymmetrically segregated fate-determinants Brat and Numb initiate INP commitment by downregulating self-renewal transcription factors.

is a classic inhibitor of Notch signaling and is thought to promote endocytosis of the Notch receptor, removing it from the membrane and preventing activation (Couturier et al., 2012 ; Giebel and Wodarz, 2012). When either *brat* or *numb* are mutated, INP commitment fails, resulting in their rapidly reversion to a type II neuroblast identity and the formation of massive numbers of supernumerary neuroblasts (Bowman et al., 2008; Xiao et al., 2012). Similarly, mis-expression of Notch, E(spl)mγ, Dpn, or Klu during the early, but not late stages of INP maturation can prevent INP commitment and drive efficient reversion to a type II neuroblast identity (Janssens et al., 2014; Xiao et al., 2012). In addition, mutation of either *dpn* or *klu* can completely suppress the formation of supernumerary neuroblasts in *brat* mutants (Janssens et al., 2014; Xiao et al., 2012). This strongly suggests the transcription factors Notch, E(spl)mγ, Dpn, and Klu promote type II neuroblst self-renewal by preventing premature INP commitment, and must be transiently downregulated to initiate the restriction of INP developmental potential. However, Notch, E(spl)mγ, Dpn, and Klu all become re-expressed in the INP upon completion of maturation, suggesting the competency of INPs to respond to these self-renewal factors is restricted.

Maintenance of the restricted developmental potential of intermediate neural progenitors

The C_2H_2 zinc finger transcription factor Earmuff (Erm) is specifically expressed in immature INPs, and functions as the master regulator of INP commitment (Janssens et al., 2014). Type II neuroblasts mis-expressing Erm prematurely differentiate; whereas *erm* null INPs spontaneously revert into supernumerary type II neuroblasts (Weng et al., 2010). Erm restricts the developmental potential of INPs by functioning primarily as a

transcriptional repressor and restricts the competency of INPs to respond to reactivation of Notch, E(spl)mγ, Dpn, and Klu (Janssens et al., 2014). Erm is the *Drosophila* homologue of mammalian Fezf1 and Fezf2 which also regulate numerous cell-fate decisions in the mammalian brain (Eckler and Chen, 2014). The molecular mechanism by which Erm, Fezf1 and Fezf2 regulate target gene transcription is likely conserved because these transcription factors all recognize the consensus binding motif AAAAGAGCAAC *in vitro* (Janssens et al., 2016) (see Chapter 3), and overexpression of Fezf1 or Fezf2 in immature INPs completely rescues the supernumerary type II neuroblast phenotype in *erm* null brains (Weng et al., 2010). Thus, understanding the mechanism by which Erm restricts the developmental potential of INPs will likely provide critical insight into the regulation of cell-fate commitment in the mammalian brain.

Maintaining *earmuff* in a poised chromatin state in type II neuroblasts balances continual self-renewal with rapid restriction of developmental potential following asymmetric division.

Similar to vertebrate stem cells, PcG and TrxG genes are important regulators of type II neuroblast lineages. Trx is required to maintain *pntP1* and *btd* expression in type II neuroblasts, and for activation of *erm* expression in immature INPs (Komori et al., 2014a). When *trx* is mutated type II neuroblasts adopt a type I neuroblast-like identity, and directly giving rise to GMCs rather than INPs (Komori et al., 2014a). The endogenous *erm* promoter and immature INP enhancer are maintained in a poised state in type II neuroblasts and display high levels of H3K4me2, and H3K27me3 and low levels of H3K27ac (Figure 4) (Janssens et al., 2016) (see Chapter 3). This facilitates rapid activation of Erm expression in immature INPs within two-hours of their birth

(Janssens et al., 2016) (see Chapter 3). However, in contrast to the aforementioned red-light/green-light model of PcG/TrxG gene regulation, mutation of critical components of PRC2 does not result in premature activation of Erm expression in type II neuroblasts, and instead causes a reduction in Erm expression in immature INPs (Janssens et al., 2016) (see Chapter 3). Thus, PRC2 is not required to maintain repression of *erm* in type II neuroblasts. Consistent with this interpretation, a transgenic reporter containing the *erm* immature INP enhancer displays high levels of H3K4me2, but low or undetectable levels of H3K27me3 in type II neuroblasts, yet it remains inactive in type II neuroblasts (Janssens et al., 2016) (see Chapter 3). Interestingly, in direct contrast to PRC2, reducing the activity of the histone deacetylase HDAC1/Rpd3 results in premature activation of the *erm* immature INP enhancer in type II neuroblasts, and causes them to prematurely differentiate (Janssens et al., 2016) (see Chapter 3). Thus, HDAC1/Rpd3, not PRC2, is required to maintain the repression of *erm* in type II neuroblasts.

How is the transition from a poised to active chromatin state regulated in immature INPs? The core self-renewal transcription factors E(spl)mγ, Dpn, and Klu all directly bind the *erm* immature INP enhancer and maintain its repression in type II neuroblasts through HDAC1/Rpd3 (Figure 4) (Janssens et al., 2016) (see Chapter 3). The type II neuroblast-specific transcription factor PntP1 also directly binds the *erm* immature INP enhancer, priming it for activation in immature INPs (Janssens et al., 2016) (see Chapter 3). In addition, Btd, Sp1 and Dll also likely bind the *erm* immature INP enhancer, potentially cooperating with PntP1 to recruit a histone acetyltransferase (Figure 4), but this remains to be tested (unpublished data). Following asymmetric type

II neuroblast division, selective down-regulation of Klu, Dpn and E(spl)mγ function in immature INPs alleviates Rpd3 mediated repression of the *poised* erm enhancer. This provides a permissive cue to allow accumulation of H3K27ac and rapid activation of Erm expression (Figure 4). Regulation of the *erm* immature INP enhancer offers a novel paradigm to explain the transition from a poised to active chromatin state, in which removing a group of transcriptional repressor proteins, rather than addition of an activator, controls the precise timing of poised enhancer activation in stem cell progeny (Figure 4).

Erm is the first example of a poised gene that is required to restrict the developmental potential of intermediate progenitors and prevent them from reverting to

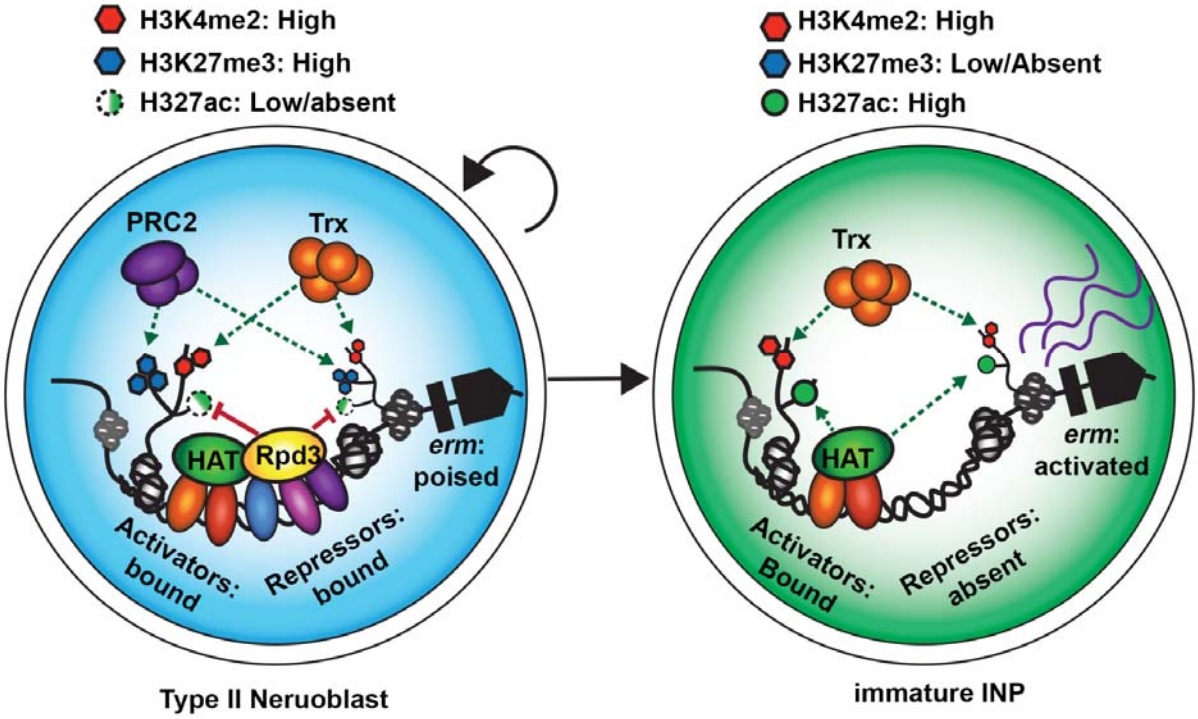

Figure 4: Maintenance of the *erm* locus in a poised chromatin state in type II neuroblasts, and the transition to an active state in their immature INP progeny

aberrantly reacquire a stem cell identity. Once activated, Erm functions as part of a negative feedback circuit, directly binding the promoter of its activator *pntP1* as well as the promoter of *grhO* and repressing their expression in INPs (Janssens et al., 2016) (see Chapter 3). This is consistent with the model that intermediate progenitor commitment requires downregulation of stem cell self-renewal pathways. However, while co-overexpression of PntP1 and GrhO together can enhancer the formation of supernumerary type II neuroblasts in an *erm* hypomorphic mutant background, overexpression of PntP1 and GrhO in a wild-type background does not produce supernumerary neuroblasts (Janssens et al., 2016) (see Chapter 3). Thus, Erm likely down-regulates additional transcriptional activators that function cooperatively with PntP1 and GrhO to promote type II neuroblast self-renewal. This strongly suggests that rapidly activating poised genes directly repress components of the stem cell transcription factor network to ensure stable commitment to a lineage-restricted or differentiated cell-fate in stem cell progeny.

Outlook

Realizing the therapeutic potential of stem cell biology requires an in-depth understanding of the molecular mechanisms controlling their self-renewal as well as the generation of specific differentiated progeny. Extensive investigation of both ES cells and tissue specific stem cells has revealed intricate transcription factor networks balance self-renewal with the capacity to generate more restricted cell types (Figure 1). While distinct stem cell populations are regulated by unique, sometimes partially overlapping collections of transcription factors, common themes underlying their control of self-renewal and differentiation have emerged. In addition to their auto-regulatory and

feedforward targets, these transcription factors also directly regulate genes that promote lineage commitment or differentiation of stem cell progeny. This group of pro-differentiation targets is often maintained in a poised chromatin state by the PcG and TrxG proteins. But how transcription factor networks maintain the poised chromatin state during stem cell self-renewal, and coordinate the transition to an active state in their differentiating progeny remains unclear. Studies of *Drosophila* type II neuroblasts suggest the transition from a poised to active chromatin state is likely regulated by selective downregulation of repressive components of the stem cell transcription factor network to alleviate HDAC1/Rpd3 mediated repression of these poised enhancers (Figure 3 and 4). Once activated, these poised genes likely facilitate lineage-commitment or differentiation by forming a negative feedback circuit, and directly repressing components of the stem cell transcription factor network. Continued investigation of type II neuroblast regulation will likely continue to break new ground in our understanding of poised enhancer regulation and the fundamental mechanisms balancing stem cell self-renewal and differentiation.

The identification of similar poised regulatory circuits in other stem cell lineages will depend on several key advances including: (1) identification of stem cell specific poised genes that are upregulated in their immediate progeny, (2) identification of the functional consequences of stem cell transcription factor binding to poised enhancers (i.e activation versus repression), and (3) identification of the mechanisms that alter the activity of stem cell transcription factor networks in the differentiating progeny. Several steps towards realizing this goal in vertebrate stem cells are already in place. For example, during asymmetric division, mammalian NSCs have been shown to

asymmetrically segregate Staufen2 into their progeny, as well as cargo mRNAs encoding the mammalian homologue of Brat, called Trim32, and another RNA binding protein called Pumilio-2 (Kusek et al., 2012; Vessey et al., 2012). This mechanism in important to promote lineage progression and differentiation, but the direct targets of Trim32 and Pumilio-2 in the progeny of vertebrate NSCs have yet to be identified. In addition, the vertebrate homologue of Erm, *Fezf2*, is bound by PRC2 in both human and mouse ES cells, and the *FezF2* 434 neurogenic enhancer displays chromatin marks indicative of a poised state (Boyer et al., 2006; Eckler et al., 2014; Rada-Iglesias et al., 2011; Shim et al., 2012). This suggests critical aspects of the relay circuit controlling INP commitment in type II neuroblast lineages are likely conserved, and may regulate cell-fate decisions in the mammalian brain. Ultimately, elucidating mammalian poised regulatory circuits will inform clinical efforts to direct stem cells to differentiate into specific cell types for regenerative medicine. Understanding these poised relay circuits will also likely provide insight into the context dependent mechanisms by which oncogenic lesions, such as mutations of PcG and TrxG genes, contribute to stem cell and intermediate progenitor cell derived tumors.

Chapter 2: dFezf/Earmuff restricts progenitor cell potential by attenuating the competence to respond to self-renewal factors

Abstract

Despite expressing stem cell self-renewal factors, intermediate progenitor cells possess restricted developmental potential, which allows them to give rise to exclusively differentiated progeny rather than stem cell progeny. Failure to restrict the developmental potential can allow intermediate progenitor cells to revert into aberrant stem cells that might contribute to tumorigenesis. Insight into stable restriction of the developmental potential in intermediate progenitor cells could improve our understanding of the development and growth of tumors, but the mechanisms remain largely unknown. Intermediate neural progenitors (INPs) generated by type II neural stem cells (neuroblasts) in fly larval brains provide an *in vivo* model for investigating the mechanisms that stably restrict the developmental potential of intermediate progenitor cells. Here, we report that the transcriptional repressor protein Earmuff (Erm) functions temporally after Brain tumor (Brat) and Numb to restrict the developmental potential of uncommitted (immature) INPs. Consistently, endogenous Erm is detected in immature INPs but undetectable in INPs. Erm-dependent restriction of the developmental potential in immature INPs leads to attenuated competence to respond to all known

neuroblast self-renewal factors in INPs. We also identified that the BAF chromatin-remodeling complex likely functions cooperatively with Erm to restrict the developmental potential of immature INPs. Together, these data led us to conclude that the Erm-BAF-dependent mechanism stably restricts the developmental potential of immature INPs by attenuating their genomic responses to stem cell self-renewal factors. We propose that restriction of developmental potential by the Erm-BAF-dependent mechanism functionally distinguishes intermediate progenitor cells from stem cells, ensuring the generation of differentiated cells and preventing the formation of progenitor cell-derived tumor initiating stem cells

Introduction

Tissue-specific stem cells often generate differentiated cell types indirectly through intermediate progenitor cells during normal development and the maintenance of homeostasis (Chang et al., 2012; Franco and Müller, 2013; Homem and Knoblich, 2012; Lui et al., 2011; Ming and Song, 2011; Weng and Lee, 2011). Intermediate progenitor cells possess restricted developmental potential, which allows them to give rise to exclusively differentiated progeny, thereby amplifying the output of stem cells. Accumulating evidence suggests that the acquisition of aberrant stem cell properties by intermediate progenitor cells might be an underlying mechanism that leads to the initiation of tumorigenesis (Haenfler et al., 2012; Komori et al., 2014b; Liu et al., 2011; Schwitalla et al., 2013; Weng et al., 2010; Xiao et al., 2012). Thus, understanding the mechanisms that restrict the developmental potential of intermediate progenitor cells might lead to the discovery of novel strategies to attenuate tumor growth.

The type II neuroblast lineage in the fly larval brain provides an excellent genetic model to investigate the mechanisms that restrict the developmental potential of intermediate progenitor cells *in vivo* (Bello et al., 2008; Boone and Doe, 2008; Bowman et al., 2008; Komori et al., 2014b; Weng et al., 2010; Xiao et al., 2012). A type II neuroblast can be unambiguously identified by the expression of Deadpan (Dpn^{+}) and lack of Asense (Ase^{-}), and divides asymmetrically to self-renew and to generate a newly born immature INP (Figure 6A). While the expression of self-renewal factors is maintained in the type II neuroblast, their expression becomes rapidly extinguished in the newly born immature INP (Xiao et al., 2012). This newly born INP undergoes a stereotypical maturation process during which its developmental potential becomes

stably restricted and the expression of Ase is activated. Upon completing maturation, an INP divides only five to six times to generate exclusively differentiated progeny despite reactivating the expression of all known neuroblast self-renewal factors. Thus, it is likely that the restriction of developmental potential during the maturation of an immature INPs results in attenuated competence to respond to the neuroblast self-renewal factors in an INP, but the mechanisms are not understood.

The neuroblast self-renewal factors include Dpn, Klumpfuss (Klu), Enhancer of split mγ (E(spl)mγ) and Notch (San-Juán and Baonza, 2011; Weng et al., 2010; Xiao et al., 2012; Zacharioudaki et al., 2012; Zhu et al., 2012). Removal of *Notch* function alone or *dpn* and *E(spl)mγ* function simultaneously leads to premature neuroblast differentiation whereas over-expression of any of the neuroblast self-renewal factors in type II neuroblasts leads to massive formation of supernumerary neuroblasts. Unexpectedly, while over-expression of *klu* in Ase^{-} immature INPs driven by the *Erm-Gal4(II)* driver induces a robust supernumerary neuroblast phenotype, over-expression of *klu* in Ase^{+} immature INPs driven by the *Erm-Gal4(III)* failed to induce supernumerary neuroblast formation (Xiao et al., 2012). The expression level of *Erm-Gal4(III)* is approximately 50% of *Erm-Gal(II)* (Janssens and Lee, unpublished observation). However, over-expression of two copies of the *UAS-klu* transgenes driven by two copies of the *Erm-Gal4(III)* driver was not sufficient to induce a supernumerary neuroblast phenotype remotely comparable to over-expression of one copy of the *UAS-klu* transgene driven by one copy of the *Erm-Gal4(II)* driver (Xiao et al., 2012). Although we cannot quantitatively control the exact expression level of the *UAS-klu* transgenes driven by *Erm-Gal4(II)* versus *Erm-Gal4(III)* in these experiments, these results suggest

that Ase^+ immature INPs are significantly less responsive to the expression of neuroblast self-renewal factors than Ase^- immature INPs. Understanding the mechanisms that alter the responsiveness to neuroblast self-renewal factors in Ase^+ immature INPs will provide critical insight into the restriction of developmental potential.

The transcription factor Erm functionally distinguishes an INP from a neuroblast (Weng et al., 2010). Erm encodes an evolutionarily conserved C_2H_2 zinc-finger transcription factor, and the vertebrate orthologs of Erm can activate or repress gene expression in a context dependent manner (Hirata et al., 2006; Weng et al., 2010; Yang et al., 2012). Erm is dispensable for the formation of INPs, but INPs in *erm* null brains spontaneously revert into supernumerary type II neuroblasts. Importantly, restoring *erm* function by over-expressing *erm* or the vertebrate ortholog of *erm* (*fez* or *fezl*) rescued the supernumerary neuroblast phenotype, strongly suggesting that the function of Erm is evolutionarily conserved. Erm suppresses the reversion of INPs by antagonizing Notch signaling (Weng et al., 2010). However, the mechanisms by which Erm restricts the functional output of Notch signaling in INPs are completely unknown. In addition, understanding if Erm might exert a similar regulatory effect on other neuroblast self-renewal factors will provide critical insight into the mechanisms that functionally distinguish an INP from a neuroblast.

In this study, we show that Erm functions as a transcriptional repressor to stably restrict their developmental potential in immature INPs. Erm functions temporally after Brat and Numb in immature INPs to suppress the formation of supernumerary neuroblasts, and endogenous Erm protein is exclusively expressed in immature INPs. Erm-dependent restriction of the developmental potential in immature INPs leads to

attenuated competence to respond to all known neuroblast self-renewal factors in INPs. Thus, the Erm-dependent mechanism stably and globally restricts the genomic response to neuroblast self-renewal factors. We identified that the BAP chromatin-remodeling complex also functions temporally after Brat and Numb to restrict the developmental potential of immature INPs. Importantly, over-expression of a dominant negative form of Brm strongly enhanced the supernumerary neuroblast phenotype in *erm* hypomorphic brains. Thus, we propose that Erm and the BAP complex function cooperatively to stably restrict the developmental potential of immature INPs and to functionally distinguish an INP from a neuroblast.

Results

Erm functions in immature INPs to suppress the formation of supernumerary type II neuroblasts

We hypothesized that restriction of the developmental potential in immature INPs alters the responsiveness to neuroblast self-renewal factors, preventing INPs from aberrantly reverting into supernumerary neuroblasts in response to the re-activation of neuroblast self-renewal factors. We used the *brat*$^{DG19310/11}$ hypomorphic genetic background to investigate the mechanisms that restrict the developmental potential of immature INPs (Komori et al., 2014b; Xiao et al., 2012). Briefly, Brat prevents the formation of supernumerary neuroblasts by acting at two temporally distinct stages during maturation (Figure 6A). First, Brat prevents a newly born immature INP, which lacks the expression of both *Erm-Gal4(II)* and Ase (Figure 6A, 5D), from reverting into a supernumerary neuroblast by rapidly extinguishing the function of neuroblast self-renewal factors. Newly born immature INPs mutant for *brat* rapidly revert into supernumerary neuroblasts instead of progressing through maturation, and removing the function of the neuroblast self-renewal gene *klu* or *dpn* suppressed the supernumerary neuroblast phenotype (Figure 5 A-C) (Xiao et al., 2012). Second, Brat continues to play an important role in the Ase^{-} immature INP, which shows the expression of *Erm-Gal4(II)* (Figure 6A), to promote the maturation of immature INPs. We confirmed that the temporal expression pattern of *Erm-Gal4(II)* and *Erm-Gal4(III)* is not altered in *brat*$^{DG19310/11}$ brains (Figure 5D-G). Restoring *brat* function in Ase^{-} immature INPs suppressed the supernumerary neuroblast phenotype in *brat*$^{DG19310/11}$ brains while

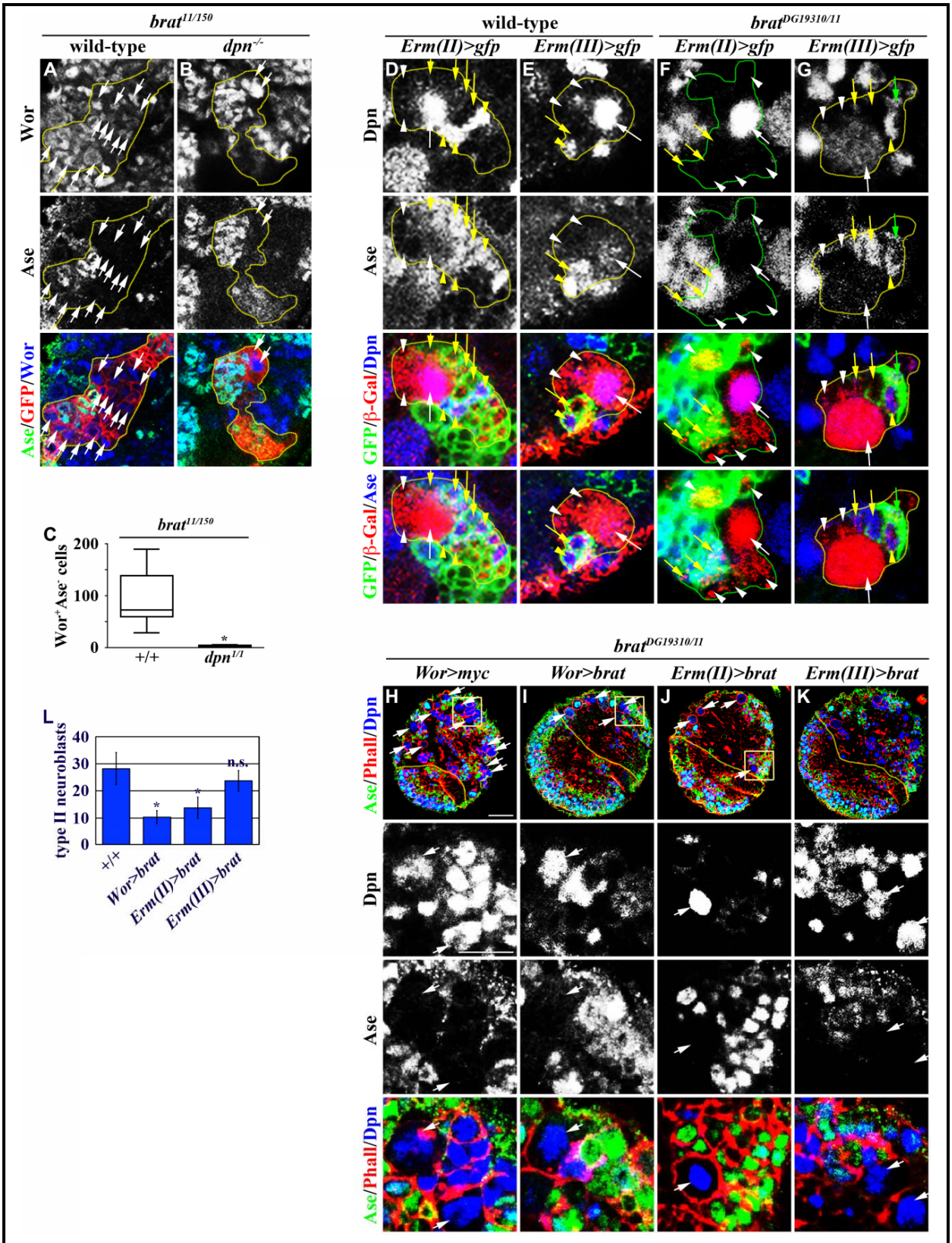

Figure 5: Brat functions in the newly born immature INP or Ase$^-$ immature INP to suppress the formation of supernumerary neuroblasts. *(legend continued on next page)*

Figure 5 (continued): (A-C) Removal of *dpn* function suppressed the supernumerary neuroblast phenotype in *brat* null brains. (C) The quantification of supernumerary neuroblasts in wild-type or *dpn* mutant type II neuroblast clones in *brat* null brains. (D-G) The expression pattern of *Erm-Gal4(II)* and *Erm-Gal4(III)* appeared indistinguishable between wild-type and *brat* hypomorphic brains. wild-type or $brat^{DG19310/11}$ larvae carrying the *UAS-mCD8-GFP*, *hs-flp*, Act-FRT-FRT-lacZ, *Erm-Gal4 (II)* or *Erm-Gal4(III)* transgenes were genotyped at hatching, and heat-shocked at 37°C for 90 minutes at 24 hours after hatching to induce the lineage clones. Larvae were dissected and processed for immunofluorescent staining at 96 hours after hatching. The specificity of *Erm-Gal4(II)* or *Erm-Gal4(III)* expression was examined in the β–Gal-marked lineage clones (outlined in yellow) derived from single type II neuroblasts in wild-type or $brat^{DG19310/11}$ brains. (H-L) Over-expression of *brat* in neuroblasts or in Ase^- immature INPs suppressed the supernumerary neuroblast phenotype in *brat* hypomorphic brains, but over-expression of *brat* in Ase^+ immature INPs had no effect. The high magnification image of the boxed area in the low magnification image is shown below. Scale bars, 40 μm in the low magnification image and 10 μm in the high magnification image. (L) The quantification of the average number of type II neuroblasts per brain lobe of the indicated genotypes. **Key:** White arrow: type II neuroblast. White arrowhead: newly born immature INP and Ase^- immature INP. Yellow arrow: Ase^+ immature INP. Yellow arrowhead: INP. The dotted yellow line separates the brain from the optic lobe (OL). Single asterisks indicate a statistically significant (p-value <0.05) difference between the marked genotype and the control genotype in the same bar graph as determined by the Student's t-test. n.s. indicates that the difference is not statistically significant.

restoring *brat* function in Ase^+ immature INPs had no effects (Figure 5H-L). Thus, Brat functions in the newly born immature INP and the Ase^- immature INP to prevent supernumerary neuroblast formation.

The unstable nature of Ase^- immature INPs provides an excellent *in vivo* system to elucidate the mechanisms that restrict developmental potential during the maturation of immature INPs. We identified the *erm* gene as a genetic enhancer of *brat* by screening for haploinsufficient loci that further exacerbate the supernumerary neuroblast phenotype in $brat^{DG19310/11}$ brains. While the heterozygosity of *erm* alone did not lead to a supernumerary neuroblast phenotype, it doubled the number of supernumerary neuroblasts in $brat^{DG19310/11}$ brains (Figure 6B-C). To examine whether the enhancement of the supernumerary neuroblast phenotype in $brat^{DG19310/11}$ brains by the heterozygosity of *erm* originated from Ase^- or Ase^+ immature INPs, we induced βgal-marked lineage clones derived from either a single Ase^+ immature INP or an INP via FRT-mediated

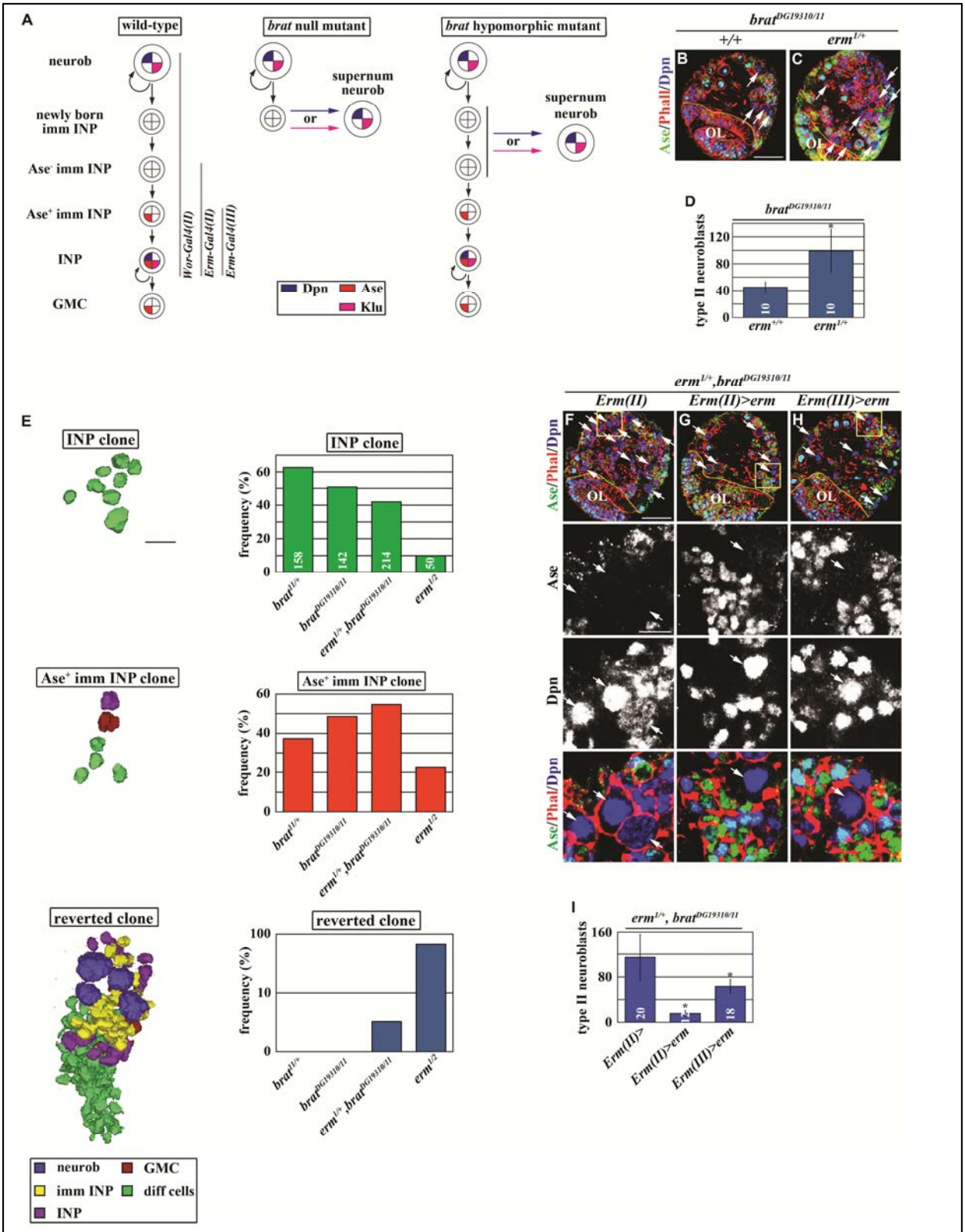

Figure 6: Erm functions in immature INPs to suppress supernumerary type II neuroblast formation *(legend continued on next page)*

Figure 6 (continued): (A) A summary of the *brat* mutant phenotype and the expression patterns of the *Gal4* drivers used in this study. neurob: neuroblast. Imm INP: immature INP. GMC: ganglion mother cell. (B-D) The heterozygosity of *erm* enhances the supernumerary neuroblast phenotype in $brat^{DG19310/11}$ brains. Phalloidin (Phall) marks the cell cortex. Scale bars, 40 μm. (D) Quantification of the average number of type II neuroblast ($Dpn^{+}Ase^{-}$) per brain lobe in larvae of the indicated genotypes. Error bars indicate s.d. (E) Reduction in *erm* function increases the frequency of the formation of supernumerary neuroblasts originating from the Ase^{-} immature INPs or INPs. Cell identity in β-Gal marked lineage clones were induced and analyzed following the scheme shown in Fig. S2. INP clone: a clone derived from a single INP. Ase^{+} imm INP clone: a clone derived from a single Ase^{+} immature INP. reverted clone: a clone containing supernumerary neuroblasts. The bar graphs show the frequency of clones observed in larval brains of the indicated genotype, and the total number of clones used to determine the frequency of the clones is shown in the bar graph for the INP clone. (F-I) Restoring *erm* function in the Ase^{-} immature INPs or Ase^{+} immature INPs rescues the enhancement of the supernumerary neuroblast phenotype in $brat^{DG19310/11}$ brains induced by the heterozygosity of *erm*. The high magnification image of the boxed area in the low magnification image is shown below. Scale bars, 40 μm in the low magnification image and 10 μm in the high magnification image. (I) The quantification of the average number of type II neuroblasts per brain lobe of the indicated genotypes. Key for all figures: The dotted yellow line separates the brain from the optic lobe (OL). White arrow: type II neuroblast. White arrowhead: newly born immature INP and Ase^{-} immature INP. Yellow arrow: Ase^{+} immature INP. Yellow arrowhead: INP. Single asterisks indicate a statistically significant (p-value <0.05) difference between the marked genotype and the control genotype in the same bar graph, as determined by the Student's t-test. n.s. indicates that the difference is statistically insignificant.

recombination (Figure 7A). Briefly, first instar larvae carrying a *UAS-flipase* transgene and a flip-out reporter transgene under the control of *Erm-Gal4(III)* and $Tub\text{-}Gal80^{ts}$ were heat-shocked at 30°C for 0-12 hours (Figure 7B). We determined that in the absence of heat-shocking, the leaky basal level of *Erm-Gal4(III)* expression was sufficient to induce an average of 3 clones per lobe in the control brain (Figure 7C). The low frequency of clone induction under this condition is ideal for analyzing the identity of cells in an individual clone. We only recovered Ase^{+} immature INP clones, which contain one INP per clone, GMCs and differentiated cells, and INP clones, which contain only differentiated cells, in control $brat^{DG19310/+}$ or $erm^{1/+}$ brains (Figure 6E). This is consistent with a wild-type INP maintaining restricted developmental potential. In

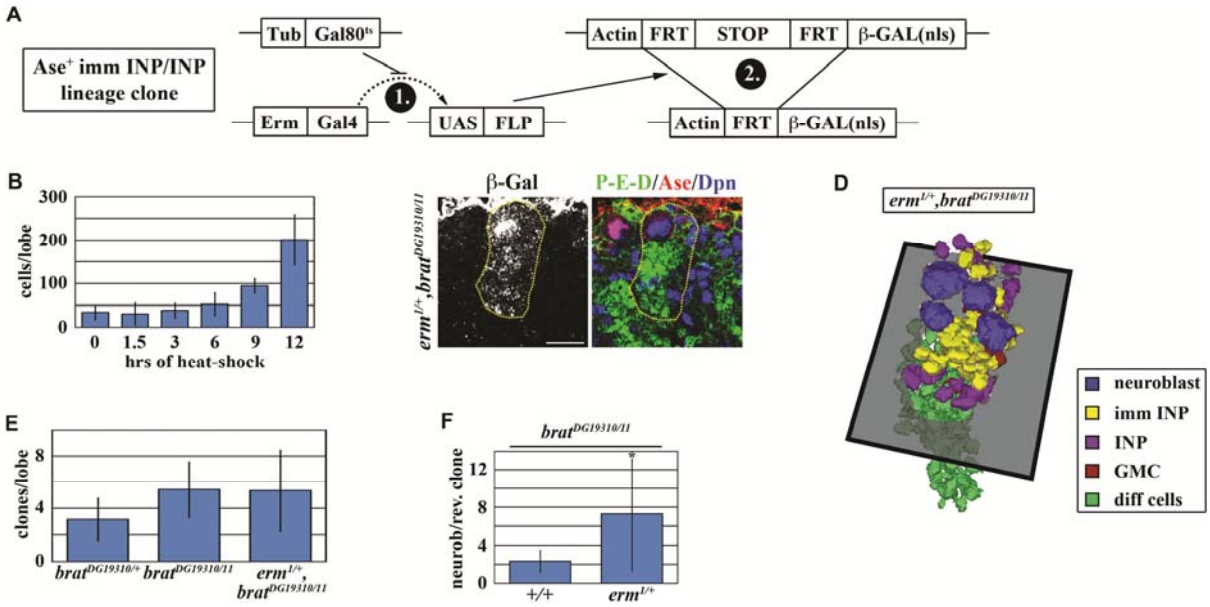

Figure 7: Empirical determination of the condition required for inducing a low number of clones derived from single Ase^{+} immature INPs or INPs per brain lobe. (A) The scheme used to induce clones derived from single Ase^{+} immature INPs or INPs. (B) The total number of cells per clone under the conditions indicated. (C) The image of a reverted clone derived from a single Ase^{+} immature INP or an INP in *brat* hypomorphic brains heterozygous for *erm*. (D) A three-dimensional reconstruction of a reverted clone. (E) The total number of clones per brain lobe induced by the basal leaky expression of *Erm-Gal4(III)* at 25^{o}C in the genotype indicated. (F) The average number of supernumerary neuroblasts in the reverted clones in *brat*$^{DG19310/11}$ brains or *brat*$^{DG19310/11}$ brains heterozygous for *erm*.

brat$^{DG19310/11}$ brains, more than 99% of the clones were either Ase^{+} immature INP clones or INP clones, and only 0.7% of the clones contained supernumerary neuroblasts (the reverted clone) (Figure 6E). This result is consistent with Brat mainly functioning in the newly born immature INP and the Ase^{-} immature INP to prevent the formation of -supernumerary neuroblasts. Importantly, 3.5% of the clones in *brat*$^{DG19310/11}$ brains heterozygous for *erm* were the reverted clones, and these clones consistently possessed more supernumerary neuroblasts than the reverted clones in *brat*$^{DG19310/11}$ brains (Figure 6E and 7D-F). Thus, heterozygosity of *erm* increases the frequency that Ase^{+} immature INPs or INPs revert into neuroblasts in *brat*$^{DG19310/11}$ brains. The occurrence of the reverted clones increased dramatically in *erm* null brains, consistent

with *erm* playing a critical role suppressing supernumerary neuroblast formation (Figure 6E). These data strongly suggest that *erm* functions temporally after *brat* in immature INPs to prevent supernumerary neuroblast formation.

We tested whether *erm* indeed functions temporally after *brat* in immature INPs by restoring *erm* function in either Ase^- or Ase^+ immature INPs in $brat^{DG19310/11}$ brains heterozygous for *erm*. Consistent with our hypothesis, restoring *erm* function in either Ase^- or Ase^+ immature INPs rescued the enhancement of the supernumerary neuroblast phenotype in $brat^{DG19310/11}$ brains induced by the heterozygosity of *erm* (Figure 6F-I). Thus, we conclude that *erm* functions temporally after *brat* in immature INPs to suppress the formation of supernumerary neuroblasts.

Erm functions temporally after Brat and Numb in immature INPs

We assessed the expression pattern of endogenous Erm to confirm that *erm* indeed functions in Ase^- and Ase^+ immature INPs. We generated a transgenic fly line carrying a BAC clone containing the entire *erm* genomic locus fused in frame to a RFP epitope (*erm-rfp*). In the type II neuroblast lineage, the expression of *erm*-RFP was detectable in immature INPs located immediately adjacent to the type II neuroblast but became rapidly down-regulated in INPs (Figure 8A). The relative position of these Erm-expressing immature INPs to the type II neuroblast strongly suggests that endogenous Erm is expressed in Ase^- immature INPs. To unambiguously verify the identity of cells where endogenous Erm is expressed, we generated a specific antibody against the Erm protein. Co-immunolocalization using specific antibodies against Ase and Erm confirmed that endogenous Erm was absent from the newly born immature INP but became detectable in both Ase^- and Ase^+ immature INPs (Figure 8C). These data are

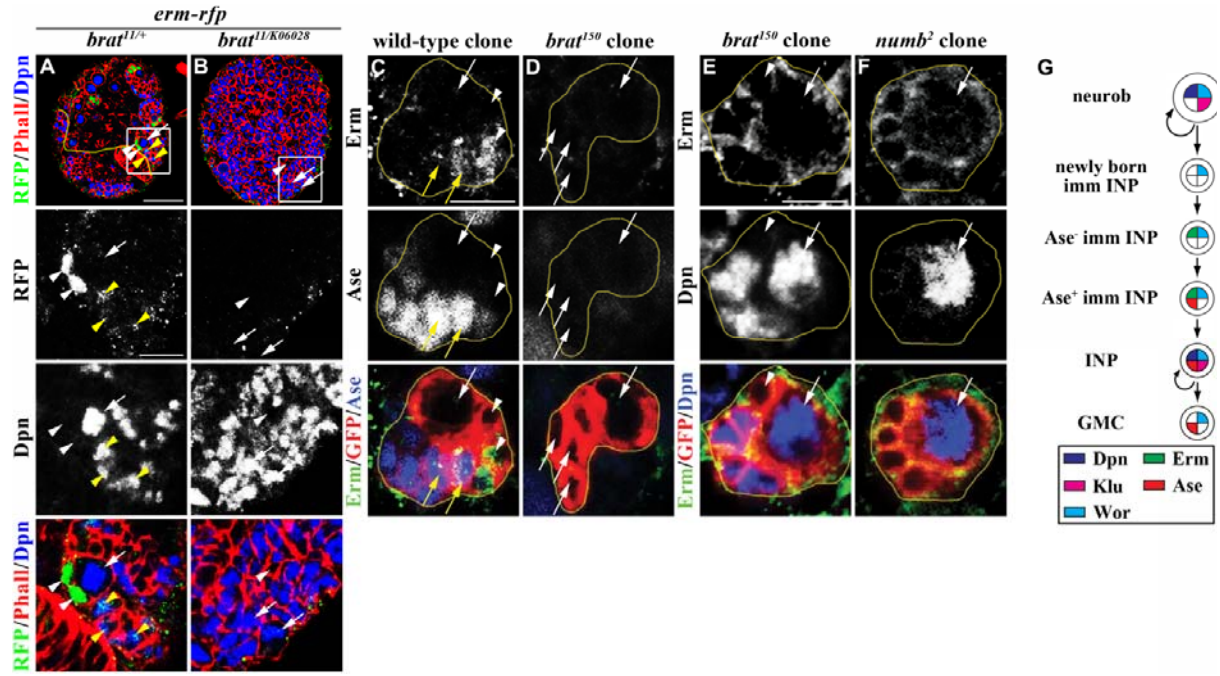

Figure 8: Erm is exclusively expressed in Ase$^-$ and Ase$^+$ immature INPs. (A-B) The expression of *erm-rfp* is detected in immature INPs in wild-type brains but undetectable in *brat* null brains. The high magnification image of the boxed area in the low magnification image is shown below. Scale bars, 40 μm in the low magnification image and 10 μm in the high magnification image. (C-D) Endogenous Erm is undetectable in the newly born immature INP. The GFP-marked lineage clones are outlined in yellow. Scale bar, 10 μm. (E-F) Erm is undetectable in *brat* or *numb* null mutant clones. The GFP-marked lineage clones were outlined in yellow. Scale bar,10 μm. (G) A cartoon summarizes the expression pattern of Erm in the type II neuroblast lineage.

consistent with *erm* functioning in Ase$^-$ and Ase$^+$ immature INPs to restrict developmental potential.

We net examined the expression pattern of endogenous Erm in *brat* null brains to confirm that *erm* indeed functions temporally after *brat* in immature INPs. Indeed, the expression of *erm*-RFP was completely absent from the *brat* null brain, and endogenous Erm was undetectable in the newly born immature INP in *brat* null type II neuroblast clones (Figure 8B, D-E). Thus, these results confirm that Erm functions temporally after Brat in immature INPs.

Numb functions in parallel to Brat to prevent the formation of supernumerary neuroblasts (Xiao et al., 2012). A *numb* null type II neuroblast clone contained many supernumerary neuroblasts and showed an aberrant accumulation of immature INPs lacking Ase expression. Importantly, we never detected the expression of Erm in immature INPs lacking Ase expression in *numb* null clones, indicating that these cells are newly born immature INPs (Figure 8F). Thus, a *numb* null clone aberrantly accumulates newly born immature INPs. Taken together, these data indicate that Erm functions temporally after Brat and Numb to restrict the developmental potential of immature INPs.

Erm restricts the developmental potential of immature INPs by repressing gene transcription

Because the vertebrate orthologs of Erm can activate or repress gene expression in a context dependent manner (Hirata et al., 2006; Yang et al., 2012), we investigated whether Erm restricts developmental potential by activating or repressing gene expression. While mis-expression of wild-type Erm in neuroblasts induced premature differentiation of all eight type II neuroblasts in a larval brain lobe, mis-expression of Erm^{zf} (containing only the zinc-fingers) had no effect (Figure 9A-B). Thus, the N-terminus of the Erm protein is essential to confer its function in restricting developmental potential. We fused the Engrailed repressor domain to Erm^{zf} converting it to act solely as a transcriptional repressor (ERD-Erm^{zf}) or the VP16 transactivation domain to Erm^{zf} converting it to act solely as a transcriptional activator (VP16-Erm^{zf}) (Figure 9A). Mis-expression of ERD-Erm^{zf} in neuroblasts also led to premature differentiation of type II neuroblasts whereas mis-expression of VP16-Erm^{zf} resulted in a mild increase in type II

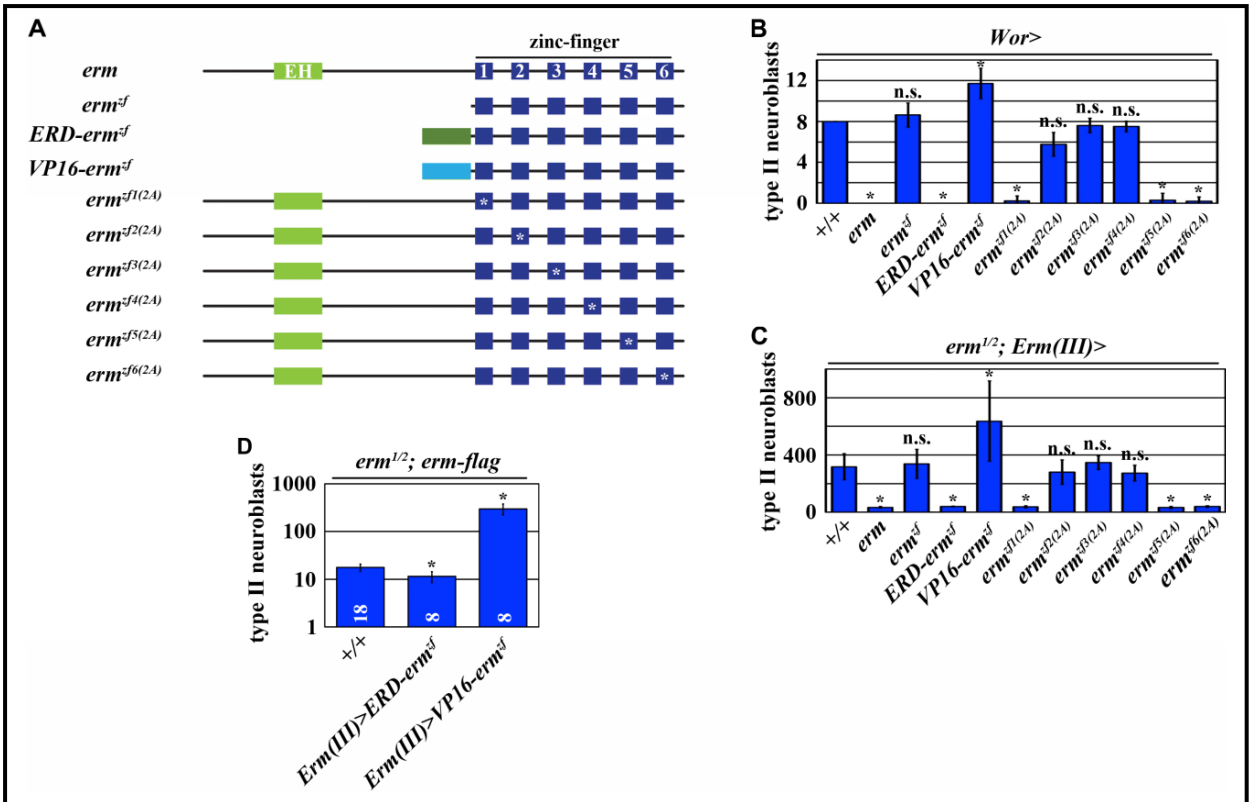

Figure 9: Erm restricts the developmental potential in immature INPs by repressing gene transcription. (A) Schematics of the *UAS-erm* transgenes used in this series of experiments. ERD: engrailed repressor domain. VP16: transactivation domain. zf: zinc-finger. (B) Over-expression of *erm* induces premature neuroblast differentiation by repressing gene transcription. Third instar larval brains of the indicated genotype were stained for Dpn, Ase and Phall, and the quantification of total type II neuroblasts ($Dpn^{+}Ase^{-}$) per brain lobe is shown. (C) Restoring *erm* expression rescues the supernumerary neuroblast phenotype in *erm* null brains by repressing gene transcription. Third instar larval brains of the indicated genotypes were stained for Dpn, Ase and Phall, and the quantification of total type II neuroblasts ($Dpn^{+}Ase^{-}$) per brain lobe is shown. (D) Over-expression of *VP16-erm^{zf}* exerts a dominant negative effect and further exacerbates the supernumerary neuroblast phenotype in *erm* hypomorphic brains. Third instar larval brains of the indicated genotypes were stained for Dpn, Ase and Phall, and the quantification of total type II neuroblasts ($Dpn^{+}Ase^{-}$) per brain lobe is shown.

neuroblasts (Figure 9B). These data strongly suggest that Erm restricts developmental potential by acting as a transcriptional repressor. We tested this hypothesis by taking two complementary approaches. First, we tested whether over-expression of the *erm* transgene can rescue the supernumerary neuroblast phenotype in *erm* null brains. Restoring wild-type Erm function driven by the *Erm-Gal4(III)* driver rescued the

supernumerary neuroblast phenotype in *erm* null brains (Figure 9C) (Weng et al., 2010). Importantly, over-expression of ERD-Erm^{zf} under the identical conditions also rescued the supernumerary neuroblast phenotype in *erm* null brains, but over-expression of VP16-Erm^{zf} enhanced the supernumerary neuroblast phenotype (Figure 9C). Second, we tested whether over-expression of the *erm* transgene can rescue the supernumerary neuroblast phenotype in an *erm* hypomorphic genetic background (*erm$^{1/2}$; erm-flag*) (Figure 9D). We confirmed that the temporal expression pattern of *Erm-Gal4(III)* is not altered in *erm* hypomorphic brains (data not shown). Consistently, over-expression of ERD-Erm^{zf} driven by the *Erm-Gal4(III)* driver rescued the supernumerary neuroblast phenotype in *erm* hypomorphic brains, but over-expression of VP16-Erm^{zf} enhanced the supernumerary neuroblast phenotype (Figure 9D). Together, these data led us to conclude that Erm restricts the developmental potential in immature INPs by acting as a transcriptional repressor, and that VP16-Erm^{zf} can exert a dominant-negative effect on the restriction of developmental potential

We next examined which C_2H_2 zinc-finger elicits the function of Erm in restricting developmental potential. We generated the *UAS-erm$^{zf(2A)}$* transgenes that encode Erm transgenic proteins containing substitutions of alanine for cysteine in individual zinc-fingers (Figure 9A). Mis-expression of *erm$^{zf2(2A)}$*, *erm$^{zf3(2A)}$* or *erm$^{zf4(2A)}$* failed to induce premature differentiation of type II neuroblasts in wild-type brains and failed to rescue the supernumerary neuroblast phenotype in *erm* null brains (Figure 9B-C). By contrast, mis-expression of *erm$^{zf1(2A)}$*, *erm$^{zf5(2A)}$* or *erm$^{zf6(2A)}$* induced premature differentiation of type II neuroblasts and rescued the supernumerary neuroblast phenotype in *erm* null brains (Figure 9B-C). Thus, the zinc-finger 2-4 are essential to confer Erm function.

Together, we conclude that Erm restricts the developmental potential in immature INPs by repressing gene transcription through the zinc-finger 2-4.

Erm-dependent restriction of the developmental potential in immature INPs leads to attenuated competence to respond to Klu in INPs

To begin investigating the mechanisms by which Erm restricts the developmental potential of immature INPs, we examined whether over-expression of *erm* can substitute for the function of *brat* and suppress the supernumerary neuroblast phenotype in $brat^{DG19310/11}$ brains. Indeed, over-expression of *erm* in Ase^{-} immature INPs efficiently suppressed the supernumerary neuroblast phenotype in $brat^{DG19310/11}$ brains, but over-expression of *erm* in Ase^{+} immature INPs cannot (Figure 10A-C). These results strongly suggest that *brat* and *erm* suppress supernumerary neuroblast formation by regulating similar downstream mechanisms. Brat suppresses supernumerary neuroblast formation by antagonizing Klu (Xiao et al., 2012). Similar to over-expression of *klu* in wild-type brains, mis-expression of *klu* in Ase^{-} immature INPs in $brat^{DG19310/11}$ brains led to supernumerary neuroblast formation, but mis-expression of *klu* in Ase^{+} immature INPs had no effect (Figure 10D). The inefficiency in inducing supernumerary neuroblasts by mis-expression of *klu* in Ase^{+} immature INPs correlates with Erm mainly functioning in Ase^{+} immature INPs to restrict developmental potential. Thus, we hypothesized that Erm restricts developmental potential by antagonizing Klu function. Consistently, co-expression of *erm* completely suppressed supernumerary neuroblast formation induced by mis-expression of *klu* in Ase^{-} immature INPs in wild-type brains (Figure 10D-F). Furthermore, while mis-expression of $VP16\text{-}erm^{zf}$ or *klu* alone in Ase^{+} immature INPs did not have any effect, co-expression of $VP16\text{-}erm^{zf}$ and

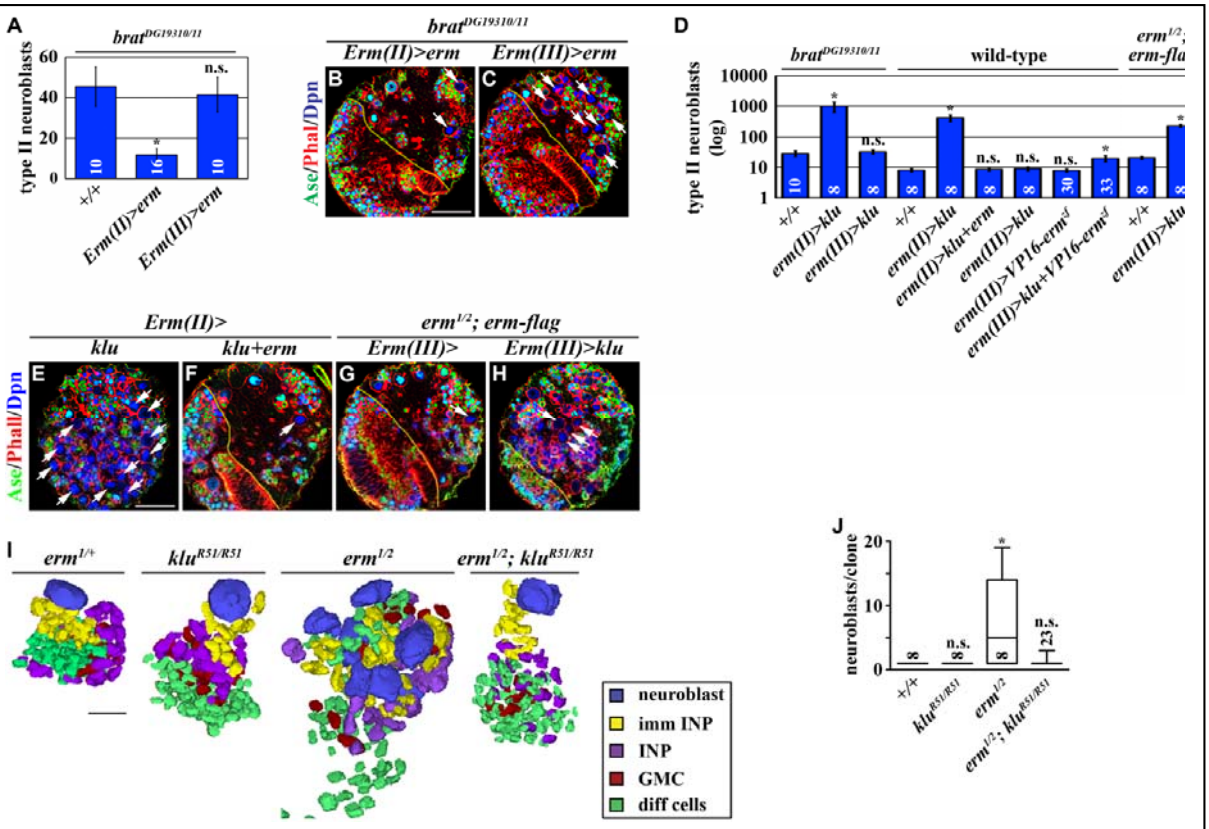

Figure 10: Erm-dependent restriction of developmental potential in immature INPs leads to attenuated competence to respond to Klu in INPs. (A-C) Over-expression of *erm* in Ase$^-$ immature INPs can suppress the supernumerary neuroblast phenotype in *brat* hypomorphic brains. (A) The quantification of total type II neuroblasts (Dpn$^+$Ase$^-$) per brain lobe of the indicated genotypes. Scale bar, 40 μm. (D-H) Co-expression of *erm* can suppress the supernumerary neuroblast phenotype induced by mis-expression of *klu*. (D) The quantification of total type II neuroblasts (Dpn$^+$Ase$^-$) per brain lobe of the indicated genotypes. Scale bar, 40 μm. (I-J) Removing *klu* function suppresses supernumerary neuroblast formation in *erm* null brains. (I) Three-dimensional reconstructed images of the clones of the genotype indicated. Third instar larval brains carrying GFP-marked mosaic clones derived from single neuroblasts of the genotype indicated were stained for GFP, Dpn, Ase, Pros and Elav. Scale bar,10 μm. (J) The quantification of total type II neuroblasts (Dpn$^+$Ase$^-$) per clone for the indicated genotypes.

klu induced supernumerary neuroblast formation (Figure 10D). This result indicates the downstream mechanisms regulated by Erm can act cooperatively with Klu to induce supernumerary neuroblast formation. Finally, mis-expression of *klu* in Ase$^+$ immature INPs also enhanced supernumerary neuroblast formation in *erm* hypomorphic brains

(Figure 10D, G-H). Together, these data strongly suggest that Erm restricts developmental potential by antagonizing Klu function.

We directly tested whether removing *klu* function can suppress supernumerary neuroblast formation in *erm* null brains. In *erm* null brains, GFP-marked mosaic clones derived from single type II neuroblasts contained multiple neuroblasts per clone (Figure 10I-J). Clonally removing *klu* function for 72 hours was not sufficient to induce premature differentiation of type II neuroblasts (Berger et al., 2012; Xiao et al., 2012). By contrast, clonally removing *klu* function strongly suppressed supernumerary neuroblasts in *erm* null brains (Figure 10I-J). Thus, *klu* is required for supernumerary neuroblast formation in *erm* null brains. Since Klu expression is extinguished in immature INPs but becomes re-activated in INPs (Xiao et al., 2012), INPs are most likely the cells of origin for supernumerary neuroblasts in *erm* null brains. Thereby, Erm most likely restricts developmental potential by indirectly antagonizing Klu function. We conclude that Erm-dependent restriction of the developmental potential in immature INPs leads to attenuated competence to respond to Klu in INPs.

Erm-dependent restriction of the developmental potential in immature INPs leads to attenuated competence to respond to Dpn and E(spl)mγ

Similar to *klu*, *dpn* is also required for supernumerary neuroblast formation in *brat* null brains (Figure 5A-C). In addition, mis-expression of *dpn* in Ase^{+} immature INPs also led to a significantly milder supernumerary neuroblast phenotype in wild-type as well as in $brat^{DG19310/11}$ brains as compared to mis-expression in Ase^{-} immature INPs (Figure 11A). These results prompted us to test whether Erm restricts developmental potential by antagonizing Dpn function. Consistent with our hypothesis, co-expression of *erm*

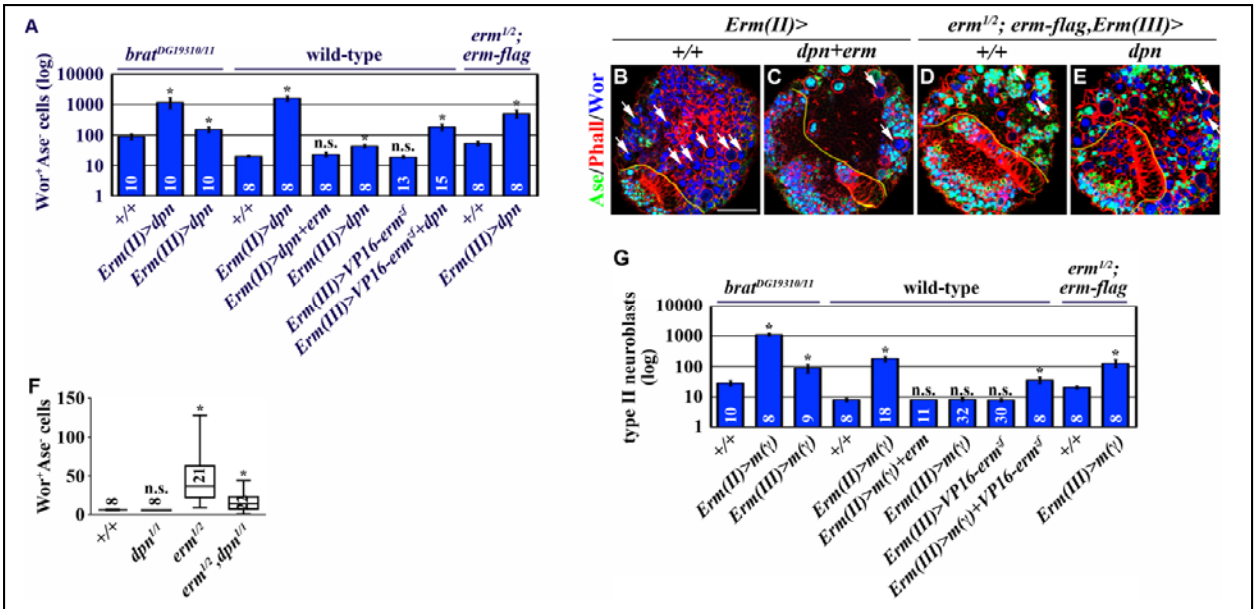

Figure 11: Erm-dependent restriction of developmental potential in immature INPs leads to attenuated competence to respond to Dpn and E(spl)mγ in INPs. (A-E) Co-expression of *erm* can suppress the supernumerary neuroblast phenotype induced by mis-expression of *dpn*. (A) The quantification of total Wor^{+}Ase^{-} cells (including type II neuroblasts and Ase^{-} immature INPs) per brain lobe of the indicated genotypes. Scale bar, 40 μm. (F) Removing *dpn* function suppresses supernumerary neuroblast formation in *erm* null brains. The quantification of total Wor^{+}Ase^{-} cells (including type II neuroblasts and Ase^{-} immature INPs) per clone for the indicated genotypes. Third instar larval brains carrying GFP-marked mosaic clones derived from single neuroblasts of the indicated genotypes were stained for GFP, Wor, Ase, Pros and Elav. (G) Co-expression of *erm* can suppress the supernumerary neuroblast phenotype induced by mis-expression of *E(spl)mγ*. The quantification of total type II neuroblasts (Dpn^{+}Ase^{-}) per clone for the indicated genotypes.

completely suppressed supernumerary formation induced by mis-expression of *dpn* in Ase^{-} immature INPs in wild-type brains (Figure 11A-C). Furthermore, co-expression of *VP16-erm^{zf}* and *dpn* in Ase^{+} immature INPs led to a significant increase in supernumerary neuroblasts as compared to mis-expression of *dpn* alone under the identical conditions (Figure 11A). Finally, mis-expression of *dpn* in Ase^{+} immature INPs enhanced supernumerary neuroblast formation in *erm* hypomorphic brains (Figure 11A,D-E). Together, these data strongly suggest that Erm restricts developmental potential by antagonizing Dpn function. Importantly, while not affecting the maintenance of type II neuroblasts (Zacharioudaki et al., 2012; Zhu et al., 2012) (Figure 11F),

clonally removing the function of *dpn* strongly suppressed the supernumerary neuroblast phenotype in *erm* null brains (Figure 11F). Because Dpn expression is extinguished in immature INPs but becomes re-activated in INPs (Xiao et al., 2012), INPs are most likely the cells of origin for supernumerary neuroblasts in *erm* null brains. Thus, Erm-dependent restriction of the developmental potential in immature INPs leads to attenuated competence to respond to Dpn in INPs.

A recent study showed that E(spl)mγ also functions as a neuroblast self-renewal factor (Zacharioudaki et al., 2012). Similar to *klu* and *dpn*, co-expression of *erm* strongly suppressed supernumerary formation induced by mis-expression of *E(spl)mγ* in Ase^{-} immature INPs in wild-type brains (Figure 11G). In addition, co-expression of *VP16-erm*^{zf} and *E(spl)mγ* in Ase^{+} immature INPs induced supernumerary neuroblasts, and mis-expression of *E(spl)mγ* in Ase^{+} immature INPs enhanced supernumerary neuroblast formation in *erm* hypomorphic brains (Figure 11G). Because E(spl)mγ expression is extinguished in immature INPs but becomes re-activated in INPs (Anhezini De Araujo and Lee, unpublished observation), E(spl)mγ also likely contributes to the reversion of INPs into supernumerary neuroblasts in *erm* null brains. Taken together, Erm-dependent restriction of the developmental potential in immature INPs leads to attenuated competence to respond to all known neuroblast self-renewal factors in INPs.

The BAP complex suppresses supernumerary neuroblast formation by restricting the developmental potential of immature INPs

To elucidate the mechanisms by which Erm restricts the developmental potential of immature INPs, we characterized additional haploinsufficient loci that enhanced the

supernumerary neuroblast phenotype in *brat*$^{DG19310/11}$ brains. We identified that the *brm*, *mor* and *osa* genes act as genetic enhancers of *brat*. Specifically, while the heterozygosity of *brm*, *mor* or *osa* did not have effects on the type II neuroblast lineage in wild-type brains, the heterozygosity of any of these three genes enhanced the supernumerary neuroblast phenotype in *brat*$^{DG19310/11}$ brains (Figure 12A-E). Since *brm*, *mor* and *osa* encode the core components of the BAF chromatin-remodeling complex (Carrera et al., 2008; Mohrmann et al., 2004), we hypothesize that the BAF complex functions in immature INPs to suppress supernumerary neuroblast formation. Consistently, over-expression of a *UAS-brm*^{DN} transgene, which encodes a dominant-negative form of Brm, specifically in Ase^{-} immature INPs enhanced the supernumerary neuroblast phenotype in *brat*$^{DG19310/11}$ brains (Figure 12F-I). These data support our hypothesis that the BAF complex functions temporally after Brat in immature INPs to suppress supernumerary neuroblast formation. Consistent with the observations from a previous study (Neumüller et al., 2011), we confirmed that knocking down or removing the function of *brm*, *osa* or *mor* led to supernumerary neuroblast formation (data not presented). We ruled out the possibility that supernumerary neuroblasts induced by the loss of the BAP complex function arise from symmetric neuroblast division because a mitotic *osa* mutant type II neuroblast displayed normal establishment and maintenance of the apical-basal cortical polarity (data not presented). Together, these results strongly suggest that the BAF complex functions temporally after Brat in immature INPs to prevent supernumerary neuroblast formation.

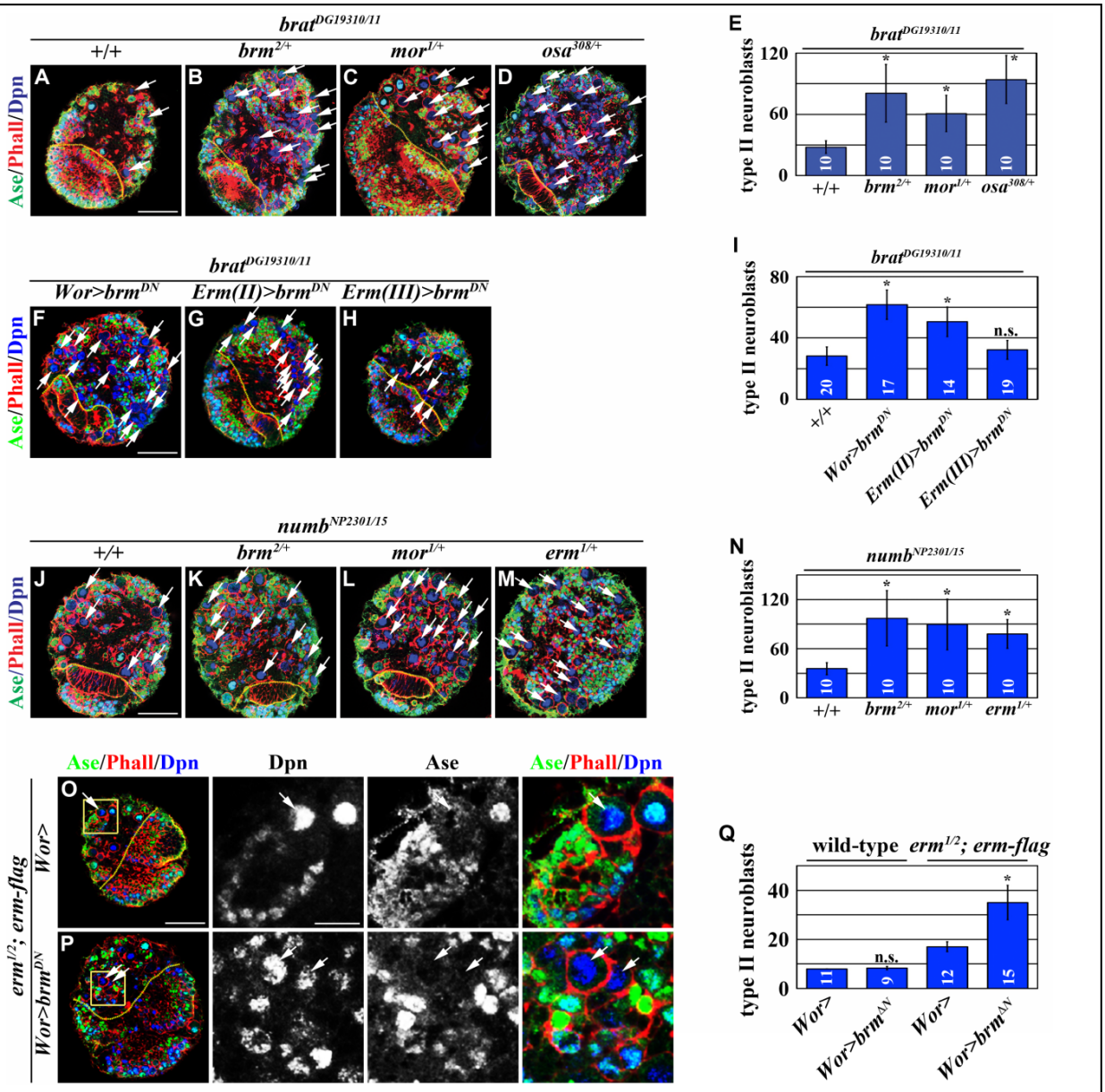

Figure 12: The BAP complex functions cooperatively with Erm to restrict the developmental potential in immature INPs. (A-E) Reduced function of the BAP complex enhances the supernumerary neuroblast phenotype in *brat* hypomorphic brains. (E) The quantification of total type II neuroblasts per lobe for the indicated genotypes. Scale bar, 40 μm.(F-I) Reducing *brm* function in Ase$^-$ immature INPs enhances the supernumerary neuroblast phenotype in *brat* hypomorphic brains. (I) The quantification of total type II neuroblasts per lobe for the indicated genotypes. Scale bar, 40 μm. (J-N) Reducing the function of the BAP complex or *erm* enhances the supernumerary neuroblast phenotype in *numb* hypomorphic brains. (N) The quantification of total type II neuroblasts per lobe for the indicated genotypes. Scale bar, 40 μm.(O-Q) Reducing *brm* function enhances the supernumerary neuroblast phenotype in *erm* hypomorphic brains. (O-P) The high magnification image of the boxed area in the low magnification image is shown below. Scale bars, 40 μm in the low magnification image and 10 μm in the high magnification image.(Q) The quantification of total type II neuroblasts per lobe for the indicated genotypes.

We next tested whether the BAF complex also functions temporally after Numb to suppress supernumerary neuroblast formation. Similar to Brat, Numb also functions to prevent the newly born immature INP from aberrantly reverting into a supernumerary neuroblast. However, the supernumerary neuroblast phenotype displayed by a *numb* null type II neuroblast clone is too severe to test gene function in immature INPs (Xiao et al., 2012). By contrast, a $numb^{NP2301/15}$ hypomorphic brain lobe, which contained 35.7 ± 7.5 type II neuroblasts and many INPs, provides a sensitized genetic background for testing gene function in immature INPs (Figure 12J, N). Consistent with our hypothesis, the heterozygosity of *brm* or *mor* enhanced the supernumerary neuroblast phenotype in $numb^{NP2301/15}$ brains (Figure 12K-L; data not presented). These results strongly suggest that the BAF complex also functions temporally after Numb in immature INPs to suppress supernumerary neuroblast formation.

Both Erm and the BAF complex function temporally after Brat and Numb in immature INPs to suppress supernumerary neuroblast formation. Thus, we tested whether Erm and the BAF complex might function cooperatively to restrict the developmental potential of immature INPs. Similar to the BAF complex, the heterozygosity of *erm* also enhanced the supernumerary neuroblast phenotype in $numb^{NP2301/15}$ brains (Figure 12M-N). Most importantly, while over-expression of the *UAS-*brm^{DN} transgene alone did not have any effect on the type II neuroblast lineage, over-expression of brm^{DN} significantly increased the formation of supernumerary neuroblasts in *erm* hypomorphic brains (Figure 12O-Q). Taken together, these data strongly suggest that Erm and the BAF complex function cooperatively to restrict the developmental potential of immature INPs.

Discussion

Understanding the molecular mechanisms that stably restrict the developmental potential of progenitor cells may lead to the identification of novel therapeutic targets to selectively target progenitor cell-derived tumor-initiating stem cells. However, restriction of developmental potential may occur while intermediate progenitor cells acquire their functional identity. Thus, well-established stem cell lineage information is essential for investigating the molecular mechanisms that restrict developmental potential. The type II neuroblast lineage in fly larval brains offers a unique model system to investigate the restriction of the developmental potential in uncommitted intermediate progenitor cells (Komori et al., 2014b; Weng et al., 2010; Xiao et al., 2012). In this study, we show that

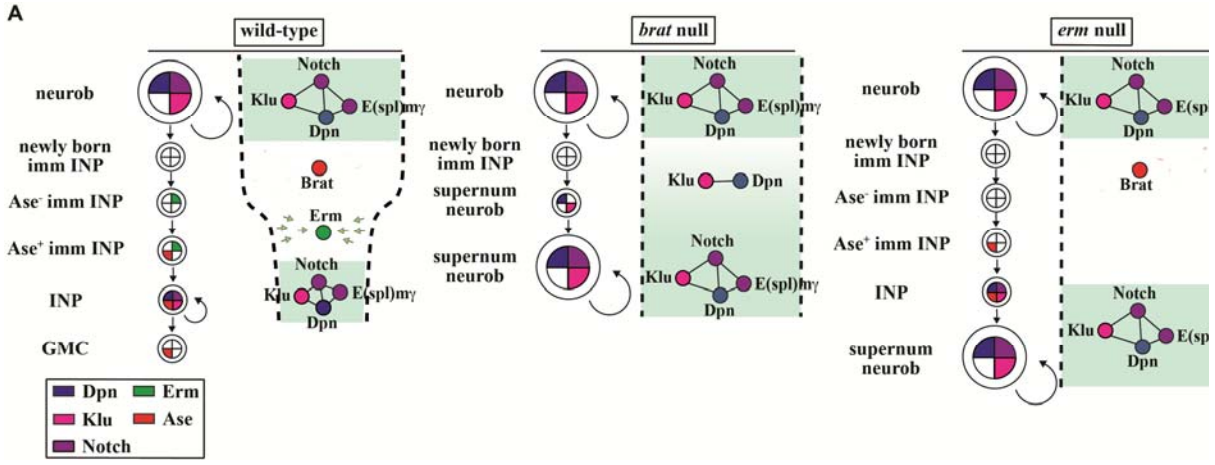

Figure 13: Summary models depict the role of Brat and Erm in the regulation of immature INPs. In wild-type brains, Erm functions temporally after Brat to restrict the competence of immature INPs to respond to the self-renewal network (indicated by the width between dotted lines of the funnel). The Self-renewal network is expressed in type II neuroblasts (light blue area), but is deactivated during maturation by Brat (white area). An Erm-dependent restriction of developmental potential (green arrows) in immature INPs, leads to an attenuated competence to respond to the re-activation of neuroblast self-renewal factors in INPs (light blue area). In *brat* amorphic brains, the newly born immature INPs fail to undergo maturation and rapidly revert into supernumerary neuroblasts. In *erm* amorphic brains, immature INPs undergo successful maturation, but their competence to respond to neuroblast self-renewal factors is not attenuated. Thus, upon re-expression of neuroblast self-renewal factors, INPs revert to form supernumerary neuroblasts.

stable restriction of developmental potential in immature INPs required a temporally coordinated effort of the asymmetrically inherited proteins Brat and Numb and the transcriptional repressor protein Erm. Brat and Numb function in the newly born immature INP where these two proteins prevent the reversion into a supernumerary neuroblast induced by the activities of self-renewal factors (Figure 13). Erm functions downstream of Brat and Numb in the Ase^{-} and Ase^{+} immature INPs to restrict their genomic response to neuroblast self-renewal factors, leading to permanently attenuated competence to respond to these factors in INPs (Figure 13). Furthermore, we also identified that the BAP chromatin-remodeling complex functions synergistically with Erm in immature INPs to suppress the formation of supernumerary neuroblasts. Taken together, we propose that Erm functions cooperatively with the BAP complex to implement a stable restriction of the developmental potential in immature INPs by modifying their genome, which leads to an attenuated response to all neuroblast self-renewal factors in INPs (Figure 13).

Erm-dependent restriction of the developmental potential in immature INPs leads to an attenuated competence to respond to all self-renewal transcription factors in INPs

Several pieces of evidence led us to conclude that Erm mainly restricts the developmental potential in the Ase^{+} immature INPs. Erm is primarily detected in the Ase^{-} and Ase^{+} immature INPs but become undetectable in the INP, strongly suggesting that Erm functions in the Ase^{-} and Ase^{+} immature INPs (Figure 8). Consistently, heterozygosity of *erm* further exacerbated supernumerary neuroblast formation originated from the Ase^{+} immature INPs in *brat* hypomorphic brains, and restoring *erm*

function in the Ase^{+} immature INPs rescued the enhancement of the supernumerary neuroblast phenotype (Figure 6E-I). Furthermore, restoring *erm* function in the Ase^{+} immature INPs also rescued the supernumerary neuroblast phenotype in *erm* null brains (Weng et al., 2010). Finally, over-expression of VP16-Erm^{zf}, a dominant-negative form of Erm, in the Ase^{+} immature INPs significantly increased supernumerary neuroblasts in various genetic backgrounds (Figure 9). Although these data do not exclude the possibility that *erm* might still function in the INP, *erm* most likely functions mainly in immature INP to restrict developmental potential and suppress supernumerary neuroblast formation.

Erm restricts the developmental potential of immature INPs by acting as a transcriptional repressor, and removing the function of *klu* or *dpn* completely suppressed the supernumerary neuroblast phenotype in *erm* null brains (Figure 9-11). Thus, Erm might restrict the developmental potential of immature INPs by directly repressing the transcription of the genes encoding neuroblast self-renewal factors or indirectly attenuating the competence to respond to these factors. However, Ase^{+} immature INPs in *erm* null type II neuroblast clones never showed a premature onset of Dpn expression, and over-expression of *erm* in neuroblasts did not affect Dpn expression (Weng et al., 2010). In addition, transcriptome analyses indicated that *dpn* and *klu* become up-regulated to a similar level in *brat* and *erm* null brains as compared to control brains (Komori and Lee, unpublished). Thus, it is unlikely that Erm directly regulates the transcription of neuroblast self-renewal genes. We favor the mechanism that Erm indirectly attenuates the competence to respond to these neuroblast self-renewal factors in INPs by restricting the developmental potential in immature INPs.

Consistently, while over-expression of the dominant-negative VP16-Erm^{zf} or a single neuroblast self-renewal factor alone induced a very weak supernumerary neuroblast phenotype, co-expression of VP16-Erm^{zf} and a single neuroblast self-renewal factor led to a very robust supernumerary neuroblast phenotype (Figure 10-11). Taken together, these data strong suggest that stable restriction of developmental potential by the Erm-dependent mechanism in immature INPs leads to attenuated competence to respond to the re-activation of neuroblast self-renewal factors in INPs.

Erm restricts the developmental potential in immature INPs by repressing gene transcription

The vertebrate orthologs of Erm, Fezf1 and Fezf2, regulate cortical development either by activating or repressing gene expression (Hirata et al., 2006; Yang et al., 2012). Since over-expression of either *fezf1* or *fezf2* can functionally substitute the role of Erm in the Ase^{+} immature INPs (Weng et al., 2010), the results from the vertebrate studies prompted us to investigate the molecular mechanism by which Erm restrict the developmental potential in immature INPs. Over-expression of ERD-Erm^{zf}, which functions solely as a transcriptional repressor protein, efficiently rescued the supernumerary neuroblast phenotype in the Ase^{+} immature INPs (Figure 9). By contrast, over-expression of VP16-Erm^{zf} exerted a dominant negative effect and led to a further increase in supernumerary neuroblasts in *brat* or *erm* hypomorphic brains (Figure 9). Taken together, these data strongly suggest that Erm restricts developmental potential in immature INPs by repressing gene transcription.

We previously mapped the molecular lesion induced by the *erm^{1}* null allele to a single amino acid substitution in the third C_2H_2 zinc-finger of Erm, indicating that the

third zinc-finger is essential for the function of Erm. The C_2H_2 zinc-finger transcription factor typically binds to DNA with two or three zinc fingers (Brayer and Segal, 2008). Consistently, perturbing the folding of zinc-finger 2 ($Erm^{zf2(2A)}$) or 4 ($Erm^{zf4(2A)}$) also render the transgenic protein unable to restrict the developmental potential in the Ase^{+} immature INPs whereas perturbing the folding of zinc-finger 1 ($Erm^{zf1(2A)}$), 5 ($Erm^{zf5(2A)}$) or 6 ($Erm^{zf6(2A)}$) had no effects (Figure 9). These data indicate that the zinc-finger 2, 3 and 4 most likely mediate the binding of Erm to DNA.

Erm might function cooperatively with the BAF chromatin-remodeling complex to modify the genomic response to neuroblast self-renewal factors

A genome-wide RNAi study showed that knocking down the function of several subunits in the BAP complex results in supernumerary neuroblast formation in fly larval brains (Neumüller et al., 2011). We independently identified that *brm*, *mor* and *osa*, which encode the core components of the BAF complex, likely function temporally after Brat and Numb to restrict the developmental potential in the Ase^{-} immature INPs (Figure 12). Because Brm and Osa are expressed ubiquitously in all cells in larval brains (Komori and Lee, data not presented), the BAP complex most likely functions cooperatively with a transcription factor that is uniquely expressed in the immature INPs to elicit its function in restricting developmental potential. Erm is the only known transcriptional factor that is uniquely expressed in the immature INPs, and is an excellent candidate for functioning cooperatively with the BAP complex to restrict the developmental potential in the immature INPs (Figure 8G). Consistently, reducing the function of Brm enhanced the supernumerary neuroblast phenotype in *erm* hypomorphic brains (Figure 12O-Q). Thus, we propose that Erm restricts the developmental potential in the immature INPs by

recruiting the BAP complex to specific genomic loci where the BAP complex alters the nucleosome structures, leading to attenuated competence to respond to the re-activation of neuroblast self-renewal factors. Additional functional and biochemical experiments in the future will be required to validate this hypothesis.

Materials and Methods

Fly strains

Mutant and transgenic fly strains used include *erm*^{1}, *erm*^{2} (Weng et al., 2010), *klu*^{R51} (Kaspar et al., 2008), *dpn*^{1} (Younger-Shepherd et al., 1992), *brat*^{150} (Betschinger et al., 2006), *numb*^{15} (Berdnik et al., 2002), *Erm-GAL4(II)* and *Erm-GAL4(III)* (Pfeiffer et al., 2008; Weng et al., 2010), *Wor-GAL4* (Lee et al., 2006b), *UAS-erm-HA* (Weng et al., 2010), *UAS-klu-HA* (Xiao et al., 2012), *UAS-brat-myc* (Xiao et al., 2012), *UAS-dpn* (Wallace et al., 2000), *UAS-E(spl)mγ* (Ligoxygakis et al., 1998) and *UAS-brm*^{DN} (Herr et al., 2010). The following fly stocks were obtained from the Bloomington *Drosophila* Stock Center: Oregon R, *brat*^{DG19310}, *brat*^{k06028}, *brat*^{11}, *brm*^{2} and *mor*^{1}, *osa*^{308}, *Act-FRT-Stop-FRT-GAL4*, *tub-GAL80, UAS-mCD8-GFP, FRTG13, FRT2A and hs-flp*, *tub-GAL80*^{ts}*, Elav-GAL4, Act-FRT-stop-FRT-lacZ(nls)*, *UAS-GFP(nls)* and *UAS-flp*. *numb*^{NP2301} was obtained from the Kyoto stock center.

The P[acman] BAC CH321-65B19 construct was used to generate *erm-flag* and *erm-rfp* transgenic fly lines following previously established protocol (Bischof et al., 2007; Venken et al., 2009; Venken et al., 2006).

Immunofluorescent staining and antibodies

Larval brains were dissected in 1X PBS solution. Larval brains were fixed in 4% formaldehyde in 1XPBS containing 0.3% Triton X-100 (PBST) for 24 minutes and processed for immunofluorescent staining according to a previously published protocol (Weng et al., 2012). Antibodies used in this study include rabbit anti-Erm (1:100; this study), guinea pib anti-Ase (1:1000; this study), rat anti-Dpn (1:1000) (Xiao et al., 2012),

rat anti-Wor (1:1) (Lee et al., 2006b), rabbit anti-Ase (1:400) (Weng et al., 2010), mouse anti-Pros (MR1A, 1:100) (Lee et al., 2006c), mouse anti-Elav (1:100; 9F8A9, DSHB), mouse anti-Dlg (1:50; 4F3E3E9, DSHB), mouse anti-Osa (Treisman et al., 1997), rabbit anti-Brm (Nakayama et al., 2012), chicken anti-GFP (1:2000; cat # 1020, Aves Labs), chicken anti-β-Gal (1:2000; cat# 1040, Aves Labs), and rabbit anti-RFP (1:100; cat# 600-401-379, lot# 25003, Rockland). Secondary antibodies were from Molecular Probes and Jackson Labs (details are available upon request). We used Rhodamine phalloidin (1:100; Invitrogen) to visualize cortical actin. The confocal images were acquired on a Leica SP5 scanning confocal microscope.

Generation of a polyclonal antibody against Erm

The cDNA region encoding the C-terminal 332-611 amino acids of Earmuff (Erm-C) was amplified by PCR and subsequently cloned into EcoRI and SalI sites of pGEX-4T-1, using In-Fusion HD Cloning Kit (Clontech, Cat# 639649). The primers used were: TGGATCCCCGGAATTCCTCACCCGCCACATGCCC (forward) and GGCCGCTCGAGTCGACCTAAAACACCTTGGCTATGA (reverse). The expression of GST-Erm-C was induced by Isopropyl β-D-1-Thiogalactopyranoside (IPTG) and purified using Glutathione Sepharose (GE Healthcare, Cat# 71-5027-54) and eluted by Glutathione. GST-Erm-C was injected into one rabbit and purified by GenScript (Hong Kong).

Clonal analysis

1. To induce the lineage clone derived from a single Ase^{+} immature INP or INP: $brat^{DG19310/+}$, $brat^{DG19310/11}$, $erm^{1/+}$,$brat^{DG19310/11}$ or $erm^{1/2}$ larvae carrying the *UAS-flp,*

Erm-Gal4(III), Tub-gal80^{ts} and *Act-FRT-stop-FRT-lacZ(nls)(III)* transgenes were genotyped at hatching, raised at 25^{o}C and dissected at 96 hours after larval hatching. We empirically determined the experimental condition to obtain a small number of clones per brain lobe (Figure 7).

2. The protocol to examine the expression pattern of *Erm-Gal4(II)* or *Erm-Gal4(III)* in *brat* or *erm* hypomorphic brains is described in the legend for Figure 5.

3. GFP-marked mosaic clones derived from single mutant neuroblasts in the various genetic background was induced following a standard protocol (Lee and Luo, 2001).

Over-expression of *UAS*-transgene

Mutant larvae carrying the *Wor-Gal4 and Tub-Gal80ts* in combination with the *UAS*-transgene were genotyped at hatching, and raised at 31^{o}C for 72 hours after larval hatching. Larvae were dissected and processed for immunofluorescent staining.

3-dimentional modeling of clones

The model was generated using the *Mimics* software from *Materialize.* Confocal images were acquired using a Z-step size of 1um and the identity of each cell within a clone was determined

Acknowledgements

We thank Drs. C. Delidakis, C. Doe, S. Hirose, H. Richardson, G. Rubin, J. Treisman, H. Vaessin and Y.N. Jan for fly stocks and antibody reagents. We thank the Bloomington *Drosophila* Stock Center, Kyoto stock center and the Developmental Studies Hybridoma Bank for fly stocks and antibodies. We thank the BestGene Inc. for

generating transgenic fly lines. We thank Krista L. Golden for technical assistance throughout the course of this work and proofreading the manuscript. We thank the members of the Lee lab for their intellectual input during the course of this study. D. H. J. was supported by a Cellular and Molecular Biology training grant (T32-GM007315). H.K. was supported by a fellowship from the Japan Society for the Promotion of Science. D.G. would like to express his gratitude to the Marshallplan Foundation for the generous financial support during his stay in the Lee lab. C.-Y.L is supported by the University of Michigan start-up fund, a Sontag Foundation Distinguished Scientist Award and an NIH grant R01-GM092818.

Chapter 3: A novel Hdac1/Rpd3-poised circuit balances continual self-renewal and rapid restriction of developmental potential during asymmetric stem cell division

Abstract

Stem cells divide asymmetrically to regenerate while producing intermediate progenitors that rapidly acquire restricted developmental potential. How the developmental competency of intermediate progenitors becomes precisely restricted remains unknown. In the fly larval brain *earmuff* (*erm*) uniquely functions to restrict the developmental potential of intermediate neural progenitors (INPs). Here, we elucidate a novel Hdac1/Rpd3-dependent mechanism through which transcriptional repressors that promote self-renewal maintain the *erm* enhancer in an inactive but poised state in neural stem cells (neuroblasts). Down-regulation of these self-renewal transcriptional repressors alleviates Hdac1/Rpd3-mediated repression, leading to the activation of Erm expression in immature INPs within two-hours of their birth. Erm acts as a negative feedback mechanism, restricting the developmental potential of INPs by repressing genes encoding neuroblast transcriptional activators. We propose poising the expression of master regulators of differentiation through active histone deacetylation in stem cells maintains continual self-renewal while enabling rapid restriction of developmental potential following asymmetric division.

Introduction

To produce the astounding number and diversity of cells that comprise our body, stem cells undergo continual rounds of asymmetric division to self-renew while simultaneously giving rise to more restricted cell types. To amplify the output of each division, tissue-specific stem cells generate intermediate progenitors that possess a restricted developmental and produce exclusively differentiated cell types (Bond et al., 2015; Paridaen and Huttner, 2014). If their developmental potential is not stably restrained, intermediate progenitors may become susceptible to oncogenic transformation (Alcantara Llaguno et al., 2015; Chen et al., 2012; Chen et al., 2010). Thus, the mechanisms that restrict the developmental potential of intermediate progenitors must be executed in an extremely efficient and robust manner following asymmetric stem cell division. Understanding how developmental potential becomes restricted in intermediate progenitors will not only improve our knowledge of organogenesis, but also the cell-of-origin for certain tumors.

It has been shown that in embryonic stem cells cell-type-specific enhancers of key developmental regulators that control lineage restriction and cell fate commitment are maintained in a poised state (Calo and Wysocka, 2013; Heinz et al., 2015; Zentner et al., 2011). These poised enhancers are enriched for mono- and di-methylated lysine 4 on histone H3 (H3K4me1/2), catalyzed by the Trithorax (Trx) family of proteins, and trimethylated lysine 27 on histone H3 (H3K27me3), catalyzed by Polycomb Repressive Complex 2 (PRC2). This led to the prevailing model that PRC2 prevents premature activation of these poised enhancers in stem cells, while Trx proteins maintain these enhancers for activation during lineage commitment. During the activation of poised

enhancers, H3K27 is demethylated to permit subsequent H3K27 acetylation (H3K27ac). In vertebrates, this mechanism has been attributed to the activation of poised enhancers during lineage commitment of embryonic stem cells and in the differentiating progeny of tissue-specific stem cells (Amador-Arjona et al., 2015; Lodato et al., 2013; Park et al., 2014; Rada-Iglesias et al., 2011). Nonetheless, whether H3K27me3 is essential for maintaining the inactivity of all poised enhancers and whether the conversion of H3K27me3 to H3K27ac indeed plays an instructive role in activating a poised enhancer remains unclear. It also remains untested if this stepwise mechanism of activating a poised enhancer is kinetically feasible to initiate expression of the fast activating genes that trigger restriction of developmental potential in differentiating stem cell progeny.

Mechanistic investigation of how the developmental potential of intermediate progenitors becomes restricted has been hindered in most stem cell lineages by the lack of a well-defined window during which this critical change in developmental competency occurs. A subset of neural stem cells in the fly larval brain called type II neuroblasts undergo repeated rounds of asymmetric division to generate immature intermediate neural progenitors (INPs) that acquire restricted developmental potential during a maturation process lasting approximately six hours from the time of their birth (Bello et al., 2008; Boone and Doe, 2008; Bowman et al., 2008; Homem and Knoblich, 2012; Homem et al., 2013; Janssens and Lee, 2014; Weng and Lee, 2011). Immature INPs can be unambiguously identified based on proximity to their parental type II neuroblast and a well characterized set of molecular markers, providing an excellent genetic model for investigating restriction of developmental potential *in vivo* (Figure

14A)(Bello et al., 2008; Boone and Doe, 2008; Bowman et al., 2008; Homem and Knoblich, 2012; Janssens and Lee, 2014; Weng and Lee, 2011). Following the completion of maturation, INPs re-enter the cell cycle, and undergo 5-6 rounds of asymmetric divisions to produce exclusively differentiating progeny (Bayraktar and Doe, 2013; Viktorin et al., 2011). Newly born immature INPs inherit tumor suppressor proteins Brain tumor and Numb through the asymmetric division of type II neuroblasts (Haenfler et al., 2012; Janssens et al., 2014; Xiao et al., 2012). Brat and Numb initiate restriction of the developmental potential by transiently down-regulating the function of type II neuroblast self-renewal genes *klumpfuss* (*klu*), *deadpan* (*dpn*) and *Enhancer of split mγ* (*E(spl)mγ*) (Berger et al., 2012; San-Juán and Baonza, 2011; Xiao et al., 2012; Zacharioudaki et al., 2015; Zacharioudaki et al., 2012; Zhu et al., 2012). Dpn and E(spl)mγ are the fly homologs of vertebrate Hes1/5 transcriptional repressors whereas Klu is homologous to the Wilm's tumor 1 transcription factor in vertebrates (Imayoshi and Kageyama, 2014; Pei and Grishin, 2015). Understanding how down-regulation of self-renewal factor activities is coordinated with the activation of restricted developmental potential in immature INPs will likely reveal important insight into the regulation of all asymmetrically dividing stem cell lineages.

The C_2H_2 zinc-finger transcription factor Earmuff (Erm) functions as the master regulator to restrict the developmental potential of INPs in the fly larval brain. Neuroblasts mis-expressing *erm* prematurely differentiate, whereas *erm* null INPs spontaneously revert into supernumerary type II neroblasts (Janssens et al., 2014; Weng et al., 2010). Endogenous Erm is undetectable in the self-renewing neuroblast and the newly born immature INP, but is detected in all remaining immature INPs in a

type II neuroblast lineage (Figure 14A). This strongly suggests that *erm* is rapidly activated in the immature INP after birth. The molecular mechanisms by which Erm and its vertebrate homologs Fezf1 and Fezf2 regulate gene transcription are likely conserved because over-expression of Fezf1 or Fezf2 completely rescued the supernumerary neuroblast phenotype in *erm* null brains (Weng et al., 2010). However, discrepancies between the reported consensus binding sequences of Erm and Fezf2 have hindered identification of the direct targets of this family of transcription factors (Chen et al., 2011; Koe et al., 2014). Elucidating the regulatory mechanisms that trigger *erm* expression in immature INPs, as well as physiologically relevant Erm-binding sites will significantly improve our understanding of how the developmental potential of intermediate progenitors becomes rapidly restricted. This knowledge will also significantly improve our understanding of the role of the Fezf family of transcritption factors during neurogenesis and immune responses (Guo et al., 2013; Janssens et al., 2014; Takaba et al., 2015),

In this study, we defined an immature INP enhancer from the *erm cis*-regulatory region and demonstrated that it is maintained in a poised state in type II neuroblasts, allowing it to be rapidly activated in immature INPs within two hours of their birth. Contrary to expectation, the histone deacetylase Rpd3, but not PRC2, is required to prevent premature activation of the poised *erm* immature INP enhancer in type II neurobalsts. We found the transcriptional repressors Klu, Dpn, and E(spl)mγ function cooperatively through Rpd3 to promote type II neuroblast self-renewal by directly binding the *erm* immature INP enhancer and maintaining *erm* in an inactive but poised state. In addition, we found the P1-isoform of Pointed (PntP1), a type II neuoblast

specific transcriptional activator, also binds the *erm* immature INP enhancer and mediates activation. Consequently, rapid down-regulation of Klu, Dpn, and E(spl)mγ in the immature INP provides the permissive cue to activate the poised *erm* enhancer, triggering Erm expression. Lastly, we identified and validate a functional Erm-binding sequence that is also recognized by Fezf1 and Fezf2 *in vitro*, and showed that Erm restricts the developmental potential in immature INPs partly by directly repressing the expression of *pntP1* and the O-isoform of *grainy head* (*grhO*) encoding neuroblast transcriptional activators. This work provides a novel paradigm, in which removal of self-renewal transcriptional repressors, rather than addition of a transcriptional activator, rapidly activates poised gene expression. In addition, Erm is the first example of a fast-activating poised gene that restricts the developmental potential of intermediate progenitors by directly repress components of the stem cell transcription factor network. We propose this novel HDAC1/Rpd3-poised negative feedback circuit as a highly efficient and robust mechanism to balance continual self-renewal with rapid restriction of developmental potential across asymmetric stem cell division.

Results

erm is poised in the type II neuroblast but becomes rapidly activated in the immature INP

To unravel the mechanisms that activate restriction of developmental potential in immature INPs, we examined the expression pattern of the entire collection of *9D-Gal4* drivers that are under the control of various cis-regulatory fragments from the *erm* locus (Pfeiffer et al., 2008). We found that two partially overlapping fragments, 9D11 and 9D10, can individually drive reporter transgene expression in immature INPs. We confirmed that the overlapping region can indeed drive reporter expression in immature INPs, mimicking the activation of endogenous Erm, and named this region the *erm* proximal enhancer (prox) (Figure 14B). In addition, we found and confirmed that the non-overlapping portion of 9D11 also drives reporter expression recapitulating endogenous Erm expression in immature INPs, and named this region the *erm* distal enhancer (dist) (Figure 14B). We focused on the *erm* dist immature INP enhancer and mapped it to a minimal 250-bp fragment (dist5E) that was sufficient to drive reporter expression (dist5E-*gfp::luc(nls)*) in a pattern reminiscent of endogenous Erm in immature INPs (Figure 14B-C). Thus we conclude dist5E contains many of the regulatory inputs that control the timing of *erm* activation in the immature INP and provides an excellent tool for dissecting the mechanisms regulating *erm* expression.

To estimate the kinetics of *erm* activation in the immature INP, we examined the timing of dist5E-*gfp::luc(nls)* activation following asymmetric neuroblast division by live-cell imaging. We marked the type II neuroblasts and all immature INPs with a mCherry(nls) transgene, and found that dist5E-GFP::Luc(nls) becomes detectable in the

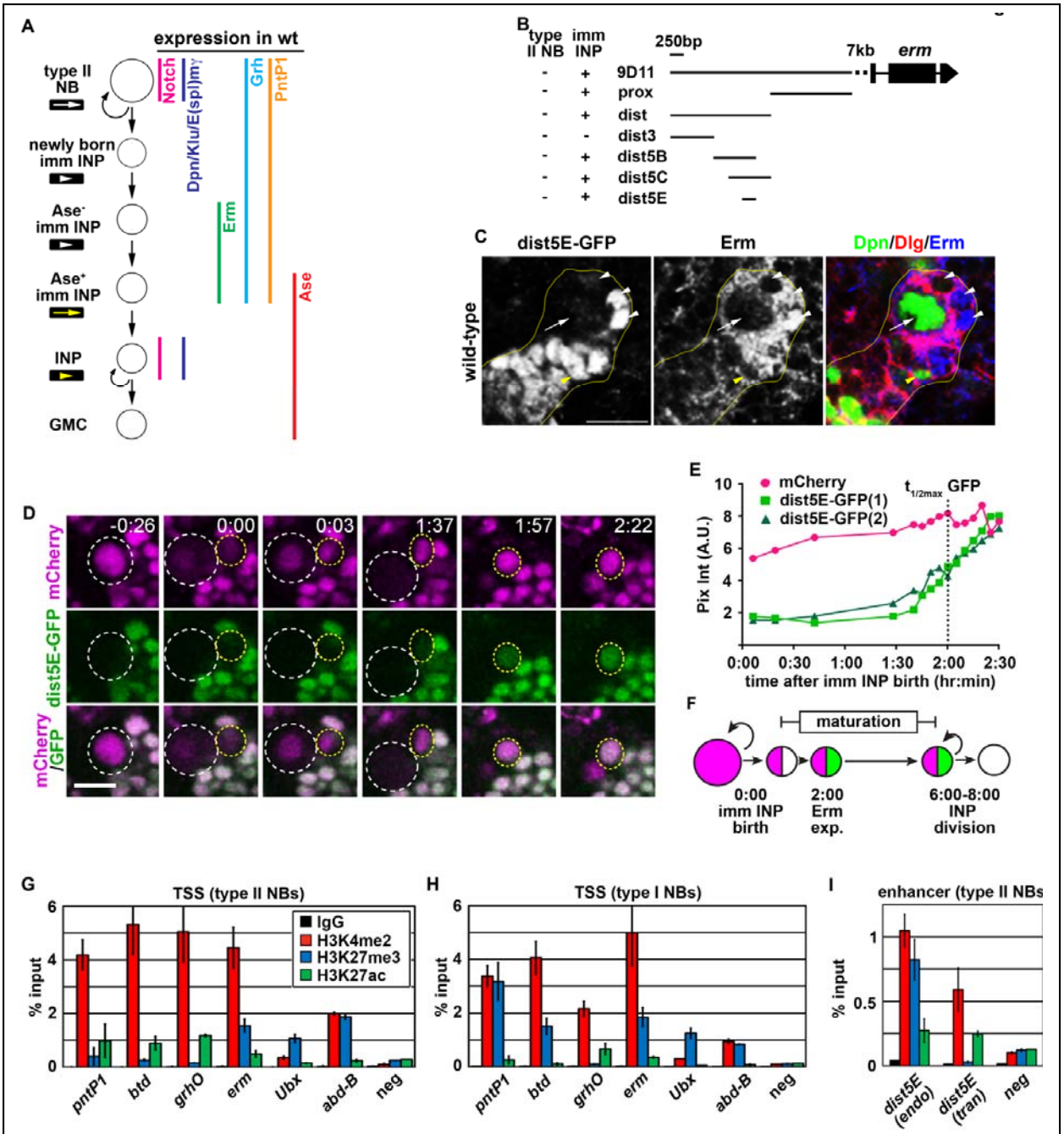

Figure 14: The dist5E enhancer recapitulates temporal-specific activation of endogenous *erm* and is poised in type II neuroblasts. (A) Diagram showing transcription factor expression patterns in the type II NB lineage. The color scheme of arrows and arrowheads used to identify various cell types in the type II NB lineage in all figures is shown. (B) A summary of a subset of reporter transgenes used for mapping the minimal *erm* immature INP enhancers in the 9D11 regulatory fragment located 7 Kb from the *erm* transcription unit. Prox: proximal. Dist: distal. (C) The dist5E-*gfp::luc(nls)* reporter contains the 250-bp dist5E enhancer fragment and recapitulates the activation of endogenous Erm expression in immature INPs. *(legend continued on next page)*

Figure 14 (continued): (D) Live-cell analyses of a type II NB lineage marked with mCherry(nls) (magenta), showing the birth of an immature INP (0:00) and the rate of dist5E-*gfp::luc(nls)* (green) activation. White dotted line: type II neuroblast, Yellow dotted line: newly born immature INP. The time stamp indicates time after the completion of NB division. (E) Quantification of the relative pixel intensity of mCherry and GFP in the immature INP nucleus, $t_{1/2max}$ indicates the length of time required for *dist5E-gfp::luc(nls)* to achieve 50% of the maximum pixel intensity of GFP in the immature INP nucleus. (F) Schematic showing the rate at which Erm is activated during INP maturation, as well as the completion of maturation and re-entry into the cell cycle. (G) ChIP analysis of the relative enrichment of H3K4me2 (red), H3K27me3 (blue), H3K27ac (green) and an IgG control (black) on the transcription start sites (TSS) of type II NB regulators as well as classic targets of PRC2 and Trx on chromatin extracted from *brat* mutant brains, which are highly enriched for type II NBs. (H) Similar ChIP analysis to (G) but performed using chromatin extracted from *Ase>>aPKC^{CAAX}* brains, which are highly enriched for type I NBs. (I) ChIP analysis examining the enrichment of chromatin marks on the endogenous dist5E enhancer fragment (dist5E(endo)) and the transgenic dist5E enhancer fragment (dist5E(tran)) performed on chromatin extracted from *brat* mutant brains.

immature INP less than 2 hours after neurobalst division (Figures 14D-E). We conclude this *erm* enhancer participates in the rapid activation of Erm in immature INPs within two hours of their birth (Figure 14F).

This rapid activation of the *erm* immature INP enhancer led us to hypothesize that *erm* is maintained in an inactive but poised state in type II neuroblasts. To test this hypothesis, we isolated nuclear extract from larval brains enriched with either type I or type II neuroblasts. A *brat* null brain aged for 120 hours after hatching contains thousands of supernumerary type II neuroblasts, whereas over-expression of a *UAS-aPKC^{caax}* transgene driven by *Ase-Gal4* leads to thousands of supernumerary type I neuroblasts per brain lobe (Haenfler et al., 2012; Komori et al., 2014a; Komori et al., 2014b; Xiao et al., 2012). Thus, the nuclear extract isolated from *brat* null brains provides a source of enriched type II neuroblast chromatin, and the nuclear extract isolated from *aPKC^{caax}* over-expressing brains provides a source of enriched type I neuroblast chromatin. We performed chromatin immunoprecipitation on the type I or type II neuroblast chromatin using specific antibodies against H3K4me2, H3K27me3,

H3K27ac and IgG coupled with quantitative PCR to assay the chromatin state of genes whose spatial expression patterns are well characterized. The transcription factors *pntP1* and *buttonhead* (*btd*) are specifically expressed in type II neuroblasts (Komori et al., 2014a; Xie et al., 2014; Zhu et al., 2011). In the type II neuroblast-enriched chromatin, the transcriptional start sites (TSS) of these two genes were marked by high levels of H3K4me2 and H3K27ac, and this combination of histone modifications is correlated with active transcription (Figure 14G). By contrast, in type I neuroblast-enriched chromatin these TSS were marked by H3K4me2 and H3K27me3, histone modifications associated with a poised state (Figure 14H). The transcription factor *grhO* is expressed in both type I and type II neuroblasts (Almeida and Bray, 2005). As was expected from this expression pattern, the TSS of *grhO* showed H3K4me2 and H3K27ac marks in both type I and type II neuroblast-enriched chromatin (Figure 14E). Lastly, we examined the TSS of two components of the Bithorax Complex, *Ultrabithorax* (*Ubx*) and *abdominal B* (*abd-B*), which are classic targets of PRC2 and Trx but are not expressed in larval central brain neuroblasts (Bello et al., 2007). Surprisingly, the TSS of *abd-B* displayed both high levels of H3K4me2 and H3K27me3, but the TSS of *Ubx* was only enriched for H3K27me3 in both type II and type I neuroblast-enriched chromatin, suggesting that *Ubx* is in a more deeply repressed state than *abd-B* (Figure 14G-H). We conclude the type I and type II neuroblast-enriched nuclear extracts provide a reliable platform to examine the chromatin signature of genes in distinct larval brain neuroblast lineages.

We next examined the chromatin state of the *erm* locus in both type I and type II neuroblast nuclear extracts. The TSS of *erm* was enriched for H3K4me2 and

H3K27me3 in both type I and type II neuroblast-enriched chromatin (Figure 14G-H). The rapid activation of *erm* expression in immature INPs together with the TSS being occupied by histones that display marks associated with poised promoters suggested that *erm* is maintained in an inactive but poised state in both type I and type II neuroblasts. Studies in vertebrates suggest that cell-type-specific enhancers can also be maintained in a poised chromatin state (Amador-Arjona et al., 2015; Park et al., 2014), prompting us to investigate whether the *erm* immature INP enhancer might also be poised in type II neuroblast to contribute to the precise pattern of *erm* expression. Consistent with this prediction, the endogenous dist5E enhancer (dist5E endo) was enriched for H3K4me2 and H3K27me3 (Figure 14I). Thus, maintenance of the *erm* promoter and its immature INP enhancer in a poised state in self-renewing type II neuroblasts likely contributes to the rapid activation of *erm* expression in immature INPs following asymmetric division.

The histone deacetylase Rpd3 and not PRC2 prevents premature activation of the poised *erm* immature INP enhancer in type II neuroblasts

Because the expression pattern of the dist5E-*gfp::luc(nls)* transgene completely co-localizes with endogenous Erm in immature INPs (Figure 14C), we used it as a tool to investigate regulation of the poised *erm* immature INP enhancer. We first examined if the dist5E enhancer fragment in our reporter transgene (dist5E tran) is enriched for H3K4me2 and H3K27me3 in type II neuroblasts, similar to the endogenous enhancer. Despite the fact that the transgenic dist5E enhancer is inactive in neuroblasts similar to endogenous *erm*, the transgenic dist5E enhancer is enriched for H3K4me2 but not H3K27me3 in the type II neuroblast-enriched chromatin (Figure 14I). Trithorax (Trx)

specifically catalyzes the formation of H3K4me1 that contributes to the maintenance of a poised enhancer (Herz et al., 2012; Tie et al., 2014). The atypical combination of histone marks on the transgenic dist5E enhancer prompted us to test if Trx is required to maintain the dist5E-*gfp::luc(nls)* transgene in a poised state. Indeed, knocking down *trx* function significantly reduced the *in vivo* Luciferase activity of dist5E-*gfp::luc(nls*) (Figure 15A). Thus, we conclude that Trx is required for activation of the transgenic dist5E enhancer, and likely functions to maintain *erm* in a poised state in type II neuroblasts.

Our finding that H3K27me3 is present on the endogenous *erm* immature INP enhancer but not on the transgenic dist5E enhancer suggested that PRC2 is not required to prevent premature activation of the *erm* immature INP enhancer in type II neurobalsts. This result led us to test if PRC2 is required to maintain repression of endogenous *erm* in type II neuroblasts. *Enhancer of zeste* (*E(z)*) and *Suppressor of zeste 12* (*Su(z)12*) encode two core components of PRC2, and are essential for catalyzing the H3K27me3 histone mark (Blackledge et al., 2015; Piunti and Shilatifard, 2016). We found that by 72 hours after clone induction *Su(z)12* null type II neuroblasts displayed undetectable H3K27me3, and that by 96 hours after clone induction the majority of *E(z)* null clones were also H3K27me3 negative (Figure 15B, B', E; data not presented). We next examined the expression of two well characterized PRC2 target genes *Ubx* and *abd-B*. Interestingly, we found that while Ubx and Abd-B were both undetectable in wild-type type II neuroblasts, only Abd-B became ectopically activated in *Su(z)12* and *E(z)* null type II neuroblasts (Figure 15C, C' and E; Figure 16A, A'; data

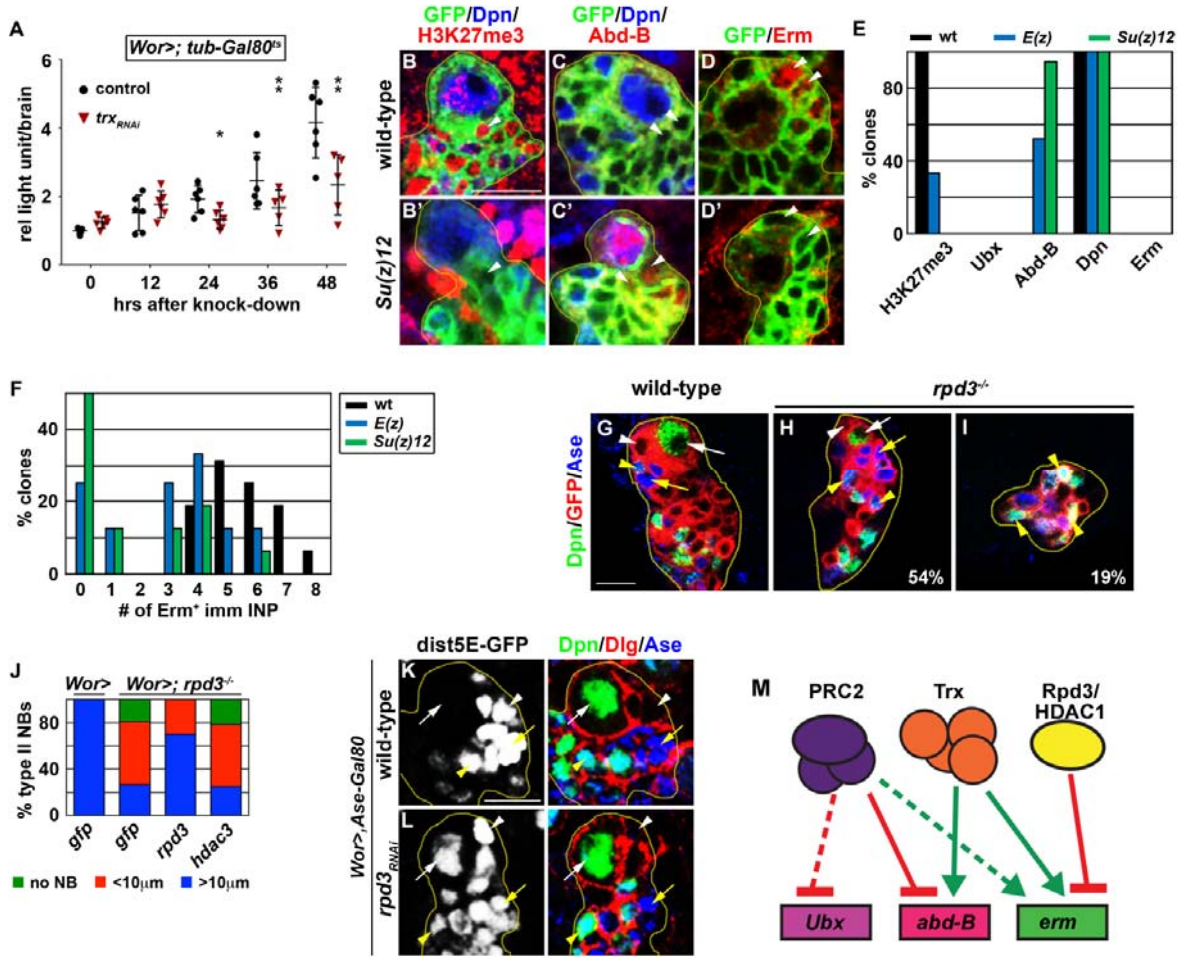

Figure 15: Rpd3-dependent deacetylation maintains the dist5E enhancer fragment poised in the type II neuroblast. (A) Knocking down *trx* function decreases the activity of dist5E-*gfp::luc(nls)* relative to the control brain as determined by a single brain luciferase assay (N ≥ 6 brains/time-point). The dot plots are represented as mean ± SD, *: P-value ≤ 0.05, **: P-value ≤ 0.005. (B-D) Confocal images of 72hr wild-type and *Su(z)12*^{4} mutant clones showing the loss of H3K27me3, ectopic expression of Abd-B, and loss of Erm expression in *Su(z)12*^{4} mutant clones. (E) Quantification of the percentage of wild-type, *E(z)*^{731}, *Su(z)12*^{4} type II neuroblasts that are positive for of H3K27me3 and the indicated proteins. (F) Quantification of the percentage of wild-type, *E(z)*^{731} or *Su(z)12*^{4} type II neuroblast clones that contain 0-8 Erm positive immature INPs. (G-I) Confocal images showing *rpd3* mutant type II neuroblasts prematurely differentiate as indicated by reduction in cell diameter (54%) and lack of identifiable neuroblasts (19%). (K) Over-expression of *rpd3* but not *hdac3* rescues type II neuroblast self-renewal defects in 72-hr *rpd3* mutant mosaic clones (N ≥ 15 clones/genotype). (J-L) Reducing *rpd3* function prematurely activates the dist5E enhancer fragment as indicated by premature expression of dist5E-*gfp::luc(nls)* in the type II neuroblast. (M) Schematic illustration of the context dependent role of PRC2 and Trx proteins on different target genes in type II neuroblasts, and the cooperation with Rpd3/HDAC1 to maintain *erm* in a poised sate. Dotted red line with bar: vestigial role in maintaining repression, Solid red line with bar: direct role in maintaining repression, Solid green line with arrow: direct role in activation, Dotted green line with arrow: potential role in activation.

not presented). These data are consistent with our ChIP qPCR results (Figure 14G-H), and suggest components of the Bithorax complex are differentially regulated in type II neuroblasts. In contrast, we found that Erm remained undetectable in *Su(z)12* and *E(z)* null type II neuroblasts, and its expression became reduced or undetectable in immature INPs (Figure 15D-F). These data indicate that PRC2 does not prevent premature Erm expression in type II neuroblasts, and led us to hypothesize that the *erm* immature INP enhancer is actively repressed through an alternative mechanism.

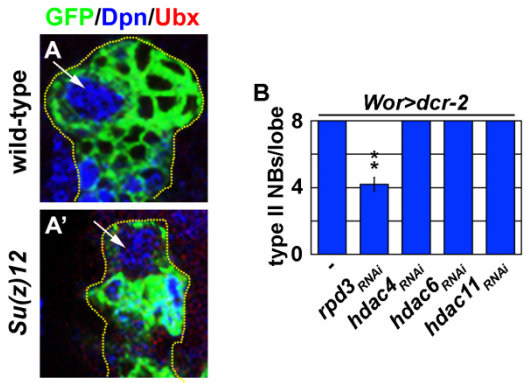

Figure 16: Analysis of chromatin modifiers in type II NB lineages. (A) Confocal images of 72hr wild-type and *Su(z)12*^{4} mutant clones showing the lack of ectopic Ubx expression in type II NBs deficient for PRC2 components (B) Quantification of type II NBs in brains over-expressing RNAi constructs targeting different histone deacetylase enzymes.

Because H3K27ac remained relatively low on the dist5E transgenic enhancer, we tested if robust histone deacetylation functions to prevent premature activation of the *erm* immature INP enhancer in type II neuroblasts. We knocked down the function of genes that encode histone deacetylases in neuroblasts by over-expressing *UAS-RNAi* transgenes, and determined that decreasing hdac1/*rpd3* function specifically and reproducibly led to a reduced number of type II neuroblasts per brain lobe (Figure 16B). To test if *rpd3* is indeed required for self-renewal, we generated mosaic clones derived from single *rpd3* null type II neuroblasts. A wild-type clone always contained a single type II neuroblast that measures approximately 10 μm in diameter (Figure 15G, J). In contrast, more than 50% of *rpd3* null type II neuroblasts displayed dramatically reduced

cell diameter, and 19% of *rpd3* null clones lacked identifiable type II neuroblasts (Figure 15H-J). Furthermore, over-expression of a *UAS-rpd3* transgene but not a *UAS-hdac3* transgene restored self-renewal in *rpd3* null type II neuroblasts (Figure 15J). These results strongly suggest that Rpd3-dependent histone deacetylation is essential for type II neuroblast self-renewal. We next tested if Rpd3 is required for maintaining the inactivity of the *erm* immature INP enhancer in type II neuroblasts. In agreement with our hypothesis, knocking down *rpd3* function led to premature activation of dist5E-*gfp::luc(nls)* in type II neuroblasts (Figure 15K-L). Thus, in contrast to PRC2, Rpd3 is required to prevent premature activation of the *erm* immature INP enhancer in type II neuroblasts. Together, these data indicate that robust Rpd3-dependent histone deacetylation works in conjunction with Trx to maintain the *erm* immature INP enhancer in a poised state in the type II neuroblast (Figure 15M).

Self-renewal transcriptional repressors and type II neuroblast transcriptional activators directly regulate *erm* expression by binding the immature INP enhancer

We next sought to identify specific transcription factors that control *erm* expression through the *erm* immature INP enhancer by using the dist5E enhancer as a platform. The self-renewal transcription factors Klu, Dpn and E(spl)mγ are excellent candidates for preventing premature activation of *erm* expression in type II neuroblasts because similar to the *rpd3* mutants, *klu* single or *dpn* & *E(spl)* double mutant type II neuroblasts also prematurely differentiate (Xiao et al., 2012; Zacharioudaki et al., 2012). Consistent with this possibility, we identified conserved Klu, Dpn and E(spl)mγ binding sites in the dist5E enhancer fragment, and found that Klu, Dpn and E(spl)mγ could directly bind

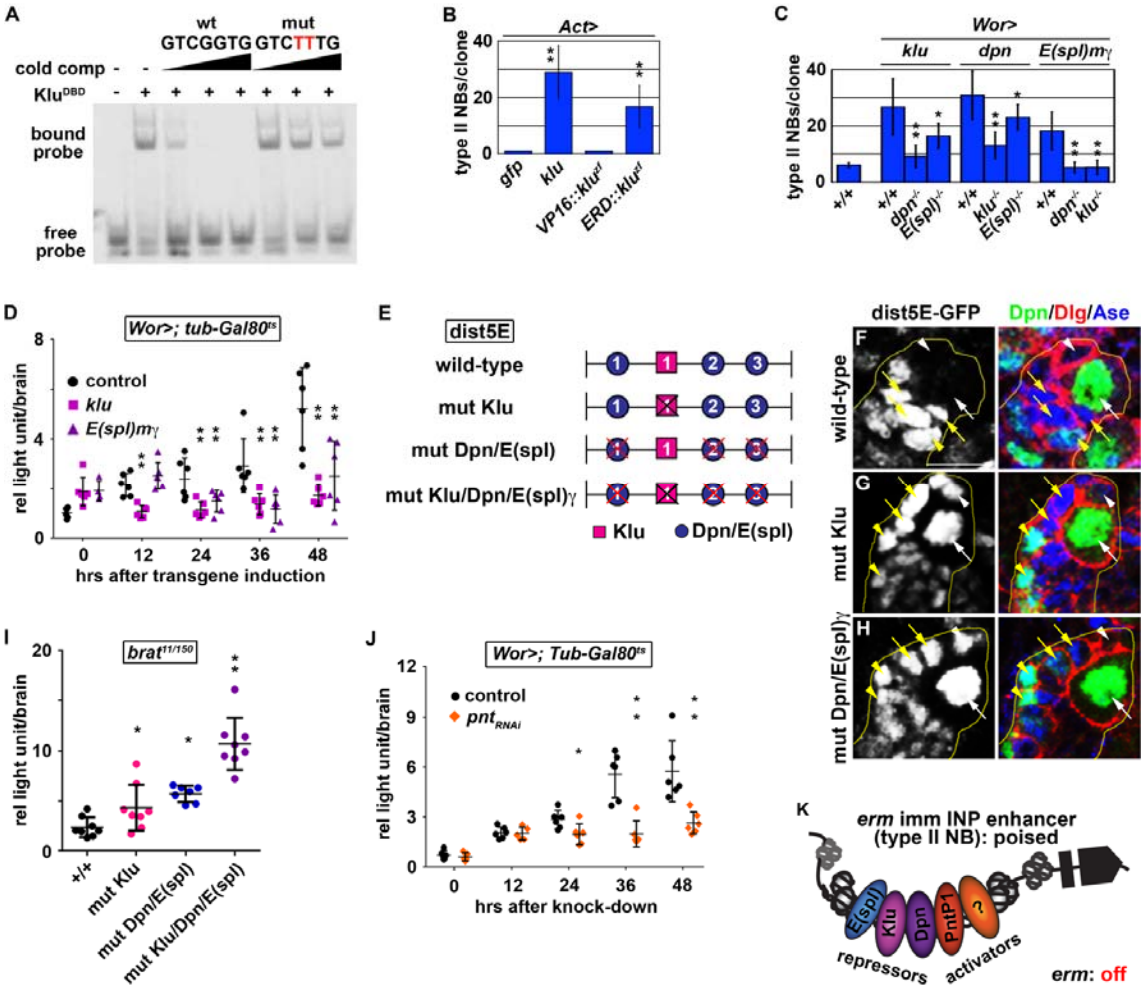

Figure 17: Dpn, E(spl)mγ, Klu and PntP1 directly bind and regulate activity of the dist5E enhancer. (A) Electromobility shift assays (EMSA) showing the interaction of the DNA-binding domain of Klu (Klu^{DBD}) with a putative Klu-binding site in the dist5E enhancer fragment. This binding can be reduced by competition with a wild-type but not a mutant cold competitor probe. (B) Quantification of the number of supernumerary type II NB-like cells in clones over-expressing wild-type Klu, a negative control (Klu^{zf}), ERD-Klu^{zf}, which works as a constitutive transcriptional repressor, or VP16-Klu^{zf}, which works as a constitutive transcriptional activator. (C) Quantification of the number of supernumerary type II neuroblasts in wild-type, and *dpn, E(spl)* or *klu* mutant clones over-expressing *klu*, *dpn* or *E(spl)mγ*. (D) Single brain luciferase assay showing the effect of overexpressing either Klu or E(spl)mγ on the activity of dist5E-*gfp::luc(nls)* relative to control brains (N ≥ 6 brains/time-point). (E) Schematic illustration of dist5E transgenes containing either wild-type or mutant Klu and Dpn/E(spl) binding sites. (F-H) Confocal images showing the expression pattern of wild-type and mutant *dist5E-gfp::luc(nls)* transgenes in type II NB lineages. (I) Single brain luciferase assay comparing the relative expression level of wild-type and mutant *dist5E-gfp::luc(nls)* transgenes in *brat* mutant brains (N ≥ 6 brains/time-point). (J) Single brain luciferase assay showing the effect of knocking down *pnt* on the expression of *dist5E-gfp::luc(nls)* relative to control brains (N ≥ 6 brains/time-point). (K) A summary of transcription factors bound to the *erm* dist5E enhancer in type II NBs. All bar graphs and dot plots are represented as mean ± SD, *: P-value ≤ 0.05, **: P-value ≤ 0.005.

these sites *in vitro* (Figure 17A; Figure 18A-C). Dpn and E(spl)mγ are evolutionarily conserved transcriptional repressors, but the mechanism by which Klu regulates gene expression is not clear (Kobayashi and Kageyama, 2014; Taelman et al., 2004b; Zacharioudaki et al., 2012). We generated a series of *UAS* transgenes that encode Klu^{zf} (the Klu DNA-binding zinc-finger motif only), VP16::Klu^{zf} (a VP16 transcriptional activation domain fused to the Klu zinc-finger motif), or ERD::Klu^{zf} (an Engrailed repression domain (ERD) fused to the Klu zinc-finger motif). Over-expression of the Klu^{zf} or the VP16::Klu^{zf} transgenic protein did not lead to supernumerary neuroblast formation (Figure 17B). By contrast, over-expression of the full-length Klu or the ERD::Klu^{zf} transgenic protein triggered the formation of supernumerary neuroblasts (Figure 17B). These data indicate that Klu promotes type II neuroblast self-renewal by acting as a transcriptional repressor. We extended our analyses to examine whether Klu functions collaboratively with Dpn and E(spl)mγ to promote type II neuroblast self-renewal. Removing *dpn* or *E(spl)mγ* function strongly suppressed supernumerary type II neuroblast formation induced by over-expression of *klu* (Figure 17C). Similarly, removing *klu* function strongly suppressed the supernumerary type II neuroblast phenotype induced by over-expression of *dpn* or *E(spl)mγ* (Figure 17C). Thus, Klu, Dpn and E(spl)mγ function interdependently as a transcriptional repressor network to promote type II neuroblast self-renewal.

To examine whether Klu, Dpn and E(spl)mγ promote type II neuroblast self-renewal by repressing *erm* expression through the dist5E enhancer, we took the following two complimentary approaches. We first tested whether Klu and E(spl)mγ are necessary and sufficient to prevent activation of dist5E-*gfp::luc(nls)* in type II

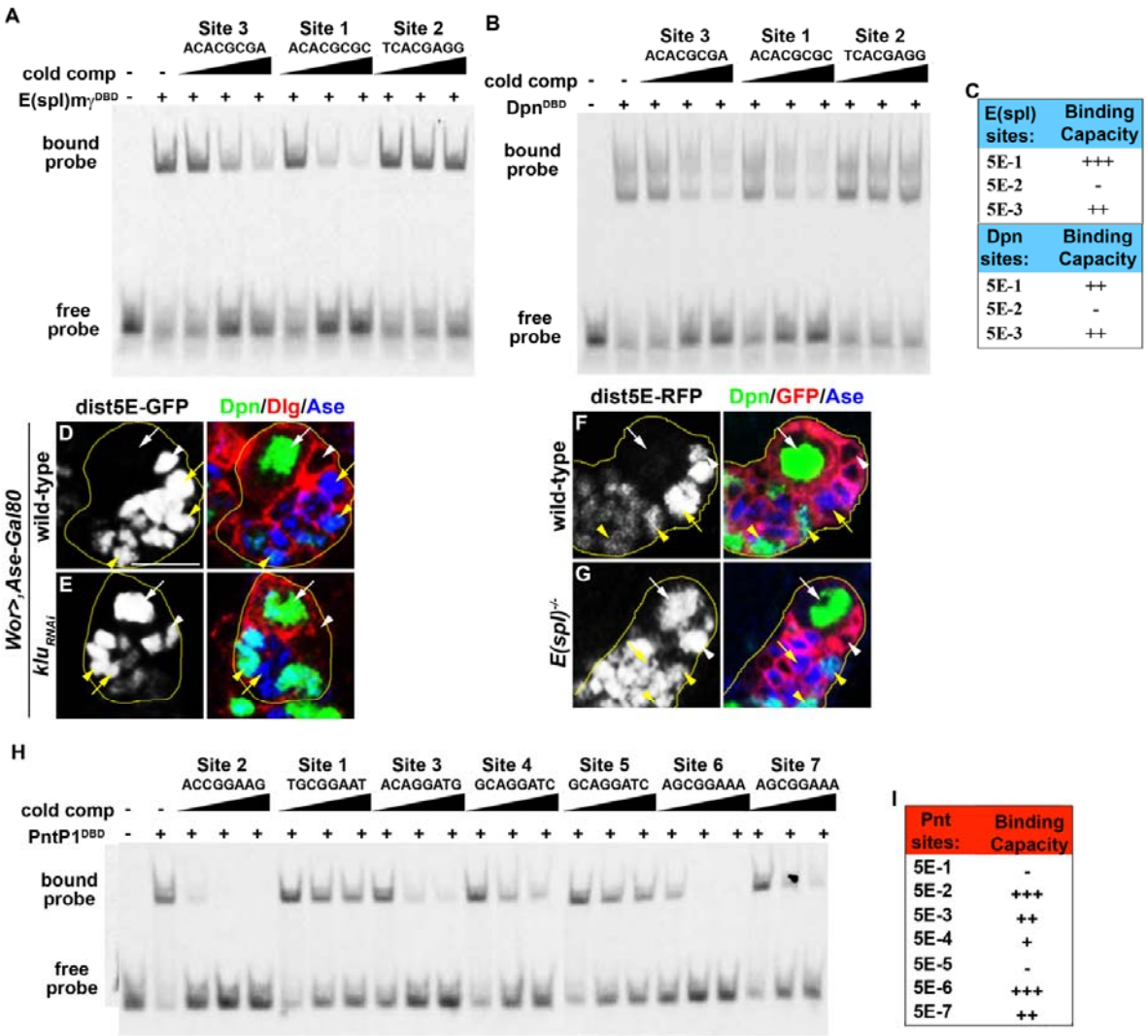

Figure 18: Dpn, E(spl)mγ, Klu and PntP1 directly bind and regulate activity of the dist5E enhancer fragment. (A-B) EMSA showing the affinity of the DNA binding domain of E(spl)mγ or Dpn to cold competitors bearing the sequence of the three predicted sites in the dist5E enhancer fragment. (C) Table summarizing the results of E(spl)mγ and Dpn EMSAs. (D-G) Confocal images showing the effect of knocking down *klu* or mutating the *E(spl)* locus on expression of dist5E reporter transgenes in type II NB lineages. (H) EMSA showing the affinity of the DNA binding domain of PntP1 to the seven predicted sites in the dist5E enhancer fragment. (I) Table summarizing the results of PntP1 EMSA.

neuroblasts. We chose to focus our analyses on *klu* and *E(spl)mγ* because Dpn and E(spl)mγ are members of the helix-loop-helix Orange transcription factors that regulate target gene expression by forming a heterodimer (Kobayashi and Kageyama, 2014; Taelman et al., 2004a; Zacharioudaki et al., 2012). Indeed, knock-down of *klu* function

or loss of the *E(spl)* locus resulted in premature activation of the dist5E-*gfp::luc(nls)* reporter in type II neuroblasts (Figure 18D-G), whereas over-expression of *UAS-klu* or *UAS-E(spl)mγ* was sufficient to reduce dist5E-*gfp::luc(nls)* activity in an *in vivo* luciferase assay (Figure 17D). Second, we examined whether Klu, Dpn and E(spl)mγ directly repress *erm* expression through the dist5E enhancer. We generated a series of mutant dist5E-*gfp::luc(nls)* reporters where the confirmed Klu-binding site or Dpn/E(spl)mγ-binding sites or both are mutated (Figure 17E). In contrast to the wild-type dist5E-*gfp::luc(nls)* reporter, the dist5E$^{\text{mut Klu}}$-*gfp::luc(nls)* or dist5E$^{\text{mut Dpn/E(spl)mγ}}$-*gfp::luc(nls)* showed detectable expression in type II neuroblasts (Figure 17F-H). To quantitatively assess this effect, we measured the *in vivo* luciferase activity of these reporters in *brat* null brains, which provided a reliable source of enriched type II neuroblast proteins. The dist5E$^{\text{mut Klu}}$-*gfp::luc(nls)* or the dist5E$^{\text{mut Dpn/E(spl)mγ}}$-*gfp::luc(nls)* reporter showed a significant increase in the luciferase activity relative to the wild-type dist5E-*gfp::luc(nls)* reporter (Figure 17I). In addition, the dist5E$^{\text{mut Klu/Dpn/E(spl)mγ}}$-*gfp::luc(nls)* reporter resulted in an even greater increase in the luciferase activity per brain (Figure 17I). Thus, Klu, Dpn and E(spl)mγ function cooperatively to promote type II neuroblast self-renewal by binding and repressing premature activation of the *erm* immature INP enhancer (Figure 17K). Furthermore, these results suggest that rapid down-regulation of Klu, Dpn and E(spl)mγ in immature INPs provides the permissive cue to allow rapid activation of the *erm* immature INP enhancer leading to Erm expression.

Because alleviating the repression by Klu, Dpn and E(spl)mγ leads to premature activation of the dist5E enhancer in type II neuroblasts, we hypothesized that

neuroblast-specific transcriptional activators function to activate the *erm* immature INP enhancer. The ETS-1 transcriptional activator PntP1 is specifically expressed in type II neuroblasts and in Ase$^-$ immature INPs making it an excellent candidate to activate *erm* expression (Figure 14A). Consistent with a potential role for PntP1 in *erm* activation, the dist5E enhancer contains seven conserved PntP1-binding sites, of which five could be bound by PntP1 (Figure 18H-I). In addition, knocking down *pntP1* function reduced the *in vivo* Luciferase activity of dist5E-*gfp::luc(nls*) (Figure 17J). Thes results are consistent with our previous findings that knocking down *pntP1* function led to supernumerary type II neuroblast formation mimicking the *erm* mutant phenotype, and that the heterozygosity of the *pnt* locus enhanced the supernumary neuroblast phenotype in *erm* hypomorphic brains (Komori et al., 2014a). Thus, PntP1 most likely contributes to the activation of the *erm* immature INP enhancer (Figure 17K). Together, these data led us to propose a novel paradigm where removing a group of transcriptional repressors, rather than addition of a transcriptional activator, facilitates rapid poised enhancer activation in stem cell progeny following asymmetric division.

Self-renewal transcriptional repressors function through Rpd3 to prevent premature activation of the *erm* immature INP enhancer in type II neuroblasts

Our data indicate that both self-renewal transcriptional repressors and Rpd3-dependent histone deacetylation play important roles in promoting self-renewal and maintaining the inactivity of the *erm* immature INP enhancer in type II neuroblasts. Thus, we tested if Klu, Dpn and E(spl)mγ function through Rpd3 to promote type II neuroblast self-renewal. We generated mosaic clones derived from *rpd3* null type II neuroblasts that over-expressed *klu*, *dpn* or *E(spl)mγ* individually. While over-expression of *klu* induced

supernumerary neuroblast formation in wild-type type II neuroblast clones, removing *rpd3* function completely suppressed the supernumerary neuroblast phenotype induced by *klu* over-expression (Figure 19A-C). Similarly, removal of *rpd3* function also strongly suppressed the supernumerary neuroblast phenotype induced by over-expression of *dpn* or *E(spl)mγ* (Figure 19C). Thus, the self-renewal transcriptional repressors function

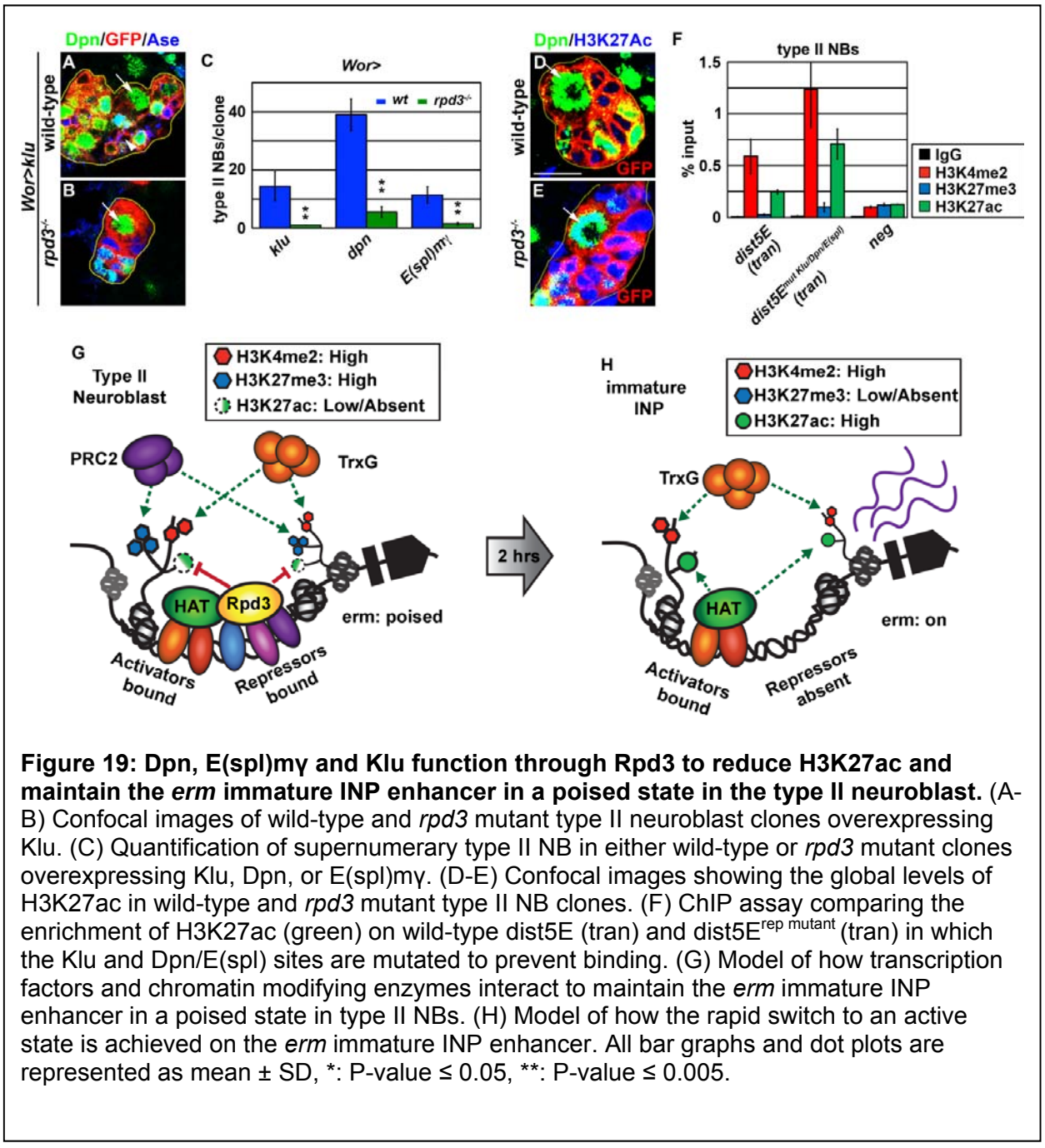

Figure 19: Dpn, E(spl)mγ and Klu function through Rpd3 to reduce H3K27ac and maintain the *erm* immature INP enhancer in a poised state in the type II neuroblast. (A-B) Confocal images of wild-type and *rpd3* mutant type II neuroblast clones overexpressing Klu. (C) Quantification of supernumerary type II NB in either wild-type or *rpd3* mutant clones overexpressing Klu, Dpn, or E(spl)mγ. (D-E) Confocal images showing the global levels of H3K27ac in wild-type and *rpd3* mutant type II NB clones. (F) ChIP assay comparing the enrichment of H3K27ac (green) on wild-type dist5E (tran) and dist5E$^{rep\ mutant}$ (tran) in which the Klu and Dpn/E(spl) sites are mutated to prevent binding. (G) Model of how transcription factors and chromatin modifying enzymes interact to maintain the *erm* immature INP enhancer in a poised state in type II NBs. (H) Model of how the rapid switch to an active state is achieved on the *erm* immature INP enhancer. All bar graphs and dot plots are represented as mean ± SD, *: P-value ≤ 0.05, **: P-value ≤ 0.005.

through Rpd3 to maintain a type II neuroblast identity. Next, we tested whether Klu, Dpn and E(spl)mγ function through Rpd3-dependent deacetylation of H3K27 to maintain the *erm* immature INP enhancer in a poised state in type II neuroblasts. Consistent with our hypothesis, all cell types within *rpd3* null type II neuroblasts clones displayed a drastic increase in H3K27ac (Figure 19D-E). Furthermore, the dist5E$^{\text{mut Klu/Dpn/E(spl)}}$-*gfp::luc(nls)* transgene showed elevated H3K27ac as compared to the dist5E-*gfp::luc(nls)* transgene in type II neuroblast enriched chromatin (Figure 19F). Thus, we conclude that continual recruitment of Rpd3 by self-renewal transcriptional repressors maintains the inactivity of the *erm* immature INP enhancer in the type II neuroblast by keeping H3K27ac below the threshold required for activation (Figure 19G). In the immature INP, down-regulation of self-renewal transcriptional repressors relinquishes the repressive effect of Rpd3, leading to increased H3K27ac and activation of the *erm* immature INP enhancer (Figure 19H).

Elucidating and validating a functional Erm-binding sequence

To elucidate how Erm restricts the developmental potential in immature INPs, we sought to identify a functional Erm-binding sequence. We screened a series of reporters that contain candidate Erm-binding sequences for their responses to the over-expression of a series of *erm* transgenes in *S2* cells and in larval brain neuroblasts. The Erm$^{\Delta N}$ transgenic protein is non-functional and serves as a negative control, and over-expression of VP16::Erm can exert a dominant negative effect on the supernumerary neuroblast phenotype in *erm* hypomorphic brains, most likely by activating Erm target gene expression (Janssens et al., 2014). Only the activity of the *gfp::luc(nls)* reporter bearing a putative Erm-binding sequence (referred to as the Erm response element

(ErmRE) hereafter) identified by the FlyFactor survey (http://mccb.umassmed.edu/ffs/TFdetails.php?FlybaseID=FBgn0031375) could be repressed by over-expression of Erm but activated by over-expression of VP16::Erm in *S2* cells (Figures 20A-B). Importantly, the *ErmRE^{mut}-gfp::luc(nls)* reporter, which contains two nucleotide substitutions in the ErmRE, was no longer responsive to expression of this collection of *erm* tansgenes in *S2* cells (Figure 20A-B). Next, we

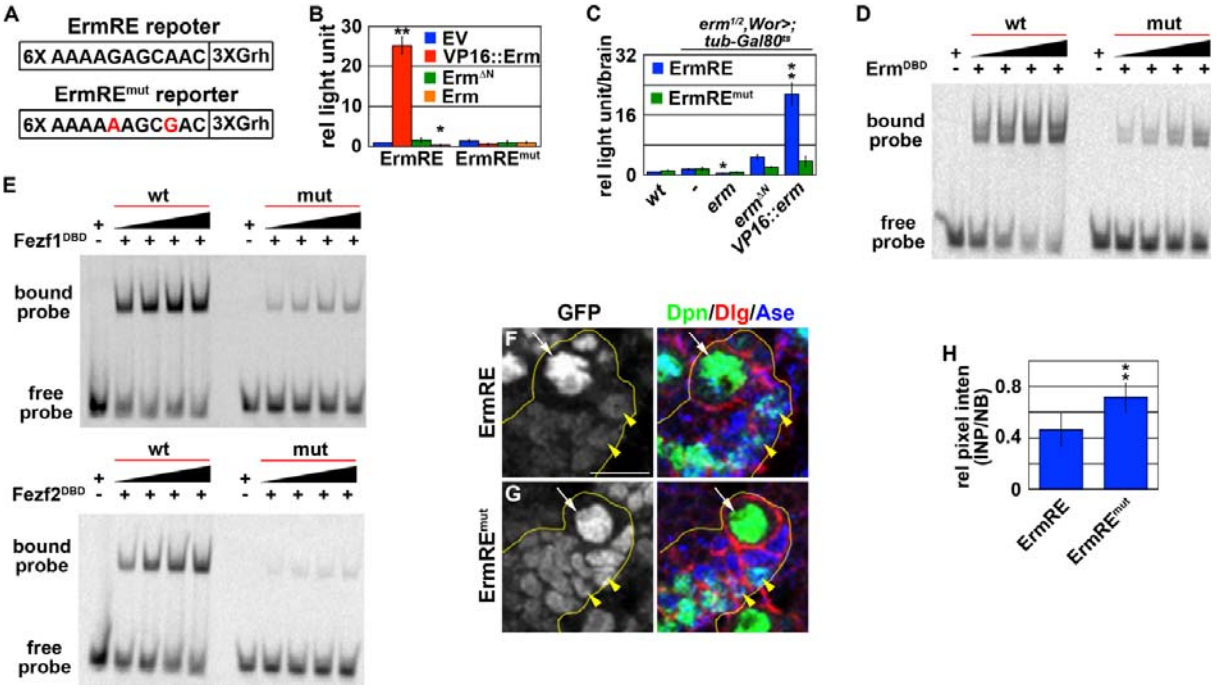

Figure 20: Identification of an Erm/Fezf consensus DNA-binding site. (A) An illustration showing the reporter transgene containing either a wild-type ErmRE or a mutant ErmRE (ErmRE^{mut}) used in *S2* cells and *in vivo* analyses. The reporter contains three Grainy head (Grh) binding sites that allow activation of reporter expression in all larval NB lineages. (B) Comparison of the relative expression levels of the ErmRE-*gfp::luc(nls)* and ErmRE^{mut}-*gfp::luc(nls* transgenes in response to contransfection with either *erm, erm$^{\Delta N}$,* or *VP16::erm* in S2 cells. N ≥ 5 transfections/sample. (C) Comparison of the relative expression levels of the ErmRE-*gfp::luc(nls)* and ErmRE^{mut}-*gfp::luc(nls* transgenes in *erm* null brains following a 12-hr pulse of *erm, erm$^{\Delta N}$,* or *VP16::erm.* N ≥ 3 pooled samples/genotype. (D-E) EMSA showing the interaction of the zinc-finger motif of Erm, Fezf1 or Fezf2 with either the ErmRE probe or an ErmRE^{mut} probe. (F-G) Confocal images showing the expression of ErmRE-*gfp::luc(nls)* or ErmRE^{mut}-*gfp::luc(nls)* in type II NBs compared to INPs within the same lineage. (H) Quantification of the relative pixel intensity of ErmRE-GFP::Luc(nls) or ErmRE^{mut}-GFP::Luc(nls) in INPs relative to type II neuroblasts. N ≥ 8 lineages/reporter. Scale bar, 10 μm.

generated transgenic flies bearing the *ErmRE-gfp::luc(nls)* or *ErmRE^{mut}-gfp::luc(nls)* transgene (Figure 20A). Consistent with the observations made in *S2* cells, *ErmRE-gfp::luc(nls)* but not *ErmRE^{mut}-gfp::luc(nls)* can be repressed by over-expression Erm and activated by over-expression of VP16::Erm in larval brains (Figure 20C). Lastly, we confirmed that the zinc-finger motif of Erm, as well as the vertebrate homologs of Erm, Fezf1 and Fezf2, bound the ErmRE with a high affinity and specificity *in vitro* (Figure 20D-E). Thus, we conclude that AAAAGAGCAAC is a consensus DNA sequence recognized by the Fezf family of transcription factors from *Drosophila* to mammals.

To functionally validate the specificity of ErmRE *in vivo*, we examined the expression of *ErmRE-gfp::luc(nls)* or *ErmRE^{mut}-gfp::luc(nls)* in the type II neuroblast lineage in wild-type brains, where endogenous Erm is exclusively expressed in Ase^{-} and Ase^{+} immature INPs (Figure 14A). The activity of *ErmRE-gfp::luc(nls)* became down-regulated in immature INPs as compared to the type II neuroblast, and its expression remained low in INPs (Figure 20F, H). In contrast, the expression of *ErmRE^{mut}-gfp::luc(nls)* did not become down-regulated in immature INPs and INPs to a similar extent as *ErmRE-gfp::luc(nls)* (Figure 20G-H). These data indicate that the ErmRE can be recognized and repressed by endogenous Erm, and AAAAGAGCAAC is a functional Erm-binding sequence.

Erm restricts the developmental potential in immature INPs by repressing *pntP1* and *grhO* transcription

To identify the direct targets of Erm that it represses to restrict the developmental potential of INPs, we started by performing a microarray analyses looking for genes whose transcript levels became up-regulated in *erm* null brains. We found multiple

genes that encode proteins highly expressed in type II neuroblasts were significantly up-regulated in *erm* mutants, and confirmed this result using qPCR (Figure 21A). To distinguish direct targets from indirect targets, we examined the responsiveness of these genes to a 12-hour pulse of transgenic Erm or VP16::Erm over-expression in *erm* null brains. We found that the transcripts for *pntP1* and *grhO* could be repressed by over-expression of *erm*, and induced by over-expression of *VP16::erm* (Figure 21A). By contrast, over-expression of these *erm* transgenes did not have as pronounced an effect on the transcription of *dpn*, *klu*, *pntP3* and *grhN* (Figure 21A). These data strongly suggest that *pntP1* and *grhO* are direct targets of Erm.

To test if *pntP1* and *grhO* are indeed direct targets of Erm, we generated a position weight matrix for our identified Erm-binding sequence and used this to scan the *pntP1* and *grhO* loci for potential Erm-binding sites. Strikingly, we found a cluster of six putative Erm-binding sites just upstream of the *pntP1* TSS and three putative Erm-binding sites just upstream of the *grhO* TSS. Consistent with the possibility that these clusters of sites may represent functional ErmREs, they are conserved in all *Drosophila* species. More importantly, the Erm DNA-binding domain can bind at least four of the sites we identified in the *pntP1* locus and three of the sites we identified from the *grhO*

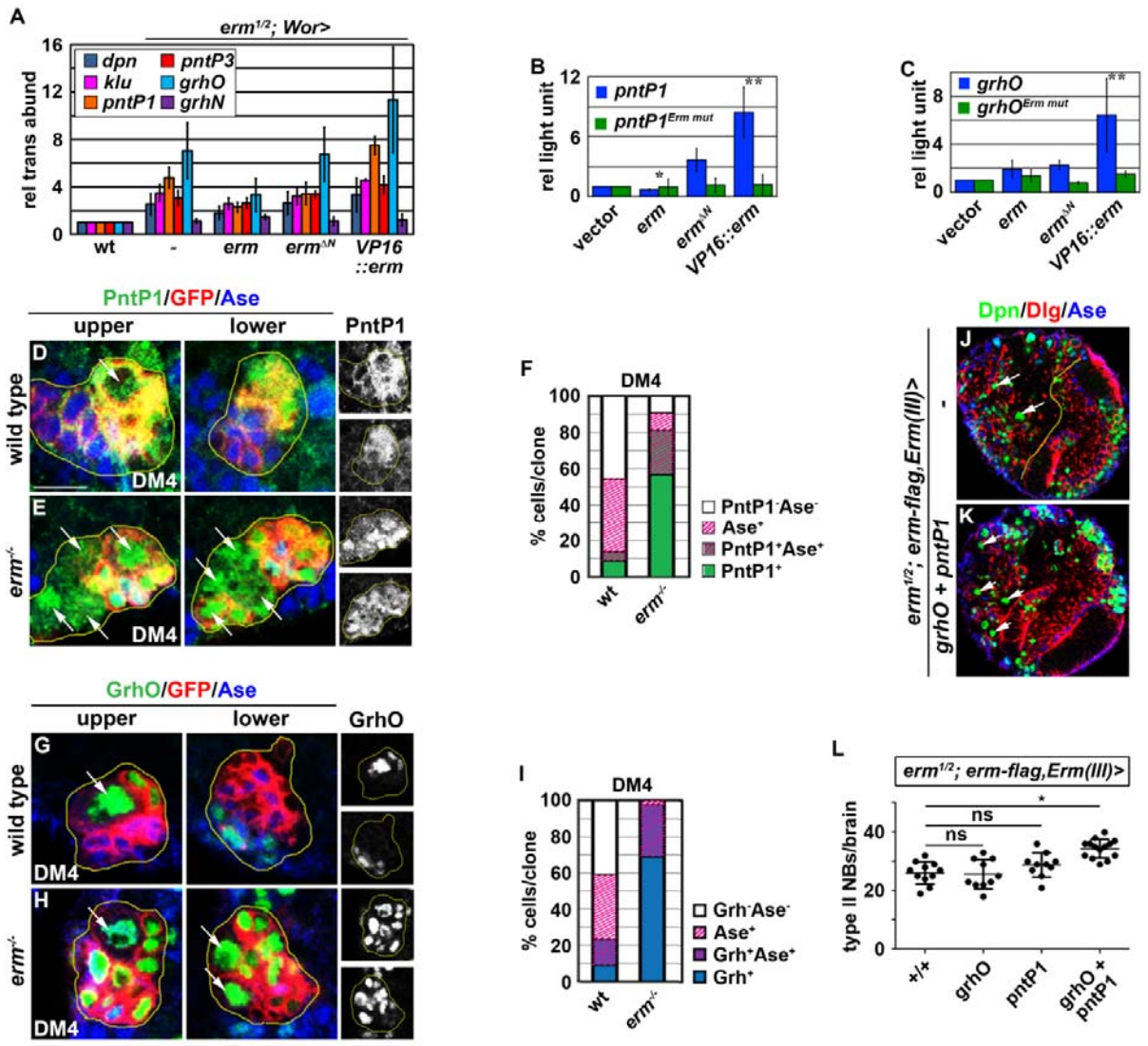

Figure 21: Erm restricts the developmental potential by repressing *pntP1* and *grhO* transcription. (A) qPCR analysis of the relative abundance of *dpn*, *klu*, *pntP1*, *pntP1*, *grhO*, and *grhN* transcripts in *erm* null brains following a 12-hr pulse of *erm, erm$^{\Delta N}$,* or *VP16::erm* N ≥ 3 samples/genotype.(B) Comparison of the relative expression levels of both a wild-type *pntP1* promoter that contains six conserved Erm-binding sites (PntP1-GFP::Luc(nls)) or a *pntP1* promoter containing mutant Erm-binding sites (PntP1$^{\text{Erm mut}}$-GFP::Luc(nls)) in S2 cells cotransfected with either *erm, erm$^{\Delta N}$,* or *VP16::erm.* N ≥ 3 transfections/sample. (C) Comparison of the relative expression levels of both a wild-type *grhO* promoter that contains three conserved Erm-binding sites (GrhO-GFP::Luc(nls)) or a *grhO* promoter containing mutant Erm-binding sites (GrhO$^{\text{Erm mut}}$-GFP::Luc(nls)) in S2 cells cotransfected with either *erm, erm$^{\Delta N}$,* or *VP16::erm.* N ≥ 3 transfections/sample. (D-E) Confocal images showing PntP1 expression in wild-type and *erm* null DM4 type II neuroblasts. Upper/lower: the upper or lower confocal optical section of the z-series. (F) Quantification of the percentage of cells per DM4 clone that are PntP1+, Ase+, or positive for both. N ≥ 5 clones/genotype.

(legend continued on next page)

Figure 21 (continued): (G-H) Confocal images showing GrhO expression in wild-type and *erm* null DM4 type II neuroblasts. Upper/lower: the upper or lower confocal optical section of the z-series. (I) Quantification of the percentage of cells per DM4 clone that are GrhO+, Ase+, or positive for both. N ≥ 5 clones/genotype (J-K) Confocal images of *erm* hypomorphic (*erm*$^{1/2}$, *erm-flag*) larval brains mis-expressing *pntP1* and *grhO* in Ase+ immature INP and INPs (*Erm(III)>*). Quantification of the number of type II NB-like cells in *erm* hypomorphic (*erm*$^{1/2}$, *erm-flag*) larval brains mis-expressing either *pntP1* or *grhO* alone or both *pntP1* and *grhO* together in Ase+ immature INP and INPs (*Erm(III)>*).

locus (Figures 22A-B). Lastly, a *pntP1-luc* reporter containing the *pntP1 cis*-regulatory region with wild-type, but not mutant, Erm-binding sites could be repressed by wild-type Erm and activated by VP16::Erm in *S2* cells (Figure 21B). Similarly, only a *grhO-luc* reporter containing wild-type Erm-binding sites was activated by VP16::Erm in *S2* cells (Figure 21C). Thus, we conclude Erm can directly bind upstream of the *pntP1* TSS and *grhO* TSS.

To determine whether Erm is required to down-regulate the expression of *pntP1* and *grhO in vivo*, we tested whether PntP1 or GrhO becomes mis-regulated in *erm* null type II neuroblast clones. Consistent with previous reports (Zhu et al., 2011), PntP1 was detected in neuroblasts and a few immature INPs in wild-type clones, but undetectable in remaining cells of the type II neuroblast lineage (Figure 21D). By contrast, we detected ectopic PntP1 expression in all *erm* null type II neuroblast clones, but the severity of mis-regulated PntP1 expression differed among type II neuroblast lineages. In the *erm* mutant clones derived from the DL1, DM2, DM4 or DM5 type II neuroblast, PntP1 became ectopically expressed in virtually all cells (Figure 21E-F, Figure 22C-D, F). In the *erm* mutant clones derived from the DL2, DM1, DM3, and DM6 type II neuroblast, PntP1 was down-regulated in immature INPs similar to wild-type clones, before becoming re-expressed in INPs as they began to revert into supernumerary neuroblasts (Figure 22C-D, F; data not presented). Similar to PntP1, we found GrhO

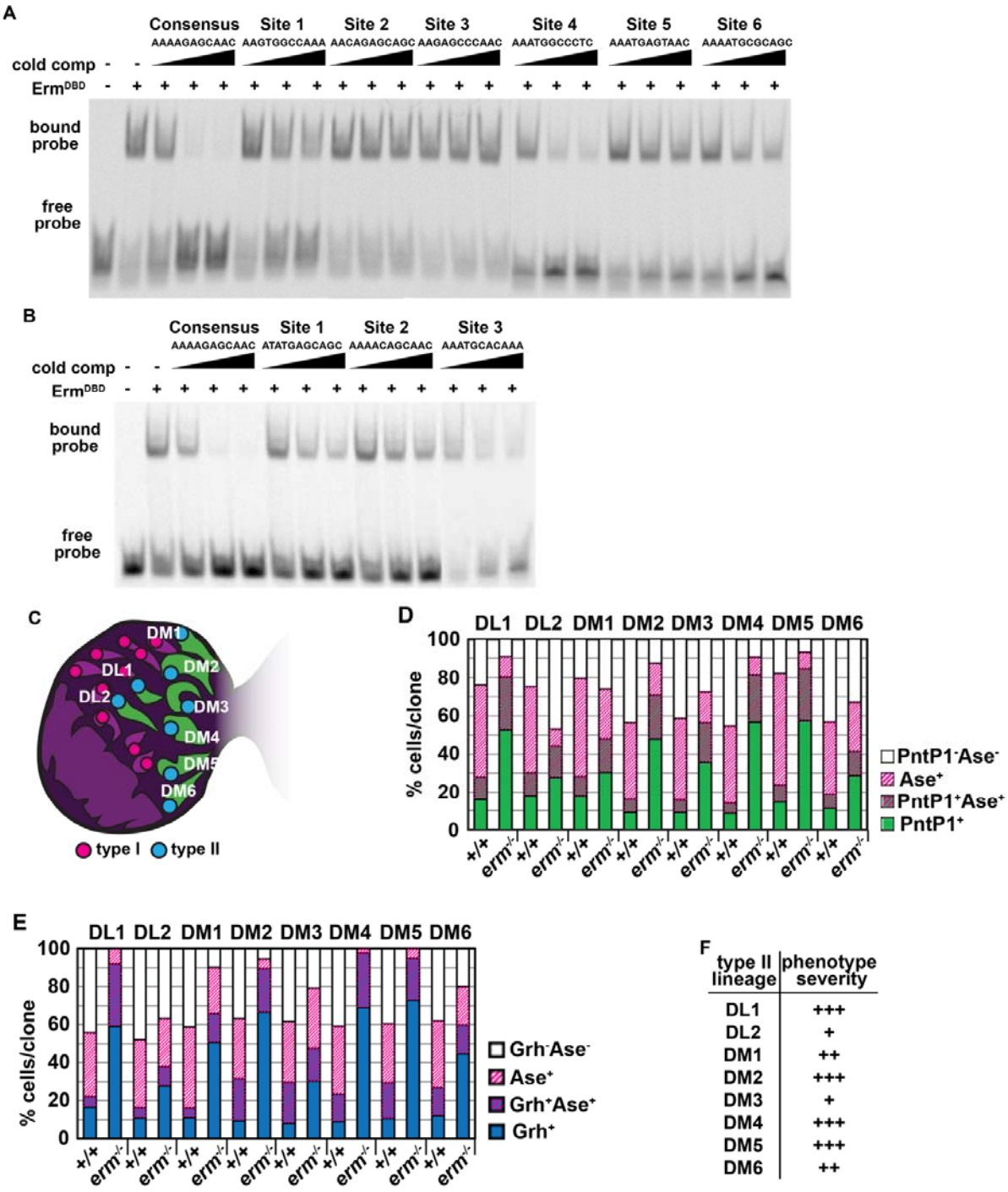

Figure 22: Erm directly binds the *pntP1* and *grhO* promoters to repress their expression during INP maturation. (A) EMSA showing the affinity of the DNA binding domain of Erm to cold competitors bearing the sequence of the six predicted sites in the PntP1 promoter. (B) EMSA showing the affinity of the DNA binding domain of Erm to cold competitors bearing the sequence of the three predicted sites in the GrhO promoter. (C) Schematic showing the position of the eight type II NB lineages in the larval brain.

(legend continued on next page)

Figure 22 (continued): (D) Quantification of the percentage of cells per clone that are PntP1+, Ase+, or positive for both in each of the eight type II NB lineages. N ≥ 5 clones/genotype. (E) Quantification of the percentage of cells per clone that are GrhO+, Ase+, or positive for both in each of the eight type II NB lineages. N ≥ 5 clones/genotype. (F) Table summarizing the severity of the *erm* mutant phenotype in the eight different type II NB lineages.

also became ectopically expressed in *erm* null type II neuroblast clones in a lineage-dependent pattern (Figure 21G-I; Figure 22C, E-F). Thus, we conclude that Erm directly represses PntP1 and GrhO expression in immature INPs, and that an additional partially redundant mechanism may work in parallel to Erm to regulate PntP1 and GrhO expression in a subset of type II neuroblast lineages.

We hypothesized that Erm restricts the developmental potential in immature INPs by repressing the transcription of genes important for the type II neuroblast functional identity. Thus, we tested if over-expression of *grhO* or *pntP1* in late stage (Ase^{+}) immature INPs as well as mature INPs, driven by *Erm-Gal4(III)*, can trigger INPs to revert into supernumerary type II neuroblasts. Over-expression of either gene individually or in combination was insufficient to induce INP reversion in wild-type brains (data not presented). These results suggested that Erm repress additional transcriptional activators that function cooperatively with PntP1 and GrhO to promote a type II neuroblast identity. Thus, we over-expressed *grhO* or *pntP1* individually or in combination under control of the *Erm-Gal4(III)* driver in *erm* hypomorphic brains. While over-expression of *grhO* or *pntP1* alone was unable to increase the reversion of INPs into supernumerary type II neuroblasts, co-expression of *grhO* and *pntP1* was sufficient to enhance INP reversion into supernumerary type II neuroblasts (Figure 21J-L). Thus, Erm restricts the developmental potential in immature INPs by acting as a negative

feedback regulator to repress components of the transcriptional activator network that maintains type II neuroblast identity (Figure 23).

Discussion

Numerous tissue-specific stem cell types amplify the output of each division by producing intermediate progenitors, and precise restriction of the developmental potential of intermediate progenitors is critical for proper differentiation following asymmetric stem cell divisions. Elucidating the molecular mechanisms that restrict the developmental potential in intermediate progenitors will provide critical insight into the precise generation of specific differentiated cell types, as well as the susceptibility of intermediate progenitors to forming tumor-initiating cells when these mechanisms go awry. We have demonstrated that in type II neuroblasts, self-renewal transcriptional repressors recruit the histone deacetylase Rpd3 to maintain the immature INP enhancer of *erm* in an inactive but poised state (Figure 17-19). Following asymmetric neuroblast division, self-renewal transcriptional repressors become rapidly downregulated by asymmetrically segregated cell fate determinants in the immature INP (Haenfler et al., 2012; Janssens et al., 2014;

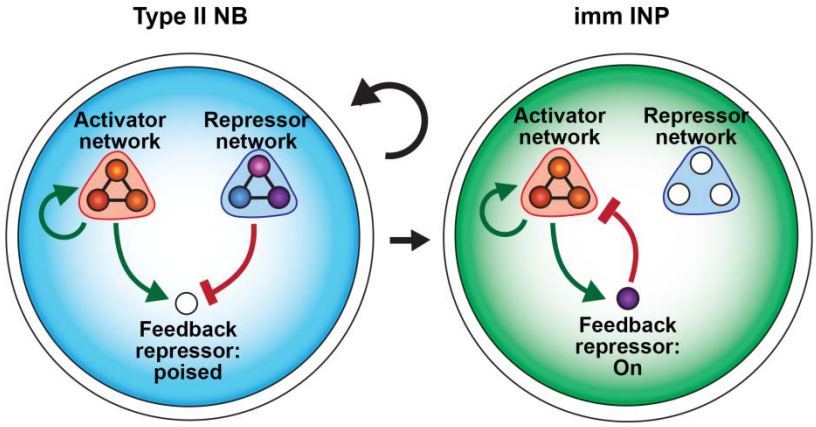

Figure 23: A poised feedback circuit balances continual self-renewal of type II neuroblasts with rapid restriction of developmental potential in immature INPs.
(A) Summary model showing how balancing the activity of an activator network with a repressor network in type II neuroblasts maintains the feedback repressor (Erm) in an inactive but poised state, facilitating continual self-renewal. Following asymmetric division, selective downregulation of this repressor network allows rapid activation of the feedback circuit in immature INPs which then represses components of the type II neuroblast activator network to stably restrict the developmental potential of INPs.

Xiao et al., 2012). Our results demonstrate this cue initiates the restriction of INP developmental potential by relinquishing Rpd3 activity on the poised *erm* enhancer and allowing for Erm activation in immature INPs within two hours of their birth. Once activated, Erm prevents INPs from reverting into supernumerary type II neuroblasts by forming a negative feedback mechanism that represses the expression of neuroblast transcriptional activators. This highly streamlined mechanism directly couples the down-regulation of self-renewal repressor activities to the activation of a master regulator of differentiation, and ensures that the developmental potential of an uncommitted intermediate progenitor becomes rapidly restrained prior to its entry into the next cell cycle (Figure 23). Previous studies in human and mouse embryonic stem cells revealed that PRC2 is bound to the promoter of *Fezf2*, a vertebrate homolog of *erm*, and the *Fezf2* neurogenic enhancer displays H3K4me1 and H3K27me3 (Boyer et al., 2006; Eckler et al., 2014; Rada-Iglesias et al., 2011; Shim et al., 2012). This suggests embryonic stem cells maintain *Fezf2* in a poised state for subsequent activation in the developing nervous system. Thus, the poised circuit we describe is likely conserved in vertebrates, and may regulate restriction of the developmental potential of intermediate progenitors in vertebrate tissue-specific stem cell lineages.

Maintaining the cell type-specific enhancer of a master regulator of differentiation in a poised state in self-renewing stem cells

To meet the fast pace of development and the fluctuating demands of tissue homeostasis, a multipotent intermediate progenitor needs to rapidly acquire restricted developmental potential before re-entering the cell cycle to produce differentiated cell types. Maintaining the cell type-specific enhancers of master regulators of lineage

commitment and differentiation in a poised chromatin state has been suggested to facilitate their efficient activation in stem cell progeny (Heinz et al., 2015). The prevailing model of poised enhancer regulation is that the H3K4me1/2 and H3K27me3 histone marks, and their associated chromatin modifiers, serve to maintain the primed state of poised enhancers while preventing premature activation respectively. This paradigm predicts that removing PRC2, which catalyzes H3K27me3 formation, should lead to premature activation of a poised enhancer and de-repression the associated gene. Surprisingly, we find that although the transgenic dist5E enhancer is inactive in type II neuroblasts it does not display H3K27me3 (Figure 14I), and removing PRC2 function led to loss of endogenous Erm expression instead of premature activation of Erm expression (Figure 15D-F). This indicates PRC2 is not required to maintain repression of the poised *erm* immature INP enhancer in type II neuroblasts. By contrast, removing *Hdac1/rpd3* function led to premature activation of the transgenic *erm* enhancer in type II neuroblasts and resulted in premature type II neuroblast differentiation, likely due to de-repression of Erm expression (Figure 15G-L). Based on these findings, we propose a new model in which Hdac1/Rpd3 but not PRC2 is required to maintain repression of the poised enhancer of a master regulator of differentiation in self-renewing stem cells. One possible explanation for this apparent difference in the role of PRC2 during poised gene regulation is that PRC2 functions in a context dependent manner on different poised enhancers, or even on the same poised enhancer in distinct stem cell types. Our characterization of the kinetics of dist5E-GFP::Luc(nls) activation *in vivo* demonstrated the poised *erm* immature INP enhancer is activated within two-hours of stem cell division, mimicking endogenous Erm expression (Figure 14C-F). Thus, we propose the

erm immature INP enhancer is part of a specific class of fast-activating poised enhancers that rely primarily on deacetylation by Hdac1/Rpd3 to maintain their repression.

Activation of a poised enhancer of a fast activating gene in uncommitted intermediate progenitors

The prevailing model suggests activation of a poised enhancer occurs in a sequential manner and is initiated by the binding of a signal-dependent transcriptional activator followed by the recruitment of a histone demethylase to remove H3K27me3 and then a histone acetytransferase to acetylate H3K27 (Heinz et al., 2015; Park et al., 2014). However, this stepwise and relatively cumbersome mechanism is likely not appropriate for a fast-activating poised gene like *erm* that is expressed in immature INPs within two-hours of their birth. In this study, we report two novel findings that enable rapid activation of a master regulator of differentiation whose expression is highly time-sensitive. First, multiple self-renewal transcriptional repressors directly bind the *erm* immature INP enhancer in type II neuroblasts and work cooperatively to maintain the poised state through continual deacetylation of H3K27 by Rpd3 (Figure 17, 19). This result strongly suggests the H3K27 histone acetyltransferase (HAT) is already present on the *erm* immature INP enhancer in type II neuroblasts (Figure 19G). One attractive possibility is that lineage-specific transcriptional activators that are expressed in type II neuroblasts and immature INPs, such as PntP1, mediate recruitment of the H3K27 HAT to the *erm* immature INP enhancer. This would explain why this Erm is specifically expressed in the progeny of type II neuroblasts. Second, selective downregulation of self-renewal transcriptional repressor proteins alleviates Rpd3-mediated deacetylation,

allowing the rapid accumulation of H3K27ac on the poised enhancer and activation of Erm expression in immature INPs (Figure 19H). This suggests the incorporation of new histones during DNA replication, together with continual recruitment of a HAT, may bypass active demethylation of H3K27 as a prerequisite for activation of fast-activating poised enhancers. Directly coupling the stem cell transcription factor network to activation of the master regulator of differentiation through its poised enhancer, and selectively downregulating self-renewal transcriptional repressors in stem cell progeny, provides a robust and efficient strategy to ensure rapid restriction of developmental potential following asymmetric division. We propose the regulatory logic described here is likely broadly applicable to numerous stem cell types in both *Drosophila* and vertebrates.

Regulation of restricted developmental potential

Restricting the developmental potential in intermediate progenitors involves restraining the mechanisms that endow stem cells with their unique functional properties. Our study identified *pntP1* and *grhO* as direct targets of Erm (Figure 21-22). Co-expression of *pntP1* and *grhO* was sufficient to enhance INP reversion into supernumerary type II neuroblasts in hypomorphic *erm* mutant brains (Figure 21J-L), suggesting that Erm restricts the developmental potential of INPs by directly repressing components of the type II neuroblast transcription factor network (Figure 23). Interestingly, PntP1 is also required for activating the *erm* immature INP enhancer, and loss of *pntP1* function leads to supernumerary type II neuroblast formation mimicking the *erm* null phenotype (Komori et al., 2014a). Thus, Erm-dependent restriction of developmental potential most likely also dismantles the mechanisms that promote activation of its own enhancer. Erm

is the first example of a fast-activating poised gene that restricts the developmental potential in intermediate progenitors by acting as a negative feedback circuit and repressing components of the stem cell transcription factor network (Figure 23). Identifying similar regulatory circuits that balance self-renewal with differentation in other stem cell lineages will require in-depth knowledge of (1) the core stem cell transcription factor network, (2) the functional consequence of the binding of specific transcription factors to the poised enhancers of pro-differentiation genes (i.e activation vs. repression), and (3) the mechanisms that alter the activity of components of the stem cell transcription factor network in stem cell progeny. Ultimately, understanding these poised regulatory circuits will facilitate the precise generation of specific differentiated cell types for regenerative medicine, and provide insight into how specific oncogenic lesions contribut to the formation and growth of stem cell and intermediate progenitor derived tumors.

Materials & Methods

Construction of *VanGlow* reporter vectors.

We created a new transgenic reporter vector (*VanGlow*) to facilitate rapid cloning of cis-regulatory elements upstream of either a GFP::Luciferase(nls) or mCherry::Renilla(nls) reporter for applications in transgenic fly lines as well as in tissue culture cells (Figure 24A-B). Synthetic nucleotides encoding a GFP::Luciferase(nls) or mCherry::Renilla(nls) (codon optimized for expression in *Drosophila*) and a yeast transcriptional terminator flanked by HindIII sites were generated by GeneArt™ (Thermofisher scientific). These constructs where then cloned into the BPGw (Addgene #17574) and BPGUw (Addgene #17575) vectors using the HindIII sites to replace GAL4, generating the promoter and enhancer *VanGlow* vectors respectively.

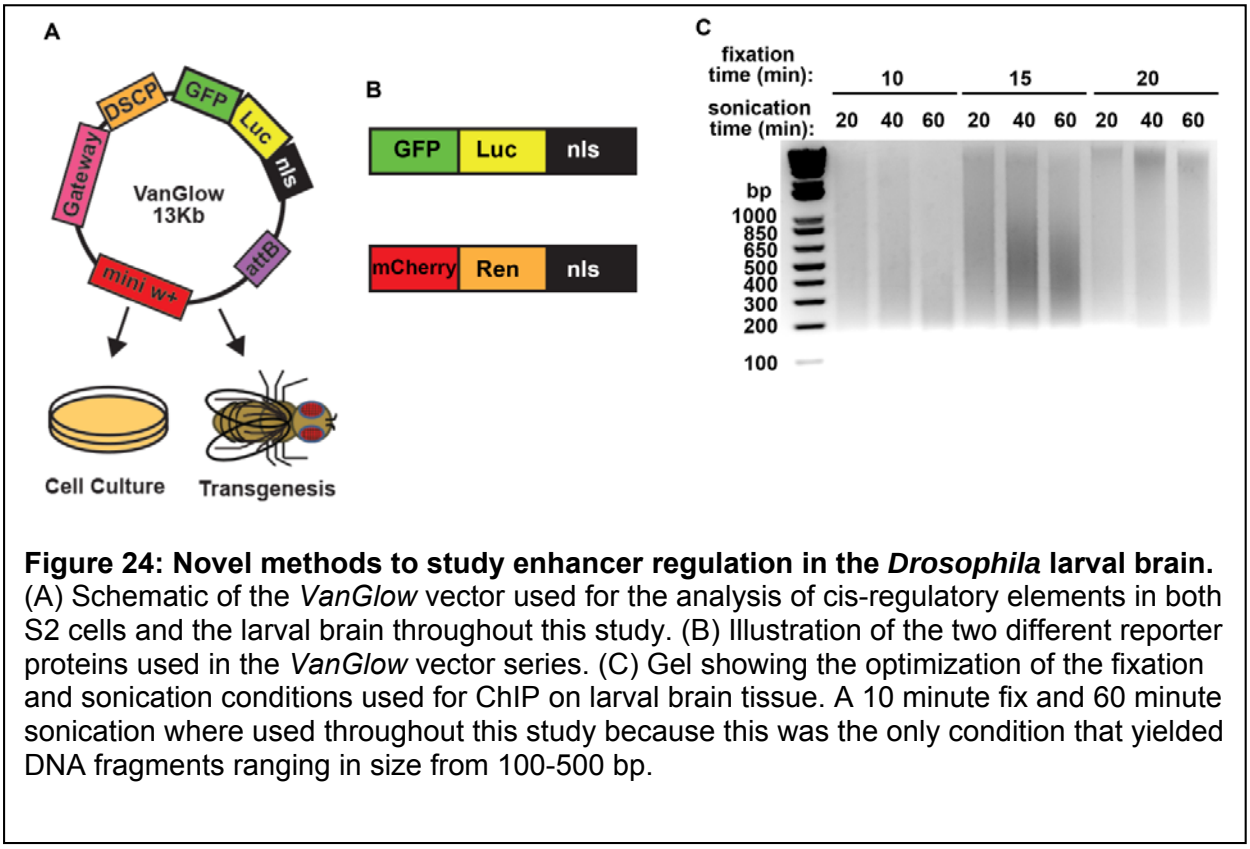

Figure 24: Novel methods to study enhancer regulation in the *Drosophila* larval brain. (A) Schematic of the *VanGlow* vector used for the analysis of cis-regulatory elements in both S2 cells and the larval brain throughout this study. (B) Illustration of the two different reporter proteins used in the *VanGlow* vector series. (C) Gel showing the optimization of the fixation and sonication conditions used for ChIP on larval brain tissue. A 10 minute fix and 60 minute sonication where used throughout this study because this was the only condition that yielded DNA fragments ranging in size from 100-500 bp.

Fly strains

Wild type and mutant *dist5E-gfp::luc(nls)* and *dist5E-rfp::ren(nls)* transgenic fly lines were generated by Gateway® cloning the wild-type and mutant sequences (generated as 500bp gBlocks® from IDT) into the *VanGlow* vector. The *ermRE-gfp::luc(nls)* and *ermRE^{mut}-gfp::luc(nls)* reporter lines were generated using a similar approach, except synthetic nucleotides bearing six copies of a putative Erm-binding motif and three Grh consensus binding motifs (included to increase basal expression levels) with a random eight nucleotide spacer between each motif were used as templates. Constructs were then inserted into the PBAC (yellow[+]-attP-3B)VK00033 docking site via ϕC31 integrase-mediated transgenesis (Bischof and Basler, 2008). Additional fly lines used in this study include *erm^{1}, erm^{2}* (Weng et al., 2010), *brat^{150}* (Betschinger et al., 2006), *Erm-GAL4(III)* (Pfeiffer et al., 2008), *Wor-GAL4* (Lee et al., 2006b), *Ase-Gal80* (Neumüller et al., 2011), *UAS-klu$_{shmiR}$* (Berger et al., 2012), *UAS-klu::HA* (Xiao et al., 2012), *UAS-dpn* (Wallace et al., 2000), *UAS-E(spl)mγ, FRT82B P[gro^{+}]Df(3R)E(spl)b32.2* (gift from C. *Delidakis), dpn^{1}* (gift from Y.Jan), *klu^{R51}* (Kaspar et al., 2008), *UAS-erm::HA*, *UAS-erm$^{\Delta N}$*, *UAS-VP16::erm* (Janssens et al., 2014), *UAS-pntP1* (Zhu et al., 2011), *UAS-grhO'* (gift from S. Bray). The following fly stocks were obtained from the Bloomington *Drosophila* Stock Center: Oregon R*, E(z)^{731}, FRT2A, Su(z)12^{4}, FRT2A, brat^{11}, Act-FRT-Stop-FRT-GAL4, tub-GAL80, FRT82B, FRT2A* and *hs-flp, tub-GAL80^{ts}, Elav-GAL4, 12E9-GAL4, UAS-GFP(nls), UAS-flp , UAS-mCD8-GFP,* and *UAS-dcr2*. We obtained the following stocks from the Vienna *Drosophila* RNAi Center: *UAS-pnt$_{RNAi}$* (7171), *UAS-trx$_{RNAi}$* (108122), *UAS-rpd3$_{RNAi}$.*

Immunofluorescence staining and antibodies

Larval brains were dissected in PBS, fixed in 100 mM PIPES (pH 6.9), 1 mM EGTA, 0.3% Triton X-100, 1 mM $MgSO_4$ containing 4% formaldehyde for 23 minutes and processed for immunofluorescence staining according to a previously published protocol (Weng et al., 2010). Antibodies used in this study include rabbit anti-Erm (1:100), and guinea pig anti-Ase (1:1000) (Janssens et al., 2014), rat anti-Dpn (1:2) and rat anti-Wor (1:2)(Lee et al., 2006b), rabbit anti-Ase (1:400) (Weng et al., 2010), rabbit anti-PntP1 (1:600; Skeath JB), rat anti-Grh (1:1000; Thor S.), rabbit anti-H3K27me3 (1:500; 07–449; Millipore, Billerica, MA), mouse anti-Ubx (1:500; FP3.38, DSHB), mouse anti-Abd-B (1:500; 1A2E9, DSHB), mouse anti-Dlg (1:50; 4F3E3E9, DSHB), chicken anti-GFP (1:2000; cat. no. 1020, Aves Labs), and rabbit anti-RFP (1:100; cat. no. 600-401-379, Rockland). Species-specific fluorophore-conjugated secondary antibodies (Jackson ImmunoResearch, 703-545-155, 112-605-167; Life Technologies, A-11034, A-11035, A-11074, A31553, A-31556) were used at 1:500. We used Rhodamine phalloidin (1:100; Invitrogen) to visualize cortical actin. The confocal images were acquired on a Leica SP5 scanning confocal microscope.

Chromatin Immunoprecipitation

We dissected groups of 100 brains from either *brat* mutant or *ase>aPKC*^{CAAX} larvae aged for 5 days at 31°C directly into Schneider's medium then fixed in cross-linking solution (1% methanol free-formaldehyde, 50mM HEPES(pH 8), 1mM EDTA, 0.5mM EGTA, 100mM NaCl) for 10 min. We stopped fixation by washing twice with Glycine solution (0.125 M, 0.01% Triton X-100) in PBS at room temperature for 5 min. Samples were then washed twice with wash buffer A (10mM HEPES(pH 7.6), 10mM EDTA,

0.5mM EGTA, 0.25% Triton X-100) and twice with wash buffer B (10mM HEPES(pH 7.6), 1mM EDTA, 0.5mM EGTA, 200mM NaCl, and 0.01% Triton X-100) and then snap frozen in liquid nitrogen. To obtain more than 2×10^6 supernumerary type II neuroblasts, we pooled 400 brains/ChIP. Samples were then homogenized in 200ul/ChIP SDS lysis buffer (1% SDS, 1 mM PMSF, 50 mM Tris–HCl pH8.1, 10 mM EDTA, 10mM Na-butyrate) containing proteinase inhibitors (Roche, Basel, Switzerland). The nuclear extracts were disrupted by sonication (60 cycles of sonicating for 30 s with 30 s intervals) using a Diagenode, Bioruptor xL. This ChIP protocol is optimized for larval brain tissue to yield chromatin fragments that range in size from 100-500bp (Figure 24C). Ten percent of the sonicated sample was stored for INPUT. The rest of the sonicated chromatin was incubated with antibodies in ChIP dilution buffer (0.01% SDS, 1.1% Trition X-100, 1.2 mM EDTA, 16.7 mM Tris–HCl pH8.1, 167 mM NaCl) on a rotator at 4°C overnight. Samples were then incubated on a rotator with 60 uL Protein A agarose/salmon sperm DNA beads (16–157; Millipore, Billerica, MA) at 4°C for 4-6 hrs, washed twice with low salt immune complex wash buffer (0.1% SDS, 1% TritonX-100, 2 mM EDTA, 20 mM Tris–HCl pH8.1, 150 mM NaCl) for 5 min, once with high salt immune complex wash buffer (0.1% SDS, 1% TritonX-100, 2 mM EDTA, 20 mM Tris–HCl pH8.1, 500 mM NaCl) for 5 min, once with LiCl immune complex wash buffer (0.25 M LiCl, 1% NP40, 1% deoxycholate, 1 mM EDTA, 10 mM Tris–HCl pH8.1) for 5 min, and twice with TE buffer, and then were eluted from beads in elution buffer (10% SDS, 0.1M $NaHCO_3$) for 5 min. Cross-linking of chromatin–protein complex was reverted at 65°C overnight. Samples were treated with RNase A at 55°C for 1 hr and incubated with 2 μg of proteinase K at 45°C for 2 hr. Samples were cleaned up by phenol:chloroform

extraction followed by EtOH precipitation. Samples were resuspended in 75 µl of water. 1.5 µl of sample was used in each qPCR reaction. Antibodies used in this experiment were rabbit anti-H3K4me2 (1:500; 07–030; Millipore, Billerica, MA), rabbit Anti-H3K27me3 (1:500; 07–449; Millipore, Billerica, MA), rabbit Anti-H3K27Ac (1:500; ab4729; Abcam) and rabbit IgG (1:500; ab46540; Abcam). Specific primer sets used for ChIP qPCR are listed in Table 1.

Target Region	Forward Primer	Reverse Primer
pntP1(TSS)	gcggcagccaatcccactt	ctagcagcgacgaacggtataaaaagat
btd(TSS)	tatttgaattatgcacgctccctctt	attctcattatccccttgcccactca
grhO(TSS)	aaccgacccgccccctcaac	gctgcttttggccgcttctaatgtg
erm(TSS)	gtcgccccatccaaatcaagtgtg	cagtgagcagagaccgcccctaaaa
Ubx(TSS)	aggcgcccacccccgataaactta	tgctctgccgactcaactcactc
abd-B (TSS)	cctccccgcccccattcc	tgctccaagtcacaggggtcatc
dist5E (endo)	ttgggaaagaaaagcgcacataac	gccaaagtccccgcaacgaa
dist5E (tran)	tatatttgtgcggctgtgacgac	aatgctttttctttctacggttgttg
neg control	gaaccgcaggcaggaacaagaaga	gtcaaggaatcggaaaataaaaacagg

Table 1: Primers used for ChIP qPCR. The sequences of forward and reverse primers used for ChIP qPCR are indicated.

Luciferase Assays

S2 Cells- 3XC-terminal-HA-tagged *erm, erm$^{\Delta N}$,* and *VP16-erm* were cloned into the pAc5.1/V5-His-A expression vector (ThermoFisher Scientific) for constitutive expression under the control of the *actin5* promoter. A total of 0.5 mL of 10 × 10^6 cells/mL S2 cells was seeded in serum free Schneider's medium (Sigma, St. Louis, MO) in 12-well plates. 1 hour later, cells were co-transfected with 700ng pcDNA3, 100ng of VanGlow luciferase reporter plasmid, 150ng of the pAC5.1 expression vector, and 10ng of pRL-CMV, which serves as an internal control. Approximately 6 hrs after transfection 0.5mL of 10%FBS Schneider's Medium was added. Cell lysis and luciferase assays were

performed 24 h after transfection using the Dual Luciferase Assay System (Promega) and a *PerkinElmer's* EnSpire Multilabel *Plate Reader.*

***Drosophila* brains-** single brains were dissected directly into 65ul of Passive Lysis buffer (Promega) and triturated to homogenize tissue, except for the analysis of *ermRE-gfp::luc(nls)*and *ermRE^{mut}-gfp::luc(nls)*for which four brains were pooled per sample. Luciferase assays were preformed using standard procedures.

Protein Expression and Purification

The DNA-binding domains of Erm (amino acids 316-482), Fezf1 (258-424), Fezf2 (270-436), Klu (560-708), PntP1 (499-604), and E(spl)mγ (2-86) were cloned into pMALc2x (New England Biolabs). Following induction, MBP-fusion proteins were purified from *E. coli* in column buffer (20 mM Hepes (pH 7.6), 0.2 M NaCl, 1 mM EDTA, 10 mM β-mercaptoethanol, 2 mM PMSF) using amylose resin (New England Biolabs). After washing, protein was eluted with 20 mM maltose in elution buffer (20 mM Hepes (pH 7.6), 100 mM NaCl, 1 mM EDTA, 10% glycerol). Dpn (28-106) was cloned into pGEX6p1. GST-Dpn was purified in column buffer (25 mM Hepes (pH 7.6), 0.15 M NaCl, 10% glycerol, 1 mM EDTA, 10 mM β-mercaptoethanol, 2 mM PMSF) using Glutathione HiCap Matrix (Qiagen). After washing, protein was eluted with 20 mM glutathione in column buffer. Protein concentrations were measured by Coomassie stained SDS-PAGE gels. Known concentrations of bovine serum albumin were used as a standard or proteins were standardized to previously determined concentrations of proteins from an earlier preparation.

Electromobility Shift Assays

EMSAs were performed as previously described (Hamm et al., 2015). 40fmol Cy5-labeled oligonucleotide probe and 75ng poly(dI-dC) were used in each reaction. Amounts of recombinant protein used per reaction were as follows: 10 pmol MBP-Klu$^{560-708}$, 0.25 pmol MBP-PntP1$^{499-604}$, 5 pmol MBP-E(spl)$^{2-86}$, 8 pmol GST-Dpn$^{28-106}$, 1-8 pmol MBP-Erm$^{316-482}$, 1-8 pmol MBP-Fezf2$^{270-436}$. For competition experiments, unlabeled competitor oligonucleotide probes were used at 10x, 250x, and 500x the concentration of the Cy5-labeled probe. All samples were incubated on ice for 20 min and electrophoresed for 35 min at 150 V and 4°C in 4% polyacrylamide gels (29:1). The sequence of the Cy5-labeled probes containing a canonical transcription factor binding site were as follows, with the DNA-binding element in bold and the bases substituted to mutate the binding sequence underlined: Erm/Fez2f: TGTCAGTG**AAAA<u>G</u>AGC<u>A</u>AC**TAGCAACG, Dpn/E(spl): AATCGCAGG**ATCG<u>CG</u>TGTC**AACAACCG, Klu: ATGATCGGC**ACA<u>CC</u>GACGC**AGGATCCT, PntP1: ATATAATTA**ACC<u>GG</u>AAGCGC**GGCACAC.

Time-lapse imaging of type II neuroblasts.

Time-lapse experiments were performed on transgenic animals expressing a single copy of *dist5E-gfp::luc(nls)* and *dist5E$^{Klu/Dpn/E(spl)}$-mcherry::ren(nls)*. Larvae hatched from synchronized egg collections were raised at 25˚C for 96h (late third instar stage). Larval brain explants were prepared for time-lapse microscopy as described (Siller et al., 2005) with the following modifications. Larval brains were cultured in D22 media (pH 6.95)

supplemented with 7.5% bovine growth serum and 10mM ascorbic acid. Time-lapse acquisition was performed on a Leica SP8 laser scanning confocal microscope equipped with 488 nm and 543 nm laser lines used for GFP and RFP excitation respectively. GFP/RFP z-stack series (8-10 focal planes with 1.5 μm spacing) were acquired at 30s intervals using sequential line scanning mode.

Acquired images series were processed using Fiji (Schindelin J et al., 2012). To compensate for moderate fluorophore photobleaching, mean whole volume fluorescence intensity was determined for the first (GFP^{t0} and RFP^{t0} and last time point (GFP^{tn} and RFP^{tn}) in each time-lapse series. The bleaching coefficient b^{coeff} was calculated separately for each fluorophore channel as GFP^{t0}/GFP^{tn} and $RFPt0/RFP^{tn}$. For composition of the time-lapse movies, image intensity levels were linearly scaled for each timepoint (tx) and fluorophore channel using the factor $b^{coeff} * (tx / tn)$. To reduce pixel noise, a Gaussian filter (sigma=1) was applied to each image after bleaching correction.

qPCR analysis of transcript abundance in *erm* mutant brains

Total RNA was extracted following the standard Trizol RNA isolation protocol (Life technologies, Grand Island, NY) and cleaned by the RNeasy kit (Qiagen, Venlo, Netherlands). First strand cDNA was synthesized from the extracted total RNA using First Strand cDNA Synthesis Kit for RT-PCR (AMV) (Roche, Basel, Switzerland). qPCR was performed using ABsolute QPCR SYBR Green ROX Mix (Thermo Fisher Scientific Inc., Waltham, MA). Data were analyzed by the comparative CT method, and the relative mRNA expression is presented. Specific primer sets used for qPCR are listed in Table 2.

Gene	Forward Primer	Reverse Primer
Rp49	atcggttacggatcgaacaa	gacaatctccttgcgcttct
dpn	catcatgccgaacacaggtt	gaagattggccggaactgag
klu	caacaataatgagacccactcc	gatcttcatcctgttcggcatc
pntP1	aatctggtgggggcgttgag	gctgttgttgatgcggtcgtgt
pntP3	gatcgtcgtccccctttta	gcagcggcggtagcatc
grhO	gccggccagcacgaggtctttgta	tgctgctgctgttgctggtggtga
grhN	cacgggctccattgtctcctct	gttctctgctggatgctgttcacg

Table 2: Primers used for qPCR analysis of transcription factor expression levels. The sequences of forward and reverse primers used for qPCR are indicated.

Acknowledgements

We thank Drs. S. Bray, C. Delidakis, J. Knoblich and S. Zhu for providing us reagents. We thank Drs. S. Barolo, K. Cadigan and Y. Dou and Ms. J. Xu for technical advice on the chromatin immunoprecipitation experiment. We thank the Bloomington *Drosophila* Stock Center and the Vienna *Drosophila* RNAi Center for fly stocks, and the *Drosophila* Genomics Resource Center for the *erm* cDNA clone. We thank BestGene Inc. for generating the transgenic fly lines. We thank Drs. T Kerppola, Dr. Y. Yamashita, Mr. Dylan Farnsworth and the members of the Lee lab for reading the manuscript and providing critical comments. D. H. J. was supported by a Cellular and Molecular Biology training grant (T32-GM007315). This work is currently supported by a NIH grant (R01NS077914).

Chapter 4: Discussion and future directions

Although PcG and TrxG genes were first discovered by genetic studies in *Drosophila* (Kennison, 1995), whether *Drosophila* stem cells maintain developmental regulators of lineage-commitment and differentiation in a poised chromatin state remained unclear. In *Drosophila*, this poised chromatin state had only been described in wing disks (Schertel et al., 2015), which do not possess a bona fide stem cell population. Thus, our finding that *Drosophila* type II neuroblasts maintain *erm*, the master regulator of INP commitment, in a poised chromatin state provides an exciting starting point for future investigation.

The power of *Drosophila* genetics combined with the ability to unambiguously identity all cell types within type II neuroblast lineages will enable mechanistic investigation of numerous aspects of the poised chromatin model that have remained intractable in other systems. Our work has already revealed self-renewal repressor proteins directly bind the *erm* immature INP enhancer and prevent premature activation through HDAC1/Rpd3 (Janssens et al., 2016) (see Chapter 3). Continuing to study the sequence of the *erm* immature INP enhancer will reveal additional transcription factor inputs that prime this enhancer for activation. Combining this knowledge with functional genetic studies will facilitate identification of the chromatin modifiers they interact with to activate *erm* expression. Second, accumulating evidence suggests that PcG genes have an important role in establishing the 3-dimensional architecture of the genome

(Bantignies et al., 2011; Sexton and Cavalli, 2015; Sexton et al., 2012). Our results suggest that in contrast to the canonical role of PRC2 to maintain transcriptional repression, PRC2 likely facilitates activation of endogenous *erm*. An attractive explanation is that PRC2 maintains the *erm* locus in a confirmation that facilitates subsequent activation. Examining the effect of PcG genes during the maintenance of the intra-genic 3D conformation of the *erm* locus will likely clarify the function of PcG genes during poised gene regulation. Lastly, our preliminary data suggests numerous components of the INP temporal cascade, which specifies the sequential generation of distinct types of neurons (Bayraktar and Doe, 2013), are also maintained in a poised state. This suggests these genes may function in parallel to the *erm* poised feedback circuit as a poised feedforward circuit to precisely specify the functional properties of INPs. Different components of this temporal cascade are activated at different times in INPs (Bayraktar and Doe, 2013), including fast-activating genes (such as *Dichaete* (*D*)) that are activated with very similar kinetics to *erm* in immature INPs, as well as genes that are activated only upon the completion of INP maturation (such as *odd paired* (*opa*) and *apterous* (*ap*)). This provides an exciting opportunity to study how distinct classes of poised genes are regulated and organized within the 3D space of the nucleus. The outcome of this line of investigation will likely continue to break new ground in the field of poised gene regulation, and provide novel insight into the universal mechanisms that control stem cell biology.

Identifying novel mechanisms that activate the poised *erm* enhancer.

Elucidating how stem cell transcription factor networks regulate the activity of poised enhancers is critical to understanding the balance between self-renewal and

differentiation. Our work shows that the self-renewal transcriptional repressors Klu, Dpn, and E(spl)mγ directly bind the *erm* immature INP enhancer (dist5E) and prevent premature activation through HDAC1/Rpd3, and that the lineage-specific activator PntP1 primes this enhancer for activation (Janssens et al., 2016) (see Chapter 3). However, our preliminary data suggest that additional activator inputs must exist in the dist5E enhancer. More specifically, mutation of the five PntP1 binding sites in dist5E did not render the enhancer inactive in type II neuroblast lineages (Figure 25A-C). By looking for additional conserved transcription factor binding motifs in the *erm* dist enhancer, we identified multiple putative binding sites for additional components of the type II specific activator network including Btd/Sp1, which share a similar binding motif, and Dll (Figure 25D). Consistent with the functional role of PntP1 during erm activation, reducing PntP1 activity by RNAi was sufficient to enhance the supernumerary neuroblast phenotype in *erm* hypomorphic mutant brains (Figure 25E-G). To determine whether Btd, Sp1 or Dll also contribute to activation of the poised *erm* enhancer we propose to take a combination of similar approaches. First, we will test whether knocking-down *btd*, *Sp1* or *Dll* also enhances the supernumerary neuroblast phenotype in *erm* hypomorphic mutant brains. Second, we will examine the consequence of mutating the Btd/Sp1 or Dll binding sites on the expression of the dist5E transgenic reporter. It is possible that PntP1, Btd, Sp1 and Dll work in a semi-redundant manner to activate the *erm* immature INP enhancer. Thus, we will also generate transgenic reporters in which the PntP1, Btd/Sp1, and Dll binding sites are mutated in combination. These experiments will likely elucidate the transcription factor inputs that activate the poised erm enhancer, demonstrate that type II neuroblast specific transcription factors

regulate common targets, and provide a useful tool to examine how the chromatin state of poised enhancers changes when the activator inputs are removed (see below).

Transcription factors often regulate expression of their target genes through recruitment of chromatin modifying enzymes. Genome-wide association studies have found that the histone acetyltransferase (HAT) p300/CBP localizes to the majority of poised enhancers (Rada-Iglesias et al., 2011). Thus, the prevailing model of poised enhancer activation includes acetylation of H3K27 by p300/CBP (Heinz et al., 2015), but this has yet to be functionally tested. In contrast to what this model would predict, we find that knocking down the function of CBP suppresses, rather than enhancers, the supernumerary neuroblast phenotype in *erm* hypomorphic mutant brains (Figure 25E, F, H). However, 8-12 type II neuroblast can still be found in these brains, indicating that reducing the function of CBP is not simply causing type II neuroblasts to die or prematurely differentiate. This strongly suggests CBP may be required for efficient INP reversion in *erm* mutants, and that an alternative HAT mediates the activation of the poised *erm* enhancer. To identify this HAT, we will reduce the function of Chameau, Tip60, MOF, or Gcn5 by RNAi in *erm* hypomorphic mutant brains, looking for enhancement of the supernumerary neurobalst phenotype. Once the HAT that most likely activates *erm* expressions is identified, we will determine whether the type II neuroblast specific activator network recruits this HAT to the poised *erm* enhancer. Briefly, HAT specific ChIP experiments will be performed on type II neuroblast enriched

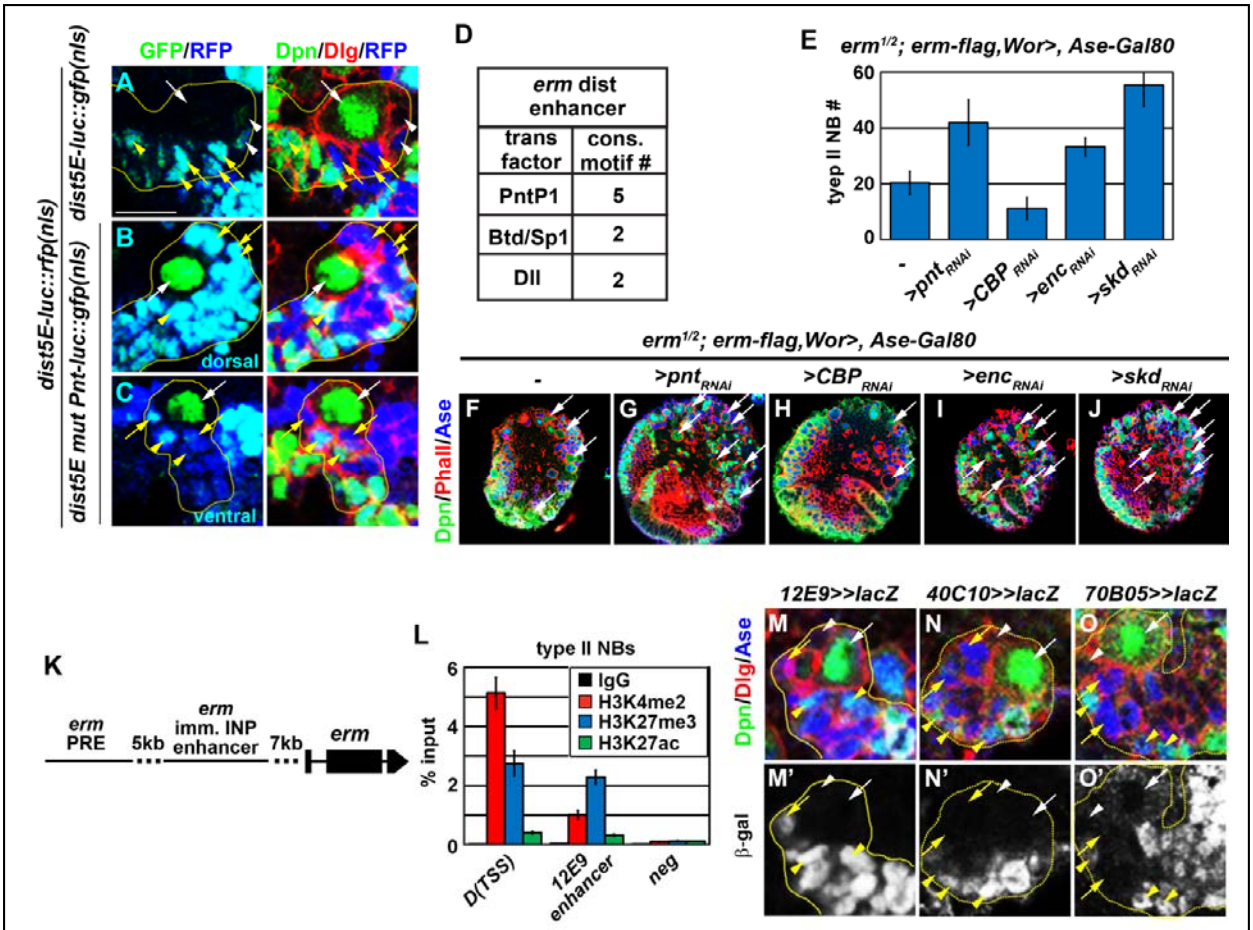

Figure 25: Preliminary Data. (A-C) Confocal images comparing the expression of wild type *dist5E-luc::rfp(nls)* and *dist5E mut Pnt-luc::gfp(nls)* in type II neuroblast lineages. (D) Table summarizing the the conserved binding motifs for type II specific transcriptional activators in the *erm* distal immature INP enhancer. (E) Quantification of the number of supernumerary type II neuroblasts in *erm* hypomorphic mutant brains overexpressing RNAi transgenes targeting the indicated genes. (F-J) Confocal images of *erm* hypomorphic mutant brains overexpressing RNAi transgenes targeting the indicated genes. (K) Schematic representation of the *erm* locus showing the relative position of the *erm* immature INP enhancer and the *erm* PRE. Kb: kilobases. (L) ChIP analysis of the relative enrichment of H3K4me2 (red), H3K27me3 (blue), H3K27ac (green) and an IgG control (black) on the transcription start sites (TSS) and 12E9 enhancer of *D* from type II neuroblast enriched chromatin. (M-O) Confocal images showing the expression pattern of a β-Gal(nls) reporter driven by the *D* 12E9 enhancer, as well as the *ap* 40C10 enhancer and *opa* 70B05 enhancer. The *ap* 40C10 enhancer and *opa* 70B05 enhancer do not become expressed until an INP completes maturation. White arrow: type II neuroblast. White arrowhead: newly born immature INP and Ase^{-} immature INP. Yellow arrow: Ase^{+} immature INP. Yellow arrowhead: INP.

chromatin. Enrichment for the wild-type dist5E transgene, but not the inactive PntP1/Btd/Sp1/Dll mutant dist5E transgene, would indicate these transcription factors

mediate poised enhancer activation through this HAT. The identification of an alternative HAT that is functionally required for *erm* activation will provide an important revision to the model of poised enhancer activation.

Interestingly, from an unbiased genetic screen we found that heterozygous mutation of the loci containing *encore* (*enc*) and *skuld* (*skd*) both enhanced the supernumerary neuroblast phenotype in *erm* hypomorphic mutant brains (data not shown). We confirmed this genetic interaction by specifically knocking-down either *enc* or *skd* by RNAi (Figure 25E, F, I, J). Interestingly, Enc and Skd are both components of the Mediator complex and have been shown to physically and genetically interact with TrxG and PcG genes in *Drosophila* (Guruharsha et al., 2011; Lindsley and Zimm, 1992). In mouse ES cells the Mediator complex facilitates enhancer-promoter interactions by physically stabilizing DNA looping (Kagey et al., 2010). The endogenous *erm* immature INP enhancer is located approximately 7kb from its promoter (Figure 25 K). Thus, an attractive possibility is that Skd and Enc facilitate this long range enhancer-promoter interaction to promote *erm* expression in immature INPs. To test this possibility experimentally we will perform a variation of the chromatin conformation capture technique, comparing the relative frequency of the enhancer-promoter interaction in a genetic background in which Skd and Enc are functional to a genetic background in which their function is reduced. In addition, we will perform a similar ChIP experiment to the one previously described, to examine whether type II specific transcription factors recruit Skd or Enc to the *erm* immature INP enhancer. Together these experiments will improve our understanding of the hierarchical relationship between transcription factor binding, chromatin modification and chromatin architecture during the activation of a

poised gene. This knowledge will likely provide novel strategies to manipulate stem cell function, and insight into the molecular mechanisms underlying numerous developmental pathologies.

Clarifying the role of PcG genes during regulation of *erm* expression.

The prevailing model is that by catalyzing H3K27me3 and repressing poised-differentiation genes, PRC2 functions to maintain stem cell identity (Boyer et al., 2006; Heinz et al., 2015; Lee et al., 2006d). Paradoxically, we find that although the endogenous *erm* promoter and immature INP enhancer are marked by H3K27me3, PRC2 is not required to maintain *erm* repression, and instead *erm* expression is reduced or lost in PCR2 mutant immature INPs (Janssens et al., 2016) (see Chapter 3). This result suggests that, in contrast to the canonical role of PRC2, it may be required for activation of endogenous *erm* expression. In support of this model, several studies have reported a role for both PRC1 and PRC2 in mediating target gene activation (Ferrari et al., 2014; Frangini et al., 2013; Lv et al., 2016; Pasini et al., 2007). A recent study of *Drosophila* imaginal discs found genes that are activated versus repressed by PcG genes could be stratified based on the presence of mono-methylation of lysine 20 on histone 4 (H4K20me1) in genes that require PRC2 for their activation (Lv et al., 2016). Consistent with this observation, the H4K20 methyltransferase PR-Set7 was found to bind these PcG activated genes, and PR-Set7 was also required for their activation (Lv et al., 2016). To follow up on the potential role of PRC2 during the activation of *erm* expression, we will examine whether knock-down of PR-Set7 or components of PRC2 enhances the supernumerary neuroblast phenotype in *erm* hypomorphic mutant brains. In addition, we will examine whether the endogenous *erm*

promoter and immature INP enhancer display H4K20me1 in type II neuroblast enriched chromatin. This work could potentially provide a mechanistic explanation for the context dependent function of PRC2 during the regulation of distinct poised genes, or even on the same poised gene in distinct stem cell types.

It remains possible that the loss of *erm* expression in PRC2 mutants is the result of an indirect effect. To test whether PRC2 has a direct role during activation of *erm* expression we plan to specifically disrupt PRC2 recruitment to the erm locus, while leaving PRC2 itself intact. The mechanisms that recruit PcG proteins to specific regions of the genome in mammalian stem cells remain unclear, preventing examination of the isolated function of PcG proteins on specific poised loci. However, in *Drosophila* PcG genes are known to be recruited to their target loci through molecularly defined Polycomb Response Elements (PREs) (Ringrose and Paro, 2007). Indeed, previous genome-wide *in silico* studies identified a PRE in the *erm* locus (Figure 25K) (Ringrose et al., 2003). To examine the function of PRC2 on the *erm* locus we will specifically knock out the PRE from the endogenous erm locus, creating the erm^{PRE} mutant allele. If homozygous erm^{PRE} mutants show a loss of endogenous *erm* expression, and recapitulate the supernumerary neuroblast phenotype of *erm* null brains, we will conclude PRC2 directly regulates activation of *erm* expression. This result would fundamentally change the current model of poised gene regulation and strongly encourage investigation of potential context dependent roles of PRC2.

Interestingly, the transgenic dist5E reporter is not expressed in type II neuroblasts and becomes activate in immature INPs with very similar kinetics to endogenous *erm*, however, PRC2 is likely not recruited to this transgene because the

surrounding chromatin is not marked H3K27me3. Why might endogenous *erm* require PRC2 for activation, while a transgene bearing the *erm* immature INP enhancer does not? One obvious difference is that the *erm* enhancer in the transgenic reporter is positioned directly adjacent to the gene promoter, whereas in the endogenous *erm* locus the immature INP enhancer is located 7 kilobases upstream of the *erm* promoter (Figure 25K). Accumulating evidence suggests PcG genes have an important role in assembling the 3 dimensional architecture of the genome (Bantignies et al., 2011; Sexton and Cavalli, 2015; Sexton et al., 2012). Thus, an attractive possibility is that PcG genes may contribute to the long rang enhancer-promoter interaction on the *erm* locus. We will test this possibility using a combination of transgenic reporters and a variation of chromosome conformation capture to compare the enhancer-promoter interactions on the wild-type erm locus with enhancer-promoter interactions on the erm^{PRE} mutant locus. This work has the potential to elucidate a novel function of PcG proteins during target gene regulation, and would suggest that, as opposed to directly promoting target gene activation versus repression per say, PcG genes are important to establish and maintain the proper confirmation of their target loci.

Determining how distinct classes of poised genes are regulated.

The precise specification of intermediate progenitor identity requires repression of stem cell self-renewal pathways and activation of the programs controlling intermediate progenitor specific functions, including the generation of specific differentiated cell types. However, the mechanisms coordinating this critical transition in cellular identity remain unclear in most stem cell lineages. Our work demonstrates that *erm* functions as a poised negative feedback circuit to ensure the maintenance of a restricted

intermediate progenitor identity by directly repressing components of the stem cell transcription factor network (Janssens et al., 2016) (see Chapter 3). Intriguingly, our preliminary data suggests that components of the temporal cascade that directs the generation of distinct types of neurons and glia through sequential round of INP division are also maintained in a poised state in type II neuroblasts. The *D* immature INP enhancer (12E9) and *D* promoter both display histone marks associated with poised genes (Figure 25L), and a transgene bearing the 12E9 enhancer activates reporter gene expression in a similar pattern to the *erm* immature INP enhancer (Figure 25M, M'). This suggests *erm* and *D* are likely regulated by a common class of fast-activating poised enhancers. Similar to the *erm* locus, the transcription factors *opa* and *ap* display high levels of H3K27me3 In S2 cells, suggesting these loci are also direct PRC2 targets (modencode). In addition, we identified an *ap* enhancer (40C10) and an *opa* enhancer (70B05) that don't become activate until completion of INP maturation (Figure 25 N-O'). This preliminary data suggests *opa* and *ap* are likely regulated by a distinct class of poised enhancers.

Our identification of distinct classes of poised genes provides an exciting opportunity to examine the regulatory mechanisms that contribute to their distinct expression patterns. For example, in mammalian adult NSC lineages the H3K27 specific demethylase JMJD3 is required for robust activation of the poised gene *Dlx2* in intermediate progenitors (Park et al., 2014). However, Utx, the *Drosophila* homologue of JMJD3, does not appear to play a functional role in *erm* activation (data not shown). Thus, we are interested in testing whether poised genes such as *opa* and *ap*, which are activated with slower kinetics, may require Utx for their activation, whereas fast-

activating poised genes such as *erm* and *D* may not. Interestingly, the type II specific transcription factors *pntP1* and *btd* are likely also maintained in a poised state, but become activated during the birth of a type II neurobalst. Once activated PntP1 and Btd likely contribute to priming the *erm* locus for activation in type II neuroblast progeny following asymmetric division. This suggests poised genes may form a relay mechanism to control the progressive restriction of developmental potential in stem cell lineages. By continuing to investigate the cell-type specific enhancers of *pntP1*, *btd*, *erm*, *D*, *opa* and *ap,* we hope to elucidate the regulatory mechanisms underlying this poised relay circuit. Lastly, we are interested in using a combination of *in situ* hybridization and chromosome confirmation capture to examine how distinct classes of poised genes are coordinated in the 3-dimensional space of the nucleus. PcG proteins have been shown to mediate functional inter-genic interactions between distal Hox clusters (Bantignies et al., 2011). Might poised genes that are expressed in type II neuroblasts, such as *pntP1* and *btd*, be maintained in a different nuclear compartment from poised genes that are expressed in their immature INP progeny, such as *erm* and *D*, or mature INPs, such as *opa* and *ap*? This aspect of poised gene regulation remains completely unexplored, and has the potential to revolutionize our understanding of developmental relay mechanisms.

References

Alcantara Llaguno, S.R., Wang, Z., Sun, D., Chen, J., Xu, J., Kim, E., Hatanpaa, K.J., Raisanen, J.M., Burns, D.K., Johnson, J.E.*, et al.* (2015). Adult Lineage-Restricted CNS Progenitors Specify Distinct Glioblastoma Subtypes. Cancer Cell *28*, 429-440.

Almeida, M.S., and Bray, S.J. (2005). Regulation of post-embryonic neuroblasts by Drosophila Grainyhead. Mech Dev *122*, 1282-1293.

Aloia, L., Di Stefano, B., and Di Croce, L. (2013). Polycomb complexes in stem cells and embryonic development. Development *140*, 2525-2534.

Amador-Arjona, A., Cimadamore, F., Huang, C., Wright, R., Lewis, S., Gage, F., and Terskikh, A. (2015). SOX2 primes the epigenetic landscape in neural precursors enabling proper gene activation during hippocampal neurogenesis. Proc Natl Acad Sci U S A *112*, E1936-1945.

Ardehali, M.B., Mei, A., Zobeck, K.L., Caron, M., Lis, J.T., and Kusch, T. (2011). Drosophila Set1 is the major histone H3 lysine 4 trimethyltransferase with role in transcription. EMBO J *30*, 2817-2828.

Bantignies, F., Roure, V., Comet, I., Leblanc, B., Schuettengruber, B., Bonnet, J., Tixier, V., Mas, A., and Cavalli, G. (2011). Polycomb-dependent regulatory contacts between distant Hox loci in Drosophila. Cell *144*, 214-226

Bayraktar, O.A., Boone, J.Q., Drummond, M.L., and Doe, C.Q. (2010). Drosophila type II neuroblast lineages keep Prospero levels low to generate large clones that contribute to the adult brain central complex. Neural Dev *5*, 26

Bayraktar, O.A., and Doe, C.Q. (2013). Combinatorial temporal patterning in progenitors expands neural diversity. Nature *498*, 449-455.

Bello, B., Holbro, N., and Reichert, H. (2007). Polycomb group genes are required for neural stem cell survival in postembryonic neurogenesis of Drosophila. Development *134*, 1091-1099.

Bello, B.C., Izergina, N., Caussinus, E., and Reichert, H. (2008). Amplification of neural stem cell proliferation by intermediate progenitor cells in Drosophila brain development. Neural Develop *3*, 5.

Berdnik, D., Török, T., González-Gaitán, M., and Knoblich, J.A. (2002). The endocytic protein alpha-Adaptin is required for numb-mediated asymmetric cell division in Drosophila. Dev Cell *3*, 221-231.

Berger, C., Harzer, H., Burkard, T.R., Steinmann, J., van der Horst, S., Laurenson, A.S., Novatchkova, M., Reichert, H., and Knoblich, J.A. (2012). FACS purification and transcriptome analysis of drosophila neural stem cells reveals a role for Klumpfuss in self-renewal. Cell Rep *2*, 407-418.

Bergsland, M., Ramsköld, D., Zaouter, C., Klum, S., Sandberg, R., and Muhr, J. (2011). Sequentially acting Sox transcription factors in neural lineage development. Genes Dev *25*, 2453-2464.

Betschinger, J., Mechtler, K., and Knoblich, J.A. (2006). Asymmetric segregation of the tumor suppressor brat regulates self-renewal in Drosophila neural stem cells. Cell *124*, 1241-1253.

Bischof, J., and Basler, K. (2008). Recombinases and their use in gene activation, gene inactivation, and transgenesis. Methods Mol Biol *420*, 175-195.

Bischof, J., Maeda, R.K., Hediger, M., Karch, F., and Basler, K. (2007). An optimized transgenesis system for Drosophila using germ-line-specific phiC31 integrases. Proc Natl Acad Sci U S A *104*, 3312-3317.

Blackledge, N.P., Farcas, A.M., Kondo, T., King, H.W., McGouran, J.F., Hanssen, L.L., Ito, S., Cooper, S., Kondo, K., Koseki, Y.*, et al.* (2014). Variant PRC1 complex-dependent H2A ubiquitylation drives PRC2 recruitment and polycomb domain formation. Cell *157*, 1445-1459.

Blackledge, N.P., Rose, N.R., and Klose, R.J. (2015). Targeting Polycomb systems to regulate gene expression: modifications to a complex story. Nat Rev Mol Cell Biol *16*, 643-649.

Bond, A.M., Ming, G.L., and Song, H. (2015). Adult Mammalian Neural Stem Cells and Neurogenesis: Five Decades Later. Cell Stem Cell *17*, 385-395.

Boone, J.Q., and Doe, C.Q. (2008). Identification of Drosophila type II neuroblast lineages containing transit amplifying ganglion mother cells. Dev Neurobiol *68*, 1185-1195.

Bowman, S.K., Rolland, V., Betschinger, J., Kinsey, K.A., Emery, G., and Knoblich, J.A. (2008). The tumor suppressors brat and numb regulate transit-amplifying neuroblast lineages in *Drosophila*. Dev Cell *14*, 535-546.

Boyer, L.A., Lee, T.I., Cole, M.F., Johnstone, S.E., Levine, S.S., Zucker, J.P., Guenther, M.G., Kumar, R.M., Murray, H.L., Jenner, R.G.*, et al.* (2005). Core transcriptional regulatory circuitry in human embryonic stem cells. Cell *122*, 947-956.

Boyer, L.A., Plath, K., Zeitlinger, J., Brambrink, T., Medeiros, L.A., Lee, T.I., Levine, S.S., Wernig, M., Tajonar, A., Ray, M.K.*, et al.* (2006). Polycomb complexes repress developmental regulators in murine embryonic stem cells. Nature *441*, 349-353.

Brayer, K.J., and Segal, D.J. (2008). Keep your fingers off my DNA: protein-protein interactions mediated by C2H2 zinc finger domains. Cell Biochem Biophys *50*, 111-131.

Calo, E., and Wysocka, J. (2013). Modification of enhancer chromatin: what, how, and why? Mol Cell Biol *49*, 825-837.

Carney, T.D., Miller, M.R., Robinson, K.J., Bayraktar, O.A., Osterhout, J.A., and Doe, C.Q. (2012). Functional genomics identifies neural stem cell sub-type expression profiles and genes regulating neuroblast homeostasis. Dev Biol *361*, 137-146.

Carrera, I., Zavadil, J., and Treisman, J.E. (2008). Two subunits specific to the PBAP chromatin remodeling complex have distinct and redundant functions during drosophila development. Mol Cell Biol *28*, 5238-5250.

Cenci, C., and Gould, A.P. (2005). Drosophila Grainyhead specifies late programmes of neural proliferation by regulating the mitotic activity and Hox-dependent apoptosis of neuroblasts. Development *132*, 3835-3845.

Chambers, I., Colby, D., Robertson, M., Nichols, J., Lee, S., Tweedie, S., and Smith, A. (2003). Functional expression cloning of Nanog, a pluripotency sustaining factor in embryonic stem cells. Cell *113*, 643-655.

Chang, K.C., Wang, C., and Wang, H. (2012). Balancing self-renewal and differentiation by asymmetric division: insights from brain tumor suppressors in Drosophila neural stem cells. Bioessays *34*, 301-310.

Chen, J., McKay, R.M., and Parada, L.F. (2012). Malignant glioma: lessons from genomics, mouse models, and stem cells. Cell *149*, 36-47.

Chen, L., Zheng, J., Yang, N., Li, H., and Guo, S. (2011). Genomic selection identifies vertebrate transcription factor Fezf2 binding sites and target genes. J Biol Chem *286*, 18641-18649.

Chen, R., Nishimura, M.C., Bumbaca, S.M., Kharbanda, S., Forrest, W.F., Kasman, I.M., Greve, J.M., Soriano, R.H., Gilmour, L.L., Rivers, C.S.*, et al.* (2010). A hierarchy of self-renewing tumor-initiating cell types in glioblastoma. Cancer Cell *17*, 362-375.

Chotinantakul, K., and Leeanansaksiri, W. (2012). Hematopoietic stem cell development, niches, and signaling pathways. Bone Marrow Res *2012*, 270425.

Couturier, L., Vodovar, N., and Schweisguth, F. (2012). Endocytosis by Numb breaks Notch symmetry at cytokinesis. Nat Cell Biol *14*.

Creyghton, M.P., Cheng, A.W., Welstead, G.G., Kooistra, T., Carey, B.W., Steine, E.J., Hanna, J., Lodato, M.A., Frampton, G.M., Sharp, P.A.*, et al.* (2010). Histone H3K27ac separates active from poised enhancers and predicts developmental state. Proc Natl Acad Sci U S A *107*, 21931-21936.

Doe, C.Q. (2008). Neural stem cells: balancing self-renewal with differentiation. Development *135*, 1575-1587.

Eckler, M.J., and Chen, B. (2014). Fez family transcription factors: controlling neurogenesis and cell fate in the developing mammalian nervous system. Bioessays *36*, 10.

Eckler, M.J., Larkin, K.A., McKenna, W.L., Katzman, S., Guo, C., Roque, R., Visel, A., Rubenstein, J.L., and Chen, B. (2014). Multiple conserved regulatory domains promote Fezf2 expression in the developing cerebral cortex. Neural Dev *9*.

Estella, C., and Mann, R.S. (2010). Non-Redundant Selector and Growth-Promoting Functions of Two Sister Genes, buttonhead and Sp1, in Drosophila Leg Development. PLoS Genet *6*, e1001001.

Ferrari, K.J., Scelfo, A., Jammula, S., Cuomo, A., Barozzi, I., Stützer, A., Fischle, W., Bonaldi, T., and Pasini, D. (2014). Polycomb-dependent H3K27me1 and H3K27me2 regulate active transcription and enhancer fidelity. Mol Cell *53*, 49-62.

Franco, S.J., and Müller, U. (2013). Shaping our minds: stem and progenitor cell diversity in the mammalian neocortex. Neuron *77*, 19-34.

Frangini, A., Sjöberg, M., Roman-Trufero, M., Dharmalingam, G., Haberle, V., Bartke, T., Lenhard, B., Malumbres, M., Vidal, M., and Dillon, N. (2013). The aurora B kinase and the polycomb protein ring1B combine to regulate active promoters in quiescent lymphocytes. Mol Cell *21*, 647-661.

Geisler, S.J., and Paro, R. (2015). Trithorax and Polycomb group-dependent regulation: a tale of opposing activities. Development *142*, 2876-2887.

Giebel, B., and Wodarz, A. (2012). Notch signaling: numb makes the difference. Curr Biol *22*, 133-135.

Guo, C., Eckler, M.J., McKenna, W.L., McKinsey, G.L., Rubenstein, J.L.R., and Chen, B. (2013). Fezf2 expression identifies a multipotent progenitor for neocortical projection neurons, astrocytes, and oligodendrocytes. Neuron *80*, 1167-1174.

Guruharsha, K.G., Rual, J.F., Zhai, B., Mintseris, J., Vaidya, P., Vaidya, N., Beekman, C., Wong, C., Rhee, D.Y., Cenaj, O.*, et al.* (2011). A protein complex network of Drosophila melanogaster. Cell *147*, 690-703.

Haenfler, J.M., Kuang, C., and Lee, C.Y. (2012). Cortical aPKC kinase activity distinguishes neural stem cells from progenitor cells by ensuring asymmetric segregation of Numb. Dev Biol *365*, 219-228.

Hamm, D., Bondra, E., and Harrison, M. (2015). Transcriptional activation is a conserved feature of the early embryonic factor Zelda that requires a cluster of four zinc fingers for DNA binding and a low-complexity activation domain. J Biol Chem *290*, 3508-3518.

Heintzman, N.D., Stuart, R.K., Hon, G., Fu, Y., Ching, C.W., Hawkins, R.D., Barrera, L.O., Van Calcar, S., Qu, C., Ching, K.A.*, et al.* (2007). Distinct and predictive chromatin signatures of transcriptional promoters and enhancers in the human genome. Nat Genet *39*, 311-318.

Heinz, S., Benner, C., Spann, N., Bertolino, E., Lin, Y.C., Laslo, P., Cheng, J.X., Murre, C., Singh, H., and Glass, C.K. (2010). Simple combinations of lineage-determining transcription factors prime cis-regulatory elements required for macrophage and B cell identities. Mol Cell *38*, 576-589.

Heinz, S., Romanoski, C.E., Benner, C., and Glass, C.K. (2015). The selection and function of cell type-specific enhancers. Nat Rev Mol Cell Biol *16*, 11.

Herr, A., Mckenzie, L., Suryadinata, R., Sadowski, M., Parsons, L.M., Sarcevic, B., and Richardson, H.E. (2010). Geminin and Brahma act antagonistically to regulate EGFR-Ras-MAPK signaling in Drosophila. Dev Biol *344*, 36-51.

Herz, H.M., Hu, D., and Shilatifard, A. (2014). Enhancer Malfunction in Cancer. Mol Cell *53*, 859–866.

Herz, H.M., Mohan, M., Garruss, A.S., Liang, K., Takahashi, Y.H., Mickey, K., Voets, O., Verrijzer, C.P., and Shilatifard, A. (2012). Enhancer-associated H3K4 monomethylation by Trithorax-related, the Drosophila homolog of mammalian Mll3/Mll4. Genes Dev *26*, 2604-2620.

Hirata, T., M., N., Muraoka, O., Nakayama, R., Suda, Y., and Hibi, M. (2006). Zinc-finger genes Fez and Fez-like function in the establishment of diencephalon subdivisions. Development *133*, 3993-4004.

Homem, C.C., and Knoblich, J.A. (2012). Drosophila neuroblasts: a model for stem cell biology. Development *139*, 4297-4310.

Homem, C.C., Reichardt, I., Berger, C., Lendl, T., and Knoblich, J.A. (2013). Long-term live cell imaging and automated 4D analysis of *Drosophila* neuroblast lineages. PLoS One *8*, e79588.

Homem, C.C., Steinmann, V., Burkard, T.R., Jais, A., Esterbauer, H., and Knoblich, J.A. (2014). Ecdysone and mediator change energy metabolism to terminate proliferation in Drosophila neural stem cells. Cell *158*, 874-888.

Hori, K., Sen, A., and Artavanis-Tsakonas, S. (2013). Notch signaling at a glance. J Cell Sci *126*, 2135-2140.

Hwang, H.J., and Rulifson, E. (2011). Serial specification of diverse neuroblast identities from a neurogenic placode by Notch and Egfr signaling. Development *138*, 2883-2893.

Imayoshi, I., and Kageyama, R. (2014). bHLH factors in self-renewal, multipotency, and fate choice of neural progenitor cells. Neuron *82*, 9-23.

Ingham, P.W. (1983). Differential expression of bithorax complex genes in the absence of the extra sex combs and trithorax genes. Nature *306*, 591 - 593.

Ingham, P.W. (1998). trithorax and the regulation of homeotic gene expression in Drosophila: a historical perspective. Int J Dev Biol *42*, 423-429.

Janssens, D.H., Hamm, D.C., Anhezini, L., Xiao, Q., Siller, K.H., Siegrist, S.E., Harrison, M.M., and Lee, C.Y. (2016). A novel Hdac1/Rpd3-poised circuit balances continual self-renewal and rapid restriction of developmental potential during asymmetric stem cell division. In Review.

Janssens, D.H., Komori, H., Grbac, D., Chen, K., Koe, C.T., Wang, H., and Lee, C.-Y. (2014). dFezf/Earmuff restricts progenitor cell potential by attenuating the competence to respond to self renewal factors. Development *141*, 1036-1046.

Janssens, D.H., and Lee, C.Y. (2014). It takes two to tango, a dance between the cells of origin and cancer stem cells in the Drosophila larval brain. . Semin Cell Dev Biol *28*, 63-69.

Kagey, M.H., Newman, J.J., Bilodeau, S., Zhan, Y., Orlando, D.A., van Berkum, N.L., Ebmeier, C.C., Goossens, J.R., P.B., Levine, S.S., Taatjes, D.J.*, et al.* (2010). Mediator and cohesin connect gene expression and chromatin architecture. Nature *467*, 430–435.

Kaspar, M., Schneider, M., Chia, W., and Klein, T. (2008). Klumpfuss is involved in the determination of sensory organ precursors in Drosophila. Dev Biol *324*, 177-191.

Kennison, J.A. (1995). The Polycomb and trithorax group proteins of Drosophila: trans-regulators of homeotic gene function. Annu Rev Genet *29*, 289-303.

Kim, J., Chu, J., Shen, X., Wang, J., and Orkin, S.H. (2008). An extended transcriptional network for pluripotency of embryonic stem cells. Cell *6*, 1049-1061.

Kobayashi, T., and Kageyama, R. (2014). Expression dynamics and functions of Hes factors in development and diseases. Curr Top Dev Biol *110*, 263-283.

Koe, C.T., Li, S., Rossi, F., Wong, J.J., Wang, Y., Zhang, Z., Chen, K., Aw, S.S., Richardson, H.E., Robson, P.*, et al.* (2014). The Brm-HDAC3-Erm repressor complex suppresses dedifferentiation in Drosophila type II neuroblast lineages. Elife *3*, e01906.

Komori, H., Xiao, Q., Janssens, D., Dou, Y., and Lee, C.-Y. (2014a). Trithorax maintains the functional heterogeneity of neural stem cells through the transcription factor Buttonhead. eLife *3*.

Komori, H., Xiao, Q., McCartney, B.M., and Lee, C.Y. (2014b). Brain tumor specifies intermediate progenitor cell identity by attenuating β-catenin/Armadillo activity. Development *141*.

Kopp, J.L., Ormsbee, B.D., Desler, M., and Rizzino, A. (2008). Small increases in the level of Sox2 trigger the differentiation of mouse embryonic stem cells. Stem Cells *26*, 903-911.

Kusek, G., Campbell, M., Doyle, F., Tenenbaum, S.A., Kiebler, M., and Temple, S. (2012). Segregation of the double-stranded RNA binding protein Stau2 during mammalian asymmetric neural stem cell division promotes lineage progression and differentiation. Cell Stem Cell *11*, 505–516.

Lamprecht, S., and Fich, A. (2015). The cancer cells-of-origin in the gastrointestinal tract: progenitors revisited. Carcinogenesis *36*, 811-816.

Lee, C.Y., Andersen, R.O., Cabernard, C., Manning, L., Tran, K.D., Lanskey, M.J., Bashirullah, A., and Doe, C.Q. (2006a). Drosophila Aurora-A kinase inhibits neuroblast self-renewal by regulating aPKC/Numb cortical polarity and spindle orientation. Genes Dev *20*, 3464-3474.

Lee, C.Y., Robinson, K.J., and Doe, C.Q. (2006b). Lgl, Pins and aPKC regulate neuroblast self-renewal versus differentiation. Nature *439*, 594-598.

Lee, C.Y., Wilkinson, B.D., Siegrist, S.E., Wharton, R.P., and Doe, C.Q. (2006c). Brat is a Miranda cargo protein that promotes neuronal differentiation and inhibits neuroblast self-renewal. Dev Cell *10*, 441-449.

Lee, T., and Luo, L. (2001). Mosaic analysis with a repressible cell marker (MARCM) for Drosophila neural development. Trends Neurosci *24*, 251-254.

Lee, T.I., Jenner, R.G., Boyer, L.A., Guenther, M.G., Levine, S.S., Kumar, R.M., Chevalier, B., Johnstone, S.E., Cole, M.F., Isono, K.*, et al.* (2006d). Control of developmental regulators by Polycomb in human embryonic stem cells. Cell *125*, 301-313.

Ligoxygakis, P., Yu, S.Y., Delidakis, C., and Baker, N.E. (1998). A subset of notch functions during Drosophila eye development require Su(H) and the E(spl) gene complex. Development *125*, 2893-2900.

Lim, D., Huang, Y.-C., Swigut, T., Mirick, A., Manuel Garcia-Verdugo, J., Wysocka, J., Ernst, P., and Alvarez-Buylla, A. (2009). Chromatin remodelling factor Mll1 is essential for neurogenesis from postnatal neural stem cells. Nature *458*, 529-533.

Lindsley, D.L., and Zimm, G.G. (1992). The Genome of Drosophila melanogaster. Book

Liu, C., Sage, J.C., Miller, M.R., Verhaak, R.G., Hippenmeyer, S., Vogel, H., Foreman, O., Bronson, R.T., Nishiyama, A., Luo, L.*, et al.* (2011). Mosaic analysis with double markers reveals tumor cell of origin in glioma. Cell *146*, 209-221.

Liu, C., and Zong, H. (2012). Developmental origins of brain tumors. Curr Opin Neurobiol *22*, 844-849.

Liu, J., Sato, C., Cerletti, M., and Wagers, A. (2010). Notch signaling in the regulation of stem cell self-renewal and differentiation. Curr Top Dev Biol *92*, 367-409.

Lodato, M.A., Ng, C.W., Wamstad, J.A., Cheng, A.W., Thai, K.K., Fraenkel, E., Jaenisch, R., and Boyer, L.A. (2013). SOX2 co-occupies distal enhancer elements with distinct POU factors in ESCs and NPCs to specify cell state. PLoS Genet *9*, e1003288.

Loedige, I., Jakob, L., Treiber, T., Ray, D., Stotz, M., Treiber, N., Hennig, J., Cook, K.B., Morris, Q., Hughes, T.R.*, et al.* (2015). The Crystal Structure of the NHL Domain in Complex with RNA Reveals the Molecular Basis of Drosophila Brain-Tumor-Mediated Gene Regulation. Cell Rep *13*, 1206-1220.

Loh, Y.H., Wu, Q., Chew, J.L., Vega, V.B., Zhang, W., Chen, X., Bourque, G., George, J., Leong, B., Liu, J.*, et al.* (2006). The Oct4 and Nanog transcription network regulates pluripotency in mouse embryonic stem cells. Nat Genet *38*, 431-440.

Lui, J.H., Hansen, D.V., and Kriegstein, A.R. (2011). Development and evolution of the human neocortex. Cell *146*, 18–36.

Luis, N.M., Morey, L., Di Croce, L., and Benitah, S.A. (2012). Polycomb in stem cells: PRC1 branches out. Cell Stem Cell *11*, 16-21.

Lupien, M., Eeckhoute, J., Meyer, C.A., Wang, Q., Zhang, Y., Li, W., Carroll, J.S., Liu, X.S., and M., B. (2008). FoxA1 translates epigenetic signatures into enhancer-driven lineage-specific transcription. Cell *132*, 958-970.

Lv, X., Han, Z., Chen, H., Yang, B., Yang, X., Xia, Y., Pan, C., Fu, L., Zhang, S., Han, H.*, et al.* (2016). A positive role for polycomb in transcriptional regulation via H4K20me1. Cell Res *26*, 529-542.

Magee, J.A., Piskounova, E., and Morrison, S.J. (2012). Cancer stem cells: impact, heterogeneity, and uncertainty. Cancer Cell *21*, 283-296.

Martello, G., Bertone, P., and Smith, A. (2013). Identification of the missing pluripotency mediator downstream of leukaemia inhibitory factor. EMBO J *32*, 2561-2574.

Mateo, J.L., van den Berg, D.L., Haeussler, M., Drechsel, D., Gaber, Z.B., Castro, D.S., Robson, P., Crawford, G.E., Flicek, P., Ettwiller, L.*, et al.* (2015). Characterization of the neural stem cell gene regulatory network identifies OLIG2 as a multifunctional regulator of self-renewal. Genome Res *25*, 41-56.

Maurange, C., Cheng, L., and Gould, A.P. (2008). Temporal transcription factors and their targets schedule the end of neural proliferation in Drosophila. Cell *133*, 891-902.

McKay, D.J., and Lieb, J.D. (2013). A Common Set of DNA Regulatory Elements Shapes Drosophila Appendages. Dev Cell *27*, 306–318.

Min, J., Zhang, Y., and Xu, R.M. (2003). Structural basis for specific binding of Polycomb chromodomain to histone H3 methylated at Lys 27. Genes Dev *17*, 1823-1828.

Ming, G.L., and Song, H. (2011). Adult neurogenesis in the mammalian brain: significant answers and significant questions. Neuron *70*, 687-702.

Mohan, M., Herz, H.M., Smith, E.R., Zhang, Y., Jackson, J., Washburn, M.P., Florens, L., Eissenberg, J.C., and Shilatifard, A. (2011). The COMPASS family of H3K4 methylases in Drosophila. Mol Cell Biol *31*, 4310-4318.

Mohrmann, L., Langenberg, K., Krijgsveld, J., Kal, A.J., Heck, A.J., and Verrijzer, C.P. (2004). Differential targeting of two distinct SWI/SNF-related Drosophila chromatin-remodeling complexes. Mol Cell Biol *24*, 3077-3088.

Müller, J., Hart, C.M., Francis, N.J., Vargas, M.L., Sengupta, A., Wild, B., Miller, E.L., O'Connor, M.B., Kingston, R.E., and Simon, J.A. (2002). Histone methyltransferase activity of a Drosophila Polycomb group repressor complex. Cell *111*, 197-208.

Nakayama, T., Shimojima, T., and Hirose, S. (2012). The PBAP remodeling complex is required for histone H3.3 replacement at chromatin boundaries and for boundary functions. Development *139*, 4582-4590.

Neumüller, R.A., Richter, C., Fischer, A., Novatchkova, M., Neumüller, K.G., and Knoblich, J.A. (2011). Genome-wide analysis of self-renewal in Drosophila neural stem cells by transgenic RNAi. Cell Stem Cell *8*, 580-593.

Nichols, J., and Smith, A. (2009). Naive and primed pluripotent states. Cell Stem Cell *4*, 487-492.

Niwa, H., Miyazaki, J., and Smith, A.G. (2000). Quantitative expression of Oct-3/4 defines differentiation, dedifferentiation or self-renewal of ES cells. Nat Genet *24*, 372-376.

Novershtern, N., Subramanian, A., Lawton, L.N., Mak, R.H., Haining, W.N., McConkey, M.E., Habib, N., Yosef, N., Chang, C.Y., Shay, T.*, et al.* (2011). Densely interconnected transcriptional circuits control cell states in human hematopoiesis. Cell *144*, 296-309.

Paridaen, J.T., and Huttner, W.B. (2014). Neurogenesis during development of the vertebrate central nervous system. EMBO Rep *15*, 351-364.

Park, D., Hong, S., Salinas, R., Liu, S., Sun, S., Sgualdino, J., Testa, G., Matzuk, M., Iwamori, N., and Lim, D. (2014). Activation of Neuronal Gene Expression by the JMJD3 Demethylase Is Required for Postnatal and Adult Brain Neurogenesis. Cell Reports *8*, 1290–1299.

Pasini, D., Bracken, A.P., Hansen, J.B., Capillo, M., and Helin, K. (2007). The polycomb group protein Suz12 is required for embryonic stem cell differentiation. Mol Cell Biol *27*, 3769-3779.

Pei, J., and Grishin, N.V. (2015). C2H2 zinc finger proteins of the SP/KLF, Wilms tumor, EGR, Huckebein, and Klumpfuss families in metazoans and beyond. Gene *573*, 91-99.

Pfeiffer, B.D., Jenett, A., Hammonds, A.S., Ngo, T.T., Misra, S., Murphy, C., Scully, A., Carlson, J.W., Wan, K.H., Laverty, T.R.*, et al.* (2008). Tools for neuroanatomy and neurogenetics in Drosophila. Proc Natl Acad Sci U S A *105*, 9715-9720.

Pierfelice, T., Alberi, L., and Gaiano, N. (2011). Notch in the vertebrate nervous system: an old dog with new tricks. Neuron *69*, 840-855.

Piunti, A., and Shilatifard, A. (2016). Epigenetic balance of gene expression by Polycomb and COMPASS families. . Science *6290*.

Ponti, G., Obernier, K., Guinto, C., Jose, L., Bonfanti, L., and Alvarez-Buylla, A. (2013). Cell cycle and lineage progression of neural progenitors in the ventricular-subventricular zones of adult mice. Proc Natl Acad Sci U S A *110*.

Rada-Iglesias, A., Bajpai, R., Swigut, T., Brugmann, S.A., Flynn, R.A., and Wysocka, J. (2011). A unique chromatin signature uncovers early developmental enhancers in humans. Nature *470*, 279-283.

Ringrose, L., and Paro, R. (2007). Polycomb/Trithorax response elements and epigenetic memory of cell identity. Development *134*, 223-232.

Ringrose, L., Rehmsmeier, M., Dura, J.M., and Paro, R. (2003). Genome-wide prediction of Polycomb/Trithorax response elements in Drosophila melanogaster. Dev Cell *5*, 759-771.

San-Juán, B.P., and Baonza, A. (2011). The bHLH factor deadpan is a direct target of Notch signaling and regulates neuroblast self-renewal in Drosophila. Dev Biol *352*, 70-82.

Saurin, A.J., Shao, Z., Erdjument-Bromage, H., Tempst, P., and Kingston, R.E. (2001). A Drosophila Polycomb group complex includes Zeste and dTAFII proteins. Nature *412*, 655-660.

Sauvageau, M., and Sauvageau, G. (2010). Polycomb group proteins: multi-faceted regulators of somatic stem cells and cancer. Cell Stem Cell *7*, 299-313.

Schertel, C., Albarca, M., Rockel-Bauer, C., Kelley, N.W., Bischof, J., Hens, K., van Nimwegen, E., Basler, K., and Deplancke, B. (2015). A large-scale, in vivo transcription factor screen defines bivalent chromatin as a key property of regulatory factors mediating Drosophila wing development. Genome Res *25*, 514--523.

Schindelin J, Arganda-Carreras I, Frise E, Kaynig V, Longair M, Pietzsch T, Preibisch S, Rueden C, Saalfeld S, Schmid B*, et al.* (2012). Fiji: an open-source platform for biological-image analysis. Nat Methods *9*, 676-682.

Schütte, J., Wang, H., Antoniou, S., Jarratt, A., Wilson, N.K., Riepsaame, J., Calero-Nieto, F.J., Moignard, V., Basilico, S., Kinston, S.J.*, et al.* (2016). An experimentally validated network of nine haematopoietic transcription factors reveals mechanisms of cell state stability. eLife *5:e11469*.

Schwitalla, S., Fingerle, A.A., Cammareri, P., Nebelsiek, T., Göktuna, S.I., Ziegler, P.K., Canli, O., Heijmans, J., Huels, D.J., Moreaux, G.*, et al.* (2013). Intestinal Tumorigenesis Initiated by Dedifferentiation and Acquisition of Stem-Cell-like Properties. Cell *152*, 25-38.

Sexton, T., and Cavalli, G. (2015). The Role of Chromosome Domains in Shaping the Functional Genome. Cell *160*, 1049–1059.

Sexton, T., Yaffe, E., Kenigsberg, E., Bantignies, F., Leblanc, B., Hoichman, M., Parrinello, H., Tanay, A., and Cavalli, G. (2012). Three-dimensional folding and functional organization principles of the Drosophila genome. Cell *148*, 458-472.

Shao, Z., Raible, F., Mollaaghababa, R., Guyon, J.R., Wu, C.T., Bender, W., and Kingston, R. (1999). Stabilization of chromatin structure by PRC1, a Polycomb complex. Cell *98*, 37-46.

Shim, S., Kwan, K.Y., Li, M., Lefebvre, V., and Sestan, N. (2012). Cis-regulatory control of corticospinal system development and evolution. Nature *486*, 74-79.

Siller, K.H., Serr, M., Steward, R., Hays, T.S., and Doe, C.Q. (2005). Live imaging of Drosophila brain neuroblasts reveals a role for Lis1/dynactin in spindle assembly and mitotic checkpoint control. Mol Biol Cell *16*, 5127--5140.

Slany, R.K. (2016). The molecular mechanics of mixed lineage leukemia. Oncogene *30*, 10.1038.

Steffen, P.A., and Ringrose, L. (2014). What are memories made of? How Polycomb and Trithorax proteins mediate epigenetic memory. Nat Rev Mol Cell Biol *15*, 340-356.

Taelman, V., Van Wayenbergh, R., Sölter, M., Pichon, B., Pieler, T., Christophe, D., and Bellefroid, E.J. (2004a). Sequences downstream of the bHLH domain of the Xenopus hairy-related transcription factor-1 act as an extended dimerization domain that contributes to the selection of the partners. Dev Biol *276*, 47-63.

Taelman, V., Van Wayenbergh, R., Sölter, M., Pichon, B., Pieler, T., Christophe, D., and Bellefroid, E.J. (2004b). Sequences downstream of the bHLH domain of the Xenopus hairy-related transcription factor-1 act as an extended dimerization domain that contributes to the selection of the partners. Dev Biol *276*, 47-63.

Takaba, H., Morishita, Y., Tomofuji, Y., Danks, L., Nitta, T., Komatsu, N., Kodama, T., and Takayanagi, H. (2015). Fezf2 Orchestrates a Thymic Program of Self-Antigen Expression for Immune Tolerance. Cell *163*, 975-987.

Teytelman, L., Özaydın, B., Zill, O., Lefrançois, P., Snyder, M., Rine, J., and Eisen, M.B. (2009). Impact of Chromatin Structures on DNA Processing for Genomic Analyses. PLoS One *0006700*.

Tie, F., Banerjee, R., Saiakhova, A.R., Howard, B., Monteith, K.E., Scacheri, P.C., Cosgrove, M.S., and Harte, P.J. (2014). Trithorax monomethylates histone H3K4 and interacts directly with CBP to promote H3K27 acetylation and antagonize Polycomb silencing. Development *141*, 1129-1139.

Treisman, J.E., Luk, A., Rubin, G.M., and Heberlein, U. (1997). eyelid antagonizes wingless signaling during Drosophila development and has homology to the Bright family of DNA-binding proteins. Genes Dev *11*, 1949-1962.

Venken, K.J., Carlson, J.W., Schulze, K.L., Pan, H., He, Y., Spokony, R., Wan, K.H., Koriabine, M., de Jong, P.J., White, K.P.*, et al.* (2009). Versatile P[acman] BAC libraries for transgenesis studies in Drosophila melanogaster. Nat Methods *6*, 431-434.

Venken, K.J., He, Y., Hoskins, R.A., and Bellen, H.J. (2006). P[acman]: a BAC transgenic platform for targeted insertion of large DNA fragments in D. melanogaster. Science *314*, 1747-1751.

Vessey, J.P., Amadei, G., Burns, S.E., Kiebler, M.A., Kaplan, D.R., and Miller, F.D. (2012). An asymmetrically-localized Staufen2-dependent RNA complex regulates maintenance of mammalian neural stem cells. Cell Stem Cell *11*, 517–528.

Viktorin, G., Riebli, N., Popkova, A., Giangrande, A., and Reichert, H. (2011). Multipotent neural stem cells generate glial cells of the central complex through transit amplifying intermediate progenitors in Drosophila brain development. Dev Biol *356*, 553-565.

Wallace, K., Liu, T.H., and Vaessin, H. (2000). The pan-neural bHLH proteins DEADPAN and ASENSE regulate mitotic activity and cdk inhibitor dacapo expression in the Drosophila larval optic lobes. Genesis *26*, 77-85.

Wang, H., Wang, L., Erdjument-Bromage, H., Vidal, M., Tempst, P., Jones, R.S., and Zhang, Y. (2004). Role of histone H2A ubiquitination in Polycomb silencing. Nature *431*, 873-878.

Wang, S., and Samakovlis, C. (2012). Grainy head and its target genes in epithelial morphogenesis and wound healing. Curr Top Dev Biol *98*, 35-63.

Weidgang, C.E., Seufferlein, T., Kleger, A., and Mueller, M. (2016). Pluripotency Factors on Their Lineage Move. Stem Cells International *2013*, 6838253.

Weng, M., Golden, K.L., and Lee, C.Y. (2010). dFezf/Earmuff maintains the restricted developmental potential of intermediate neural progenitors in Drosophila. Dev Cell *18*, 126-135.

Weng, M., Komori, H., and Lee, C.Y. (2012). Identification of neural stem cells in the Drosophila larval brain. Methods Mol Biol *879*, 39-46.

Weng, M., and Lee, C.Y. (2011). Keeping neural progenitor cells on a short leash during Drosophila neurogenesis. Curr Opin Neurobiol *21*, 36-42.

Wilson, N.K., Foster, S.D., Wang, X., Knezevic, K., Schütte, J., Kaimakis, P., Chilarska, P.M., Kinston, S., Ouwehand, W.H., Dzierzak, E.*, et al.* (2010). Combinatorial transcriptional control in blood stem/progenitor cells: genome-wide analysis of ten major transcriptional regulators. Cell Stem Cell *7*, 532-544.

Xiao, Q., Komori, H., and Lee, C.Y. (2012). klumpfuss distinguishes stem cells from progenitor cells during asymmetric neuroblast division. Development *139*, 2670-2680.

Xie, Y., Li, X., Zhang, X., Mei, S., Li, H., Urso, A., and Zhu, S. (2014). The Drosophila Sp8 transcription factor Buttonhead prevents premature differentiation of intermediate neural progenitors. eLife *3*, 10.7554/eLife.03596.

Yang, C.P., Fu, C.C., Sugino, K., Liu, Z., Ren, Q., Liu, L.Y., Yao, X., Lee, L.P., and Lee, T. (2015). Transcriptomes of lineage-specific Drosophila neuroblasts profiled via genetic targeting and robotic sorting. Development *doi: 10.1242/dev.129163*.

Yang, N., Dong, Z., and Guo, S. (2012). Fezf2 regulates multilineage neuronal differentiation through activating basic helix-loop-helix and homeodomain genes in the zebrafish ventral forebrain. J Neurosci *32*, 10940-10948.

Younger-Shepherd, S., Vaessin, H., Bier, E., Jan, L.Y., and Jan, Y.N. (1992). deadpan, an essential pan-neural gene encoding an HLH protein, acts as a denominator in Drosophila sex determination. Cell *70*, 911-922.

Zacharioudaki, E., Housden, B.E., Garinis, G., Stojnic, R., Delidakis, C., and Bray, S. (2015). Genes implicated in stem-cell identity and temporal-program are directly targeted by Notch in neuroblast tumours. Development *doi: 10.1242/dev.126326*.

Zacharioudaki, E., Magadi, S.S., and Delidakis, C. (2012). bHLH-O proteins are crucial for Drosophila neuroblast self-renewal and mediate Notch-induced overproliferation. Development *139*, 1258-1269.

Zentner, G.E., Tesar, P.J., and Scacheri, P.C. (2011). Epigenetic signatures distinguish multiple classes of enhancers with distinct cellular functions. Genome Res *21*, 1273-1283.

Zhao, S., Nichols, J., Smith, A.G., and Li, M. (2004). SoxB transcription factors specify neuroectodermal lineage choice in ES cells. Mol Cell Neurosci *27*, 332–342.

Zhu, S., Barshowa, S., Wildonger, J., Jan, L.Y., and Jan, Y.-N. (2011). Ets transcription factor pointed promotes the generation of intermediate neural progenitors in Drosophila larval brains. Proc Natl Acad Sci USA *108*, 20615-20620.

Zhu, S., Wildonger, J., Barshow, S., Younger, S., Huang, Y., and Lee, T. (2012). The bHLH repressor deadpan regulates the self-renewal and specification of Drosophila larval neural stem cells independently of notch. PLoS One *7*, e46724.

Zong, H., Parada, L.F., and Baker, S.J. (2015). Cell of origin for malignant gliomas and its implication in therapeutic development. Cold Spring Harb Perspect Biol *7*, Epub.